9-1-1972

A Program For Estimating Runoff From Indiana Watersheds, Part III: Analysis Of Geomorphologic Data And A Dynamic Contributing Area Model For Runoff Estimation

H. T. Lee

J. W. Delleur
delleur@purdue.edu

TECHNICAL REPORT NO. 24

A PROGRAM FOR ESTIMATING RUNOFF FROM INDIANA WATERSHEDS

Part III. Analysis of Geomorphologic Data And A Dynamic Contributing Area Model For Runoff Estimation

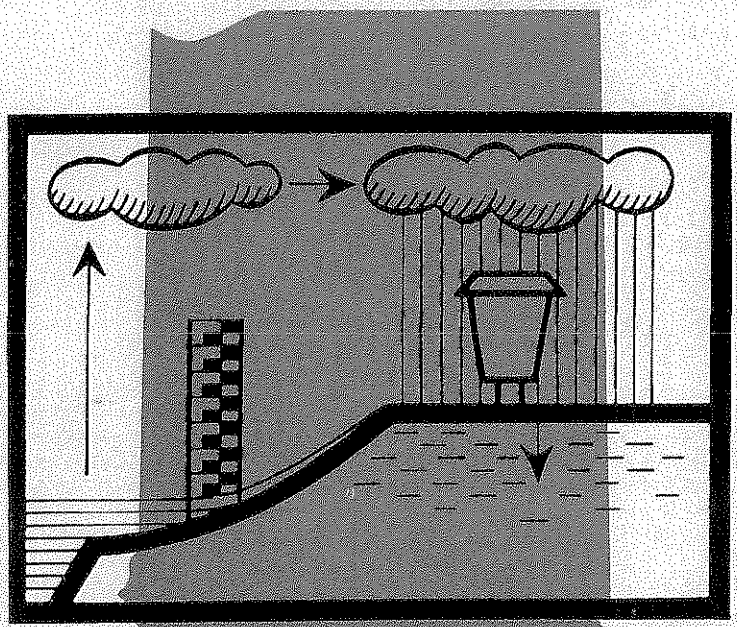

by

M. T. Lee

J. W. Delleur

SEPTEMBER 1972

PURDUE UNIVERSITY
WATER RESOURCES RESEARCH CENTER
LAFAYETTE, INDIANA

School of Civil Engineering

Purdue University

Lafayette, Indiana 47907

A PROGRAM FOR ESTIMATING RUNOFF FROM INDIANA WATERSHEDS

PART III - ANALYSIS OF GEOMORPHOLOGIC DATA AND A DYNAMIC CONTRIBUTING AREA MODEL FOR RUNOFF ESTIMATION

by

M. T. Lee

J. W. Delleur

Period of Investigation: July 1968 - September 1972

Final Report For OWRR-B-008-IND

Matching Grant Agreement No. 14-01-0001-1902

Purdue University Water Resources Research Center

Technical Report No. 24

September 1972

PREFACE AND ACKNOWLEDGMENTS

This report describes the work accomplished as part of research project OWRR-B-008-IND entitled "Assembly and Analysis of Hydrologic and Geomorphologic Data for Small Watersheds in Indiana." It is the continuation of project OWRR-A-001-IND entitled "Estimation of Runoff from Small Watersheds in Indiana." The results of the first project were reported in "A Program for Estimating Runoff from Indiana Watersheds - Part I. Linear System Analysis in Surface Hydrology and Its Application to Indiana Watersheds" by D. Blank and J. W. Delleur, Purdue University Water Resources Research Center, Technical Report No. 4, August 1968. This report included the acquisition of a library of rainfall excess and direct runoff data, and the identification of the instantaneous unit hydrographs by the Fourier and Laplace transforms and by a numerical deconvolution method.

The use of the mathematical transforms and of digital filtering in the identification of the instantaneous unit hydrograph was extended further jointly with project OWRR-B-022-IND, entitled "Effects of Urbanization in Hydrology," and was reported in "The Instantaneous Unit Hydrograph: Its Calculation by the Transform Method and Noise Control by Digital Filtering" by R. A. Rao and J. W. Delleur, Technical Report No. 20, June 1971.

To the hydrologic data bank a geomorphologic data bank was added, forming what may be called a hydrologic and geomorphologic atlas of Indiana. The compilation and use of this atlas was reported in "A Program for Estimating Runoff from Indiana Watersheds - Part II. Assembly of Hydrologic and Geomorphologic Data for Small Watersheds in Indiana" by M. T. Lee, D. Blank and J. W. Delleur, Technical Report No. 23, May 1972.

The present report summarizes the previous work and concentrates on the analysis of the data contained in the hydrologic and geomorphologic atlas of Indiana. The geomorphologic data of a number of Indiana watersheds are studied. The stream network planform and other geomorphologic characteristics are included in the formulation of a new rainfall-runoff model. This model is based on the dynamic partial response area concept and on a linearized flood routing procedure. The method is applied to Indiana watersheds.

The authors wish to express their appreciation to Dr. Dan Wiersma, Director of the Water Resources Research Center at Purdue University and to Dr. J. F. McLaughlin, Head of the School of Civil Engineering for their help in the

administration of the project. The authors are grateful to Professor W. N. Melhorn, and to Dr. D. M. Coffman for their permission to use the W.A.T.E.R. computer programs (reference 18), and for their assistance in the use of these programs and in the interpretation of the results. The authors also wish to express their thanks to Mr. M. Hale, formerly District Chief of the U.S. Geological Survey Indianapolis Office, and to Mr. McCollam of the same office for their cooperation and assistance in assembling the hydrologic data.

The work presented herein was supported partly by the Office of Water Resources Research, Department of the Interior, under matching grant project OWRR-B-008-IND (Assembly and Analysis of Hydrologic and Geomorphologic Data for Small Watersheds in Indiana), partly by the Purdue Research Foundation under grant XR5869 and partly by Purdue University. The authors wish to express their thanks to the sponsors.

TABLE OF CONTENTS

	Page
Preface and Acknowledgments	i
Table of Contents	iii
List of Tables	v
List of Figures	vi
Nomenclature	viii
Abstract	xi
CHAPTER I - Introduction	1
CHAPTER II - Related Studies	3
CHAPTER III - Previous Work on Data Acquisition and Linear Systems Analysis	5
3.1 Assembly and Retrieval of Hydrologic and Geomorphologic Data	5
3.2 Linear Systems Analysis	6
CHAPTER IV - Using W.A.T.E.R. System for Data Analysis	15
4.1 General	15
4.2 Use of the W.A.T.E.R. System	16
4.3 River Network Classification and Basic Geomorphologic Parameters	17
4.4 Analysis of Geomorphologic Data	22
4.4.1 Law of Stream Number and Stream Length	22
4.4.2 Bifurcation Ratio and Stream Length Ratio	25
4.4.3 Number of Link Magnitude	26
4.4.4 Link Length Distribution	28
4.4.5 Summary Table of Watershed Characteristics	28
4.5 Summary and Conclusions	31
CHAPTER V - Formulation of the Hydrologic Model	36
5.1 The Natural Watershed as a System	36
5.2 Areal Distribution Along Stream Reach	38

Page

5.3 Fixed Response Area and Varied Response Area 41

5.4 Flood Routing Technique 48

5.5 Formulation of the Model 52

5.6 Estimation of Parameters 53

5.7 The Unit-Variate Search Method 54

CHAPTER VI - Results and Discussions 56

6.1 Introduction 56

6.2 Contributing Area Distribution Curve 56

6.3 The Determination of "B" Horizon Loss and Weight Factor D 59

6.4 Verification of Computer Programs Used in the Analysis of Upstream Inflow Instantaneous Unit Hydrograph (UIIUH) 64

6.5 Sensitivity Analysis of Model Parameters 66

6.6 The Sample Results of Identification Mode 67

6.7 The Correlation of Identified Parameters with Geomorphologic Characteristics and Rainfall Pattern 68

6.8 Proposed Runoff Estimation Model 76

6.9 Model Regeneration Performance and Comparison with Some Other Methods 79

CHAPTER VII - Summary and Conclusions 83

Bibliography 85

Appendix 90

LIST OF TABLES

Table		Page
3-1	Watershed Summary	7
4-1	The Water System Options	18
4-2	Watersheds for Geomorphologic Analysis	23
4-3	Comparison of First-Order Stream Lengths	24
4-4	Watershed Statistics	33
5-1	Comparison of Peak and Base Flows Testing Data Set	37
5-2	Drainage Density and Source Distribution of Sub-basins of the Big Blue River at Carthage, Indiana (Watershed No. 10) and of the Salamonie River at Portland, Indiana (Watershed No. 35)	40
6-1	Stream Length Ratio and Some Basin Shape Characteristics	58
6-2	Estimation of Soil Permeability in Indiana	59
6-3	Soil Results of Permeability by Betcher et al. [Ref. No. 60]	60
6-4	Runoff Ratio of Testing Watersheds	62
6-5	Summary Information of Watershed No. 3, 10 and 24	69
6-6	Storms Selected for Regression Analysis of C_z	72
6-7	Regression Equations of C_z	71
6-8	Regression Equations of Runoff Ratio	75
6-9	Summary of Prediction Model Input Information	78
6-10	Summary Results of Regeneration Performance	80
6-11	Comparison of Wu Method of Grouping IUH's According to Peak Value and Time to Peak and Dynamic Area Models	82

LIST OF FIGURES

Figure

3-1 Data Acquisition Procedure
3-2 Location of Stream and Rain Gages
4-1 Inter-Related Scheme of Geomorphic Parameters
4-2 Laws of Stream Numbers and Stream Lengths
4-3 Distribution of Bifurcation Ratio
4-4a Bifurcation Ratios vs. Stream Orders
4-4b Stream Length Ratios vs. Stream Orders
4-5 Link Number Distribution
4-6 Means and Standard Deviations of Link Lengths
4-7 Main Stream Length and Drainage Area
4-8 Basin Slopes vs. Drainage Areas
4-9 Drainage Density and Basin Mean Slope
4-10 Drainage Density and Texture Ratio
4-11 Drainage Area vs. Elongation Ratio
4-12 Drainage Density vs. Mean Link Length
4-13 Drainage Density vs. Link Frequency and Channel Frequency
4-14 Link Magnitude vs. Drainage Area with Drainage Density as Parameter
5-1 Natural Watershed System
5-2 Drainage Area Distribution Along the Stream Reaches
5-3 Example of Drainage Area Distribution Along the Stream Reaches; Bean Blossom Creek at Bean Blossom, Indiana
5-4 Fixed and Varied Response Area Concepts
5-5 Dynamic Watershed Concept (Source: TVA, 1965)
5-6 A Time-Lapse View of a Basin Showing Expansion of the Source Area and the Channel System During a Storm (Source: Nutter and Hewlett, 1971)
5-7 Physical Diagram of Upstream Inflow Instantaneous Unit Hydrograph for Single Stream Reach
5-8 Flow Diagram of System Identification and Prediction
5-9 Unit Direction Search
6-1 Simplified Watershed, Lawrence Creek at Ft. Benjamin Harrison, Indiana (Watershed No. 1)

Figure

6-2	Simplified Watershed, Hinkle Creek Near Cicero, Indiana (Watershed No. 16)
6-3	Examples of Drainage Area Distribution Along the Stream Reaches
6-4	Drainage Area and Maximal Ordinate of Drainage Area Distribution
6-5	General Soil Types of the Regions of Indiana
6-6	Sensitivity Analysis of Weight D
6-7	Runoff Ratio vs. N
6-8	Estimated Runoff Ratio by Wu Method
6-9a	Magnitude of First Term in UIIUH
6-9b	Magnitude of First Term in UIIUH
6-10	Verification of UIIUH
6-11	Verification of UIIUH
6-12	Verification of Convolution
6-13	Sampling Scheme of Upstream Inflow Instantaneous Unit Hydrograph
6-14	Sensitivity Analysis of UIIUH Parameters
6-15	Comparison of Response Area Models
6-16	Comparison of Optimization Criteria
6-17	Sample Results of Watershed No. 2, 3 and 10
6-18	Sample Results of Watershed No. 16, 19 and 24
6-19	Sample Results of Watershed No. 35, 39 and 44
6-20	Comparison of Observed and Computed Direct Runoff Hydrographs
6-21	C_z vs. Rainfall Volume
6-22	Reference Discharge vs. Rainfall Volume
6-23	Runoff Ratio vs. N in Watersheds No. 3, 10 and 24
6-24	The Sample Results of Regeneration Performance
6-25	The Comparison with Some Other Methods

NOMENCLATURE

$A(i\Delta t)$	The dynamic response area at time $i\Delta t$
$a(L,t)$	Variable response area at stream reach L and at time t
A_0	Drainage area
$a_0(L)$	Drainage area distribution of stream reach L
B	"B" horizon infiltration
B_f	Average base flow
C_z	Roughness coefficient
D	Fraction of the antecedent rainfall contributing to the response area
D_d	Drainage density
D_N	$\frac{S_0 L}{y_0}$
D_r	Storm duration, in hours
D_t	$\frac{d}{dt}$
e	Base of natural logarithms
f_c	Infiltration rate which represents the fairly steady rate of water absorption reached after water has been applied continuously for a long period of time
F_L	Link frequency
F_N	Froude number
f_0	The initial infiltration rate at t=0
f(t)	Infiltration capacity at time t
g	Gravity acceleration
G(t)	Loss function time accumulative distribution
$H_u(x,t)$	Upstream inflow instantaneous unit hydrograph with inflow at stream reach x
I(t)	Input function
IUH	Instantaneous Unit Hydrograph
K	Parameter in storage equation
l	Basin mean link length
L_0	Main stream length
L_T	Total stream length
M	Link magnitude

N	Parameter of equation (5.3.9)
n	Parameter in Appendix
$N_0(\mu)$	$\frac{1}{2\mu-1}\binom{2\mu-1}{\mu}$
$P_m(t)$	The precipitation mass curve
P_{max}	Maximal rainfall intensity within a storm, in inches per hour
P_t	Total rainfall volume, in inches
q	Discharge
q'	Deviation from reference discharge
q_L	Lateral inflow
q_0	Reference discharge
$Q(t)$	Direct runoff hydrograph
$R_B(t)$	Rainfall at time t in excess of the "B" horizon permeability
R_b	Bifurcation ratio
R_r	Runoff ratio
$R(t)$	Rainfall at time t
S	The total number of stream reach sampling points in the idealized one dimensional watershed
S_f	Head loss per unit length
S_I	Soil index developed by USGS
S_0	The drop in elevation of stream bottom per unit length
$S_{RF}(i\Delta t)$	The accumulated rainfall in excess of "B" horizontal permeability
$S(t)$	Storage function at time t
T	Total number of sampling points of direct runoff
t	time
T_c	Time of concentration
t_f	The time at the end of storm event
T_g	The lag of the time of translation
T_{min}	Minimal daily temperature when storm occurs
T_{max}	Maximal daily temperature when storm occurs
T_{NM}	Total link number
T_0	Time to the wave head of UIIUH
T_R	Duration
T_r	Texture ratio
t_s	The starting time of the rainfall

T_T	Link - Texture ratio
U	Stream order
UIIUH	Upstream Inflow Instantaneous Unit Hydrograph
u	Flow velocity
V(μ)	The probability density function of randomly drawing a link of magnitude μ in an infinite topologically random channel network
$W(\frac{t}{T_c})$	The ordinate of dimensionless time area concentration curve
W(μ;M)	The probability of drawing a link of magnitude μ from finite topologically random networks with magnitude μ
$X_R(t)$	Excess precipitation time distribution
x	Stream reach
y	Water depth
y_0	Reference depth
y'	Deviation from the reference depth
α	Parameter of equation (5.3.7)
β	Parameter of equation (5.3.7)
γ	Parameter of equation (5.3.7)
μ	Link magnitude
τ	Parameter in time lag equation
ΔL	The sampling interval for stream link length
δ(t)	Delta function

ABSTRACT

The determination of the time distribution of the runoff from a watershed is a common and complex problem in water resources design. It depends primarily upon the watershed characteristics, the rainfall pattern and the climatic conditions. The construction of an integrated model of the rainfall-runoff process and its application to watersheds located in Indiana were the main objectives of this study.

This study consists of three major parts:

1) the development of a computer oriented assembly and retrieval system for hydrologic and geomorphologic data for watersheds 2 to 300 square miles.
2) the formulation, with the help of this assembly, of a dynamic model of the areas contributing to the watershed runoff based on the watershed stream network and on the climatic conditions.
3) the development of a method of digital simulation of the watershed behavior in order to estimate streamflow hydrographs for small Indiana basins under varying rainfall and watershed conditions.

In order to pursue these objectives, the following steps were taken.

1) The principal geomorphologic characteristics of the watersheds were quantified by analyzing the planform of the watershed networks.
2) An integrated model of the rainfall-runoff process was formulated by using the dynamic response area concept and a linear routing technique.
3) The model parameters were correlated to geomorphologic, rainfall, and climatologic characteristics.

The analysis of stream network data indicates that the small Indiana watersheds obey the Strahler and Shreve ordering system. It was found that the drainage area, the drainage density and the basin slope are the major watershed parameters.

A contributing drainage area distribution curve along the stream reaches was developed, for the purpose of runoff estimation. The dynamic contributing area model is expressed in terms of a ratio of the weighted accumulated rainfall up to the time considered to the total rainfall and this ratio is raised to a power. This power which quantifies the rate of expansion of the dynamic area was found to be related to the runoff ratio which in turn was

correlated with the rainfall pattern, the climatic conditions, the watershed condition and the major soil type.

A linear three parameter method was used to route the contributed runoff through the drainage area distribution curve. The roughness parameter was found to be correlated with the average base flow per unit area and with geomorphologic characteristics whereas the slope parameter could be estimated from topographic maps and the reference discharge parameter varied within narrow limits.

Based on the dynamic area model and the linear routing technique, a runoff simulation model is proposed. The basic input information required is: the rainfall hyetograph, the base flow, the daily minimum temperature, the soil index, and drainage and topographic maps. The model regenerates the runoff hydrographs within reasonable error limits. The model performance was compared with some of the other methods currently used in engineering design in order to evaluate its advantages and disadvantages.

CHAPTER I

INTRODUCTION

Development and management of water resources are major economic activities of all nations. Water resources are developed to ensure the satisfaction of other economic activities, such as water supply both for domestic and industrial uses, flood control, drought prevention, hydroelectric power, irrigation, water pollution abatement, navigation etc.; these activities are strongly dependent upon the knowledge of the hydrologic cycle. In the state of Indiana and many parts of the United States and other nations, a substantial portion of the water used comes from surface water. Therefore, surface water runoff estimation is one of the key problems in the water resource development.

The surface water problem needs an extensive understanding of the rainfall-runoff process. Most engineering methods currently used are based on the unit hydrograph and the instantaneous unit hydrograph. A more precise understanding of the rainfall-runoff transformation needs extensive data acquisition, application of physical laws, and integrated system modeling techniques. As a result of this demand, this study was proposed to pursue the following objectives:

1) to develop a computer oriented assembly and retrieval system for hydrologic and geomorphologic data for watersheds from 2 to 300 square miles in Indiana.
2) to study with the help of this assembly, the hydrologic response (runoff hydrograph) of small Indiana watersheds under varying climatic conditions and to correlate the parameters describing the hydrologic systems' transfer functions to the basin hydrologic and geomorphologic characteristics.
3) to develop a method of digital simulation of the watershed behavior in order to forecast streamflow hydrographs for Indiana basins under varying storm and watershed conditions.

The details of this study are given in the following Chapters. A review of related studies is given in Chapter II. Chapter III discusses the previous work on data acquisitions and linear systems analysis. Before the formulation of the hydrologic model, the understanding of the basin morphology is necessary. The analysis of the geomorphology of the stream networks is

presented in Chapter IV. Based on the stream network planform, a hydrologic model is formulated to simulate the rainfall-runoff process. The integrated system is given in Chapter V. The results and discussions are presented in Chapter VI. Finally the summary and conclusions are given in Chapter VII.

CHAPTER II

RELATED STUDIES

There are two major problems involved in the modeling of the rainfall-runoff process. The first is the identification of the rainfall volume both in time and space which produces the runoff. The second is the method of routing the rainfall to direct runoff at the basin outlet.

The first problem in lumped system analysis is the rainfall excess separation. The methods employed for this type of analysis were cited in reference [1]. The most commonly used method is based on the infiltration capacity concept proposed by Horton [2]. However, the recent studies [3, 4, 5,6,7,8,9,10,11,12] indicated that the classic Horton overland flow is a rare occurrence in time and space. Nutter and Hewlett [10] cited that the partial area response approach is more general than the traditional Horton infiltration method. The field experiment [13] by T.V.A. and the numerical simulation by Freeze [12,14] further showed that the partial response area concept is needed to simulate the field condition. Therefore, the partial response area approach was employed to simulate the hydrologic model in this study.

The second problem is concerned with the routing procedures. Essentially, those procedures may be divided into two broad categories. The first is based on the unsteady flow equations. The second one is based on the storage concept. The storage concept includes the conceptual models [15] and storage methods [15] which may be linear or nonlinear. One characteristic of this type of analysis is that the runoff response is represented by a set of functions with few parameters. The second category is based on the unsteady flow equations. There are four basic methods in this approach. They are: 1) the dynamic wave, 2) the kinematic wave, 3) the diffusion analogy and 4) the linearization method. The dynamic and kinematic wave methods are valid for simple stream reach problems. They are laborious and impractical to apply in watershed simulation. The diffusion analogy is a simplified version of linearization solution. As we know, most of the routing models based on the storage concept are valid for lumped system analysis. Hence the linearized solution was pursued further. Using unsteady flow equations, Harley [16] derived a complete linear approximation for the upstream inflow instan-

taneous unit hydrograph. Harley and Dooge [17] also compared the complete linear solution with the methods of storage approach. They concluded that the complete linear solution is as accurate or more accurate than the other models commonly used. Therefore, it was decided to employ the complete linear routing technique in this study.

In summary, there are two phases which are to be investigated in this study. They are the partial area response and the complete linear routing. Both phases need substantial information on the drainage basins. Therefore, it was decided to pursue this study in the following sequence:

1) Using W.A.T.E.R. [18] system to analyze the basin parameters which quantify the characteristics of watersheds.

2) Using the partial response area concept and the linear routing technique to form an integrated system for the rainfall-runoff process.

3) Using the geomorphologic parameters and characteristics of the rainfall pattern to correlate the system parameters found in the model for prediction of the runoff response in Indiana small watersheds.

CHAPTER III

PREVIOUS WORK ON DATA ACQUISITION AND LINEAR SYSTEMS ANALYSIS

This Chapter summarizes two phases of the research that have been previously reported. These are the assembly and retrieval of hydrologic and geomorphologic data and the application of linear systems analysis in hydrology.

3.1 Assembly and Retrieval System of Hydrologic and Geomorphologic Data

The study of the hydrologic cycle requires extensive data. Systems analysis of the rainfall-runoff process in particular needs a large bank of good quality data for model identification and verification. Hydrologic data are collected by many agencies and published in scattered reports. As a result the compilation of geomorphologic and hydrologic data banks is both time consuming and expensive.

The hydrologic data were collected by Mr. D. Blank in the early stage of this study. The hydrologic data bank included the total rainfall, the total runoff, the rainfall excess and the direct runoff discretized at 30 minute intervals for 1059 storms in 55 watersheds with areas between 3 and 300 square miles located in Indiana. The data were loaded on magnetic tapes. The complete description of the hydrologic data bank may be found in [19].

Two major types of geomorphologic data were collected. They are: the drainage network and the topography. The drainage network was compiled from the Indiana county drainage atlas prepared by Purdue University [20]. The topographic data were digitized from U.S. Geological Survey 1/24,000 quadrangle and 1/125,000 topographic maps. All these sets of data were digitized and recorded on computer cards. The CALCOMP plotter was used to display the data for checking purposes. Then the data were loaded on magnetic tapes.

The outline of data collection procedures is shown in Figure 3-1. Tape 1 and tape 2 contain the rainfall excess and direct runoff and the total rainfall and runoff data banks. Tapes 3 and 4 contain the geomorphologic data bank. Detailed procedures of the data storage and retrieval system are discussed in reference [19].

The selection of the watersheds was determined by: 1) the desire to cover most of the regions of the state of Indiana, and 2) the condition that man-made disturbances were not predominant factors controlling the behavior of the watershed. It should be realized, however, that with the increase in urbanization and with the ever increasing use of surface water in the state, most watersheds already are or will be subjected to some form of disturbance such as diversions for water supply, dams, or sewage disposal into the main stream. Table 3-1 gives a list of the watersheds selected, their area in square miles, the number of storms included, the assigned precipitation stations, and the availability of digitized topography and stream network. Figure 3-2 shows the location of the stream and rain gage stations considered.

3.2 Linear Systems Analysis

In the early part of the research only the hydrologic data bank was available. The analysis of the rainfall excess-direct runoff data was then made using the lumped linear system analysis approach which is summarized in this section.

A watershed, as defined by Eagleson [21], is an open physical system in the sense that there is import and export of matter across its closed boundaries. In the strict sense, we may define the watershed boundary as a fixed, closed curve lying on the land surface and including a chosen point, such that all surface runoff produced by precipitation falling within the curve, and no other, leaves the area in a concentration flow at that point.

In hydrology, the word "system" has been defined by Chow [22] as, "an aggregation or assemblage of parts, being either objects or concepts, united by some form of regular interaction or in(ter)dependence" (syllable in parenthesis added). Therefore, the classical hydrologic cycle may be considered as a "hydrologic system". The hydrologic cycle contains various components: interception, evaporation, transpiration, infiltration, detention, retention, surface runoff, subsurface runoff and ground water flow. In a watershed system, the rainfall is considered as the input and the runoff as the output.

In watershed mathematical simulation, there are two basic means to achieve modeling. Either a lumped-system or a distributed system is selected. A lumped system was cited by Chow [22] as a "black box". There is no interest

Table 3-I Watershed Summary

Watershed No.	Watershed Name and Location	Area (sq. mi.)	Number of Storms	Precipitation Stations	Topo-Map	Network
I	Lawrence Cr. at Ft. Benjamin Harrison	2.86	13	19,113	yes	yes
2	Bear Cr. near Treviac	7.	15	28,32,90,111	yes	yes
3	Bean Blossom Cr. at Bean Blossom	14.6	17	28,32,90,111	yes	yes
4	Wildcat Cr. at Kokomo	245.	6	57,74	no	no
5	South Hogan Cr. near Dillsboro	38.2	9	51	yes	no
6	Mississinewa River near Ridgeville	130.	39	38,61,85,139	no	no
7	Iroquois River at Rosebud	30.3	9	6,31,108	no	no
8	Fall Cr. near Fortville	172.	15	59,65,84	yes	yes
9	Sand Dr. near Brewersville	156.	31	2,4,8,115	yes	yes
10	Big Blue River at Carthage	187.	23	59,63,72	yes	yes
11	Little Calumet River at Porter	62.9	12	50	no	no

Table 3-1 (continued)

Watershed No.	Watershed Name and Location	Area (sq. mi.)	Number of Storms	Precipitation Stations	Topo-Map	Net-work
12	South Fork Wildcat Cr. near Lafayette	246.	15	14,55,56,79	yes	yes
13	White River at Muncie	242.	11	61,76,139	no	no
14	Busseron Cr. near Carlisle	228.	46	43,68,69,147	no	no
15	Laughery Cr. near Farmers Retreat	248.	18	2,51	no	no
16	Hinkle Cr. near Cicero	16.3	10	65,74,84	yes	yes
17	Dear Cr. near Delphi	278.	15	5,57,79	no	no
18	Big Raccoon Cr. near Fincastle	132.	16	54,60,96,135	yes	yes
19	Brush Cr. near Nebraska	11.7	26	5,51	yes	yes
20	West Cr. near Schneider	54.5	18	45	yes	no
21	White Lick Cr. at Morresville	212.	11	11,19,94,96,113	no	no
22	Cicero Cr. at Noblesville	219.	22	65,74,84	yes	yes
23	Dear Cr. at Putnam-ville	59.	21	39,94,103	yes	yes

Table 3-1 (continued)

Watershed No.	Watershed Name and Location	Area (sq. mi.)	Number of Storms	Precipitation Stations	Topo-Map	Net-work
24	Buck Cr. at Muncie	36.7	21	61,76,144	yes	yes
26	Clifty Cr. at Hartsville	88.8	14	8,42,109,110	yes	yes
27	Little Raccoon Cr. near Catlin	133.	15	30,54,99,107	yes	yes
28	South Fork Salt Cr. at Kurtz	38.1	14	44	yes	yes
29	Graham Cr. near Vernon	77.6	27	4,51	yes	yes
30	Middle Fork Anderson River at Bristow	41.9	15	11,25,120	yes	yes
31	Indian Cr. near Springville	60.9	12	34,68,111	yes	yes
32	Clear Cr. near Harrodsburg	55.2	12	34,111	yes	yes
33	Salt Cr. near McCool	78.7	16	50	yes	yes
34	Yellow River near Bremen	132.	8	24,47	no	no
35	Salamonie River at Portland	86.	20	38,85,128	yes	yes
36	Cedar Cr. at Auburn	87.3	12	53,71	no	no
37	Bice Ditch near South Marion	22.6	17	6,31,108	yes	yes

Table 3-1 (continued)

Watershed No.	Watershed Name and Location	Area (sq. mi.)	Number of Storms	Precipitation Stations	Topo-Map	Network
38	Patoka River near Ellsworth	171.0	11	11,20,36,91	yes	no
39	Little Cicero Cr. near Arcadia	44.7	15	65,74,84	yes	yes
40	Carpenter Cr. at Egypt	48.1	29	6,31,108	yes	yes
41	Vernon Fork near Butlerville	87.3	18	2,4,8,51	yes	yes
42	Wildcat Cr. near Jerome	148.	15	64,74	yes	yes
43	Slough Cr. near Collegeville	84.1	12	6,31,108	yes	yes
44	Little Indian Cr. near Royal Center	35.	16	41,126,143	yes	yes
45	East Fork Whitewater River at Richmond	121.	19	66	yes	no
46	Vernon Fork at Vernon	201.	25	2,4,51	no	no
47	Wabash River near New Corydon	262.	20	38,70,85	no	no
48	Youngs Cr. near Edinburg	109.	28	15	yes	yes
49	Singleton Ditch at Schneider	122.	15	45,134	no	no

Table 3-1 (continued)

Watershed No.	Watershed Name and Location	Area (sq. mi.)	Number of Storms	Precipitation Stations	Topo-Map	Network
50	Little River near Huntington	266.	28	12,62,88	yes	yes
51	Eagle Cr. at Zionville	102.	22	26,65	yes	yes
52	Indian Cr. near Corydon	129.	35	9,25,35	yes	yes
53	Mill Cr. near Cataract	241.	32	39,94,98,103	no	no
54	Big Monon Cr. near Francesville	145.	16	6,29	no	no
56	North Fork Salt Cr.	120.	22	2,8,32,90	yes	yes
57	Muscatatuck River near Deputy	296.	17	4,51	no	no

*There is no watershed with no. 25 or no. 55.

or concern given to the process going on inside the box. Other characteristics such as the space coordinates or the positions are not important and all the parts of the system are regarded as being located at a single point in space. Lumped system models do not explain the basic mechanics of flow through the watershed because they are only simulations of the black box as a whole and offer in effect only a mechanical aid to "data fitting".

The second approach is the distributed system. It was cited by Chow [22] that it involves more than one independent variable: the space coordinates, in addition to the usual time variable. Mathematically, therefore, it can be represented by a set of partial differential equations as against an ordinary differential equation for a lumped system.

The work of Sherman [23] was the starting point of the linear lumped systems analysis in hydrology. His basic ideas were the principles of proportionality and superposition. His basic assumptions are listed as follows:

(1) The rainfall is uniformly distributed within its duration or specific period of time.

(2) The rainfall is uniformly distributed over the drainage basin.

(3) The time base of the direct runoff hydrograph due to rainfall of unit duration is a constant.

(4) The coordinates of the direct storm hydrograph of the same base time are proportional to the total amount of direct runoff.

(5) For a given drainage basin, the hydrograph reflects all the combined physical characteristics of the basin.

The T-hour unit hydrograph is the time distribution of the direct runoff from a basin due to one inch of runoff producing rain. In other words, the rainfall excess has an intensity of $1/T_R$ inch per hour for a period of T_R hours.

Chow [15] interprets the instantaneous unit hydrograph as follows: assume the outlet of a basin to be constricted by a dam, and let the watershed be covered by one inch of rainfall excess. If the constriction is suddenly removed, the resulting flow is described as the instantaneous unit hydrograph.

From a system point of view, the unit hydrograph might be interpreted as a response of a system to a unit step function of rainfall excess $x(t) = [u(t) - u(t - T_R)]/T_R$, where $u(t)$ is the unit step function, and T_R is the

duration. If T_R approaches zero, then x(t) becomes a delta function $\delta(t)$ and the unit hydrograph becomes an instantaneous unit hydrograph. The introduction of the instantaneous unit hydrograph is of great value for the development of conceptual models. It also leads to the general linear system analysis in hydrology.

The transform approach was used in the early phase of this research, before the geomorphologic data were collected as this method only needs the rainfall excess and direct runoff to identify the instantaneous unit hydrograph and is not dependent upon any kind of conceptual model. The details of the method have been reported by Blank et al. [24] and by Delleur and Rao [25]. A brief outline of the transform method follows.

The rainfall excess-direct runoff relationship on a watershed are assumed to be expressible by the convolution integral

$$Y(t) = \int_0^t h(\tau)\, x(t-\tau)\, d\tau \qquad (3.2.1)$$

The Fourier transformation pair is defined by the following integrals.

$$f(\omega) = \int_{-\infty}^{\infty} f(t)\, e^{-j\omega t}\, dt \qquad (3.2.2)$$

$$f(t) = \frac{1}{2\pi} \int_{-\infty}^{\infty} f(\omega)\, e^{j\omega t}\, d\omega \qquad (3.2.3)$$

By taking the Fourier transform of both sides of Eq. (3.2.1), it can be shown that the convolution in the time domain is equivalent to the product of the transforms in the frequency domain:

$$Y(\omega) = X(\omega)\, H(\omega) \qquad (3.2.4)$$

$$H(\omega) = \frac{Y(\omega)}{X(\omega)} \qquad (3.2.5)$$

If $H(\omega)$ is known, $h(t)$ can be evaluated by means of the inverse integral, which may be written as

$$h(t) = \frac{1}{2\pi} \int_{-\infty}^{\infty} H(\omega)\, e^{j\omega t}\, d\omega \qquad (3.2.6)$$

The use of the Laplace transform is similar.

The previous methods of system analysis by the Fourier and Laplace transforms were originally developed for continuous input, output and transfer functions. The necessary approximations were developed to extend the use of these methods to the analysis of discrete data as they are usually found in hydrology. The Z-transform was developed specifically for this purpose. The Z-transform pair of a sequence number $X(\Delta t)$, $X(2\Delta t)$, ... , $X(n\Delta t)$ is defined by

$$X(Z) = \sum_{n=0}^{\infty} X(n\Delta t)Z^{-n} \tag{3.2.7}$$

The input and output of Z-transform were $X(Z)$ and $Y(Z)$ respectively. The kernel function $H(Z)$ was expressed as $H(Z) = Y(Z)/X(Z)$ or

$$\begin{aligned} H(Z) &= \frac{Y(\Delta t) + Y(2\Delta t)Z^{-1} + \ldots + Y(n\Delta t)Z^{-n+1}}{X(\Delta t) + X(2\Delta t)Z^{-1} + \ldots + X(m\Delta t)Z^{-m+1}} \\ &= H_1(\Delta t) + H_2(2\Delta t)Z^{-1} + \ldots + H_n(n\Delta t)Z^{-n+1} \\ &\quad + \ldots \end{aligned} \tag{3.2.8}$$

where

$$\begin{aligned} H(n\Delta t) = \frac{1}{X(\Delta t)} [&Y(n\Delta t) - H(\Delta t)\, X(n\Delta t) - H(2\Delta t) \\ &\cdot X(\overline{n-1}\Delta t) - \ldots - H(\overline{n-1}\Delta t)\, X(2\Delta t)] \end{aligned} \tag{3.2.9}$$

The comparison of Laplace, Fourier and Z-transform methods [25] indicated that Z-transform requires the least computer time, but the Fourier transform provides the best insight in the understanding of the methodology. Oscillations of the impulsive response are often observed. Their cause may be due to the computational procedure or to noise in the data. Proper selection of the discretization time interval and the use of digital filters effectively control the instabilities in the kernel function. For details the reader is referred to references [24] and [25].

CHAPTER IV

USING THE W.A.T.E.R. SYSTEM FOR DATA ANALYSIS

4.1 General

Recent developments in quantitative fluvial geomorphology are closely related with the classification of stream network. The study of stream networks requires a considerable amount of data to support its fundamental principles. The availability of the data bank makes such studies possible. Such an improvement leads to a possible way to handle the complex stream network by computer. The data bank also brings the study of hydrology and geomorphology together to investigate the quantitative relationship of watershed hydrologic behavior. The stream network has its own systematic and persistent characteristics. Before studying the hydrologic behavior, an understanding of the geomorphology is useful in the modeling of the hydrologic system for runoff estimation or prediction.

The research on computer applications to geomorphology were reported by earlier workers [18,26,27]. One of the most recent developments is the Water And Terrain Evaluation Research program [18] which was developed as a part of the research program of the Purdue University Water Resources Research Center. This chapter is concerned with the use of the W.A.T.E.R. system using the data bank described in the previous chapter.

The W.A.T.E.R. system has been programmed in FORTRAN IV. The programs have been tested on a CDC 6500 computer at Purdue University and on an IBM 360/65 computer at Toronto University, Toronto, Canada. The programs consist of one main program and a set of subroutines. The system was made to collect all input and output operations in a special routine. The detailed description of this system was reported in Reference [18].

The following sections will discuss the use of these computer programs for the analysis in Indiana small watersheds. Section 2 will discuss the input and the output, Section 3 the stream network classification and basic geomorphologic parameters, Section 4 the results and discussions and Section 5 will be the summary of the geomorphologic application of the data bank.

4.2 Use of the W.A.T.E.R. System

The input data of the W.A.T.E.R. System were divided into two groups. In the first group was the required information to process these data. For instance, the requested options, the name of the watershed, the scale of the coordinate grid and the format of the network data pertain to this group. The second group was called "the network data set" which contained the ordered set of data cards, including the X and Y coordinates. The first group gave the information necessary to the program for analyzing the stream network data set. The basic information which the W.A.T.E.R. system needs is: the type of input data and the types of analysis which are expected to be done. All this information was lumped into the category which was called "option". At present, there are eighteen options; seven "input options" and eleven "output options". The input or output was defined as the option which affects input or output respectively. Besides the types of options, it is also important to know that all options are not of equal importance. Some options are dependent upon others. Therefore, the classification of options was proposed. There were four classes. Class I was the required "option". Class II was the primary choice of inputs and outputs. Class III and IV were dependent on the higher classes. These options are listed in Table 4-I.

The following examples illustrate the typical input data setup and its related outputs for small watershed analysis.

Options	Output Items and Remarks
*WATER	(1)*, (2), (9)
*STRAHLER	(3)
*MAGNITUDE	(6)
*LENGTHS	(4), (7)
*HISTOGRAPH	(5), (8)
*DATA	start of co-ordinate data set
1669 1 9 3	watershed identification
Watershed No. 3	watershed identification
636.6 0.0 0.0 0.0	scale, orientation
3 (10X,3(2F2.0,I2))	data format
(Data)	network data set
*END	end of a basin data
*ENDALL	end of all sets of options and data

The corresponding outputs include:

1) Table showing input data
2) Table showing computed stream reaches Strahler order
3) Strahler stream order statistics
4) Lengths of order segments
5) Histograph of length of each order
6) Stream magnitude statistics
7) Link lengths of different magnitudes
8) Histograph of length of Shreve's magnitude
9) Table of basin statistics

---

*The output list number

Sampling outputs may be seen in Reference [18]. The next section will discuss the river network classification and basin geomorphologic parameters.

4.3 River Network Classification and Basic Geomorphologic Parameters

The study of river network classification has a long history, a detailed description of which may be found in the work of Coffman et al. [18]. In summary there are two kinds of classifications which are widely used. The first is the Strahler ordering system, and the second is Shreve's link-magnitude system. The Strahler ordering assigns the order one to every unbranched finger-tip tributary segment. Two first-order streams unite to form a second order segment. A third order segment is formed by junction of two second-order streams, but may be joined by additional first- or second-order segments. Two third order segments join to form a fourth-order segment, and so on. The general rule may be expressed as:

$$U * U = U + 1 \qquad (4.3.1)$$

where U represents the stream order of any channel segment, and * represents the operation of joining any two segments. If two unequal channels unite to form a segment its assigned order is the same as the larger order of the two upstream segments. Numerous investigators have used this classification to analyze drainage networks and several empirical "laws" have been developed.

On the other hand, Shreve used the probability theory to investigate stream networks. According to Shreve links rather than segments are the

Table 4-1 The Water System Options*

NAME	CLASS	TYPE**	PURPOSE
*IDSW		PRERUN	Identifies data as point data or order-magnitude data
*SCALE		PRERUN	Allows maps to be produced at set scale
*WATER	I	INPUT	Begin new basin, initialize all counters
*DATA	I	INPUT	Start of co-ordinate data set
*END	I	INPUT	End of all options and data for a basin
*ENDALL	I	INPUT	End of all sets of options and data
*HYPSOMETRY	II	INPUT	Elevation data being supplied
*STRAHLER	II	OUTPUT	Classify network into Strahler's orders
*MAGNITUDE	II	OUTPUT	Classify network into Shreve's magnitudes
*ANGLES	II	OUTPUT	Compute junction angle statistics
*JUNCTION	II	OUTPUT	Addition of orders and magnitude for independently analyzed sub-basin
*CONNECT	II	OUTPUT	Simultaneous analysis of multiple interconnected basins
*NETWORKS	III	OUTPUT	Make printer-maps of orders and/or magnitudes. Requires *STRAHLER and/or *MAGNITUDE
*PROFILES	III	OUTPUT	Display longitudinal profiles (max = 11) of main stream and from selected points. Requires *HYPSOMETRY
*AZIMUTHS	III	OUTPUT	List aximuths of ordered segments. Requires *STRAHLER

Table 4-I continued

NAME	CLASS	TYPE**	PURPOSE
*LENGTHS	III	OUTPUT	List lengths of segments by order and/or links by magnitude. Requires *STRAHLER and/or *MAGNITUDE
*FALLS	III	OUTPUT	List falls of segments and/or links. Requires *HYPSOMETRY AND *STRAHLER and/or *MAGNITUDE
*GRADIENTS	III	OUTPUT	List gradients of segments and/or links. Requires *HYPSOMETRY AND *STRAHLER and/or *MAGNITUDE
*HISTOGRAM	IV	OUTPUT	Display histograms of azimuths, lengths, falls, and gradients of segments and/or links. Requires combination of *HYPSOMETRY, *STRAHLER, *MAGNITUDE, and *AZIMUTHS, *LENGTHS, *FALLS, *GRADIENTS
*PUNCH	IV	OUTPUT	Causes lists produced by *AZIMUTHS, *LENGTHS, *FALLS and/or *GRADIENTS options to be punched onto cards and identified by header cards

*From ref. 18

**TYPE indicates purpose of option, PRERUN options are used with program PRERUN only, INPUT and OUTPUT options affect input and output respectively.

basic units of stream networks. He proposed that all exterior links be assigned the magnitude of one. The junction of any two links increases the magnitude of the resulting downstream link by the following formula.

$$M_1 * M_2 = M_1 + M_2 \qquad (4.3.2)$$

Thus the link magnitude increases by adding the magnitudes from two upstream links.

Based on these two systems, numerous drainage basin characteristic parameters were derived. The interrelationships between these parameters and other basin characteristics calculated directly from the stream network data form a structure shown schematically in Figure 4-1. This structure consists of three major parts based on the Strahler stream ordering system, the Shreve link-magnitude system and the direct measurements from drainage basins, respectively. The major function of Strahler's stream ordering system is the assignment of an order to each stream segment. The number of streams of a given order and the distribution of stream lengths among the same order segments were obtained. From the stream length distributions, the means and standard deviations of stream lengths were calculated. At the same time, the total stream length and the main stream length were also obtained. The order of a basin is defined [18] as the order of the largest segment which it contains. The bifurcation ratios defined as the stream number of one order divided by the stream number of the next higher order were calculated. Similarly, the stream length ratios defined as the mean stream length of one order divided by the mean stream length of the next higher order were computed.

The second part of the geomorphologic parameter structure is Shreve's link-magnitude system. It has an analogous description and its basic function is the assignment of a magnitude to each link, based on Shreve's rule. The numbers of links and the distributions of link lengths were obtained. The mean and standard deviation of the link lengths were computed. The total number of links is the sum of all the link numbers of each magnitude. The magnitude of a basin is defined as the magnitude of the largest link which it contains. The probability distribution of the link numbers in each magnitude uses the total link number as the total population.

In the third part the direct measurements from basin maps are used to estimate the geomorphologic parameters. Four important parameters describe the most important characteristics of basins. They are: the drainage area, the basin perimeter, the basin length and the basin slope. Drainage area is given in square miles and is defined as the area within which the rainfall excess drains through the basin mouth. The basin perimeter is the length of the drainage boundary, in miles. The basin length [18] is defined as the maximum straight line distance between a point on the basin perimeter and the stream mouth. The basin slope is defined as the total relief, or the difference between the highest contour and the elevation of the basin mouth, divided by the main stream length.

Secondary basin parameters were derived from the three major parts of the geomorphic parameter structure. They are defined as follows:

(1) the texture ratio: the ratio between the total number of stream and the length of the basin perimeter.

(2) the link-texture ratio: the ratio between the total number of stream links and the length of the basin perimeter.

(3) the fineness ratio: the ratio of total channel length and the length of the basin perimeter.

(4) the drainage density: the ratio of the total length of channels of all orders in a basin to the area of the basin.

(5) the constant of channel maintenance: the ratio between the area of a drainage basin and the total length of all the channels expressed in square feet per foot.

(6) the channel frequency: the number of streams (segments) per unit area in a drainage basin.

(7) the channel link frequency: the number of links per unit area.

(8) the circularity ratio: the ratio of the basin area to the area of a circle having a circumference equal to the perimeter of the basin.

(9) the elongation ratio: the ratio between the diameter of a circle with the same area as the basin and the basin length.

(10) the watershed shape ratio: the ratio of the main stream length to the diameter of a circle having the same area as the watershed.

(11) the unity shape factor: the ratio of the basin length to the square root of the basin area.

All the primary parameters obtained from the three major sources and the secondary parameters were used to quantify the basin characteristics. However, a few remarks are in order. First, it should be recognized that Strahler's ordering system and Shreve's link-magnitude system are not the only two ways of classifying drainage networks. Nevertheless, these two systems are the most frequently used. Secondly, the parameters listed do not include all the possible basin parameters. In particular, the relief was not shown on the planform of the drainage maps and parameters involving the relief are not included. Thirdly, all the geomorphologic parameters are not independent. Numerous studies reported close relationships among these parameters. One of the objectives of this study is the investigation of the inter-relationships of the geomorphic parameters of Indiana small watersheds. The understanding of these basin characteristics is expected to be useful in the study of the hydrologic behavior of the watersheds.

4.4 Analysis of Geomorphologic Data

The following sections contain the results obtained by means of the W.A.T.E.R. system using the data bank for fourteen Indiana watersheds. Table 4-2 shows the locations of watersheds for geomorphic analysis.

4.4.1 Law of Stream Number and Stream Length

Horton [28] proposed that the stream numbers and the stream lengths vary with the stream orders in a geometric progression. Accordingly, the plot of the data on semi-logarithmic paper, should result in an approximately straight line. Shreve [29] studied a law of stream number based on the statistics of a large number of randomly merging stream channels. He demonstrated that in a topological random population, the most probable networks approximately obeyed Horton's Law but that they exhibit certain systematic deviations. Smart [30] clarified Horton's Law and commented that:

> "Any attempt to apply the law in such a strong sense leads to internal inconsistencies. Horton's statement can also be interpreted in a much weaker sense, namely, simply as an approximation that becomes successively better as the order of basin increases."

All of these studies show, as Shreve [29] stated, that "Horton's law indicates the distribution of natural river networks among the possible sets of stream numbers, the most probable networks according to Horton being

Table 4-2 Watersheds for Geomorphologic Analysis

Water-shed No.	Watershed Name	Drainage Area (sq.mi.)	Basin Order	Basin Magnitude	Number of sub-basin
1	Lawrence Cr. at Ft. Benjamin Harrison	2.86	4	97	1
2	Bear Cr. near Trevlac	7.00	5	259	1
3	Bean Blossom Cr. at Bean Blossom	14.6	6	785	1
10	Big Blue River at Carthage	187.	6	3066	1
16	Hinkle Cr. near Cicero	16.3	6	624	1
19	Brush Cr. near Nebraska	11.7	5	894	4
22	Cicero Cr. at Noblesville	219.	6	3066	7
24	Buck Cr. at Muncie	36.7	6	817	5
35	Salamonie River at Portland	86.0	7	2159	8
37	Bice Ditch near South Marion	22.6	5	451	1
39	Little Cicero Cr. near Arcadia	44.7	6	1003	5
42	Wildcat Cr. near Jerome	148.	6	933	4
43	Slough Cr. near Collegeville	84.1	6	490	7
44	Little Indian Cr. near Royal Center	35.0	5	129	1

those with stream numbers close to inverse geometric series."

With these remarks in mind, it was intended to check the validity of Horton's laws for small Indiana watersheds. The stream numbers and the mean stream lengths are plotted versus the stream order for twelve basins as shown in Figure 4-2. The plots approximate a straight line, with the exception of the stream length plots of Bean Blossom Creek (WS3), Little Cicero Creek (WS39), Wildcat Creek (WS42), Slough Creek (WS43) and Little Indian Creek (WS44) which are of the "incomplete" type networks. This may be detected in two ways. First, they contained only two second highest order streams which were just barely enough to make them form the highest order streams. Secondly, their highest order stream lengths are very short. Therefore, they do not obey the geometric progression trend. In general, the law of stream number is obeyed much more strongly than that of stream length.

In Figure 4-2, the average first order stream length ranges from 0.08 to 0.20 miles in Indiana small watersheds. These small values are due to the great detail with which the drainage maps were drawn. The first order stream lengths reported by other researchers [28,31,32] were listed in Table 4-3.

Table 4-3 Comparison of First-Order Stream Lengths

Name	Mean first order stream length (mi.)	Std. Dev. (mi)	Number of basin	Geograph-ical location	Map Sources
Horton (1945)	0.885	0.157	(10)	N.Y.	U.S.G.S. Quad.
Strahler (1952)	0.154	0.0781	(5)	Va, La, Ill, NC.	U.S.G.S. Quad.
Morisawa (1962)	0.073	0.0360	(15)	Ohio, Md, Tenn, Pa, Va, W.Va.	Quad. & Aerial Photo
Lee, M.T. (1972)	0.140	0.0519	(12)	Ind. North and Center	County Drainage maps (aerial photo)

This table shows that there is no standard first-order stream length. It is strongly dependent upon the quality of maps. The study of Morisawa [33]

indicated that data from the U.S.G.S. topographic maps and aerial photographs have significant differences. The comparison of Horton's and Morisawa's data shows the difference between the results obtained using U.S.G.S. quadrangle maps and aerial photographs. If the county drainage maps were considered as standard maps, for taking the mean first order stream length, then the first order stream lengths of the quadrangle maps approximate third or fourth order stream lengths of the county drainage maps. This coincides with the conclusion from a previous study [18].

4.4.2 Bifurcation Ratio and Stream Length Ratio

The bifurcation ratio, R_b, was defined by Melton [34] as the stream number of one order divided by the stream number of the next higher order. It provides some measure of a stream segment's tendency to divide. Eagleson [21] referring to the bifurcation ratio indicates that "Strahler [32] has found R_b to be uncorrelated with relief, and to have a range from 3 to 5, but to be remarkably stable about the average value of 4." Coates [35] measured some basins in southern Indiana and found bifurcation ratios for first order to second order streamsranging from 4.0 to 5.1. Morisawa [31] cited that bifurcation ratios for first-order and second-order streams range from 3.1 to 4.6 in the Eastern United States. Shreve [29] reported that: "For a given number of first-order streams in network, the most probable network is that which makes the geometric mean bifurcation ratio closest to 4." Scheidegger [36] has suggested that "lost" stream segments make it inherently impossible for the bifurcation ratio to remain constant between consecutive orders in a basin.

The bifurcation ratio distributions of these thirteen basins were plotted in Fig. 4-3. They range from 2.8 to 7.0. Streams of ordershigher than four were eliminated, because they might contain "incomplete drainage networks". The average bifurcation ratios of the thirteen watersheds of different order streams were almost constant and equal to about 4.5. This shows that Indiana stream networks have a higher bifurcation ratio than those of a topologically random network. This might indicate that minor geological controls occur in this area.

The mean bifurcation ratio of 13 watersheds and the bifurcation ratios of watersheds 3 and 16 are plotted against stream order in Fig. 4-4a. It

indicates that each basin does not have consistent bifurcation ratios for all stream orders. The general trend indicates that the mean bifurcation ratio decreases as the stream order increases. The standard deviations are seen to increase as the stream order increases. These measurements have the same trend as reported by Smart [30] and Scheidegger [36].

The plot of stream length ratios against stream orders is also shown in Fig. 4-4. Shreve [37] hypothesized, in his study of the "Law of Stream Lengths" that all links have the same length. (The properties of link lengths are shown in Fig. 4-6 in this study.) He concluded that, "the 'Law of Stream Lengths' corresponding to the previous crude 'laws' would state that the average length of stream increases with order as a geometric series with ratio 2." That means the stream length ratio should approximately equal to 2. Fig. 4-4b shows that it is indeed true for the lower order streams. The mean stream length tends to increase slowly as the stream order increases. At the same time, the standard deviation increases as the stream order increases. The data of watersheds no. 16 and no. 3 indicate that the watersheds do not have consistent stream length ratios for different stream orders. Both the bifurcation ratio and the stream length ratio of highest order (i.e. 5-6 order) do not follow the trend, because they contain "incomplete segments".

4.4.3 Number of Link Magnitude

Shreve [37] reported that the discrete probability density function $V(\mu)$ of randomly drawing a link of magnitude μ in an infinite topologically random channel network is:

$$V(\mu) = \frac{2^{-(2\mu-1)}}{2\mu-1} \binom{2\mu-1}{\mu} \qquad (4.4.1)$$

and the probability $\omega(\mu;M)$ of drawing a link of magnitude μ from finite topological random networks magnitude M is:

$$\omega(\mu;M) = \frac{(M-\mu+1)\, N_0(M-\mu+1)\, N_0(\mu)}{(2M-1)\, N_0(M)} \qquad (4.4.2)$$

where

$$N_0(\mu) = \frac{1}{2\mu-1} \binom{2\mu-1}{\mu} \qquad (4.4.3)$$

The numerical tables of $V(\mu)$ and $\omega(\mu;M)$ in Shreve's paper [37] indicate that the differences between the probabilities for infinite and finite topo-

logically random networks were very small when M is larger than 200. The basin magnitudes of small Indiana watersheds as shown in Table 4-2 range from 97 to 3066. The average basin magnitude is 900. There are only two basins having basin magnitudes less than 200. Therefore, $V(\mu)$ was used as a standard to investigate the properties of small Indiana watersheds. Fig. 4-5 shows the function $V(\mu)$ and the observed frequency distribution for six basins. The semi-logarithmic scale was used because the frequency decreases very rapidly as the magnitude increases. The link number probability density distribution function is the discrete function. For the reasons of comparing and easier visualization, the discrete density functions were connected by lines. The streams with magnitudes greater than 10 were neglected, because they represent a very small portion of the total population. Some magnitudes even do not occur for magnitudes larger than 10.

In Fig. 4-5, the departures from the infinite random network have definite patterns. Once the observed frequency is lower than that of the infinite random network, then the consecutive frequencies maintain this trend for a few magnitudes. This is the result of the network joining properties. Magnitude 1 has an almost constant frequency of 50% of total link population. The magnitude 2 is formed only by two links of magnitude 1. Similarly, magnitude 3 is formed by magnitude 1 and 2. Magnitude 4 has two possibilities: either by two links of magnitude 2 or one magnitude 1 and one magnitude 3. By the same token, the higher the order, the more the different combinations. As links of magnitude 1 have a 50% frequency, if links of magnitude 2 have a lower frequency than that of an infinitely random network (this means magnitude 1 has higher probability to join higher magnitudes), then the opportunities to form the magnitude 3 are relatively reduced. Watershed no. 1 is a typical example. This property indicates that the frequency distribution of neighboring magnitudes have close correlations.

The departures from the topologically random network magnitude frequency were not too large for most of the networks. The differences showed the lower magnitudes have lower frequencies than those of random networks. This property causes the bifurcation ratio to increase at low Strahler stream order. This conclusion coincides with the results from bifurcation ratios.

4.4.4 Link Lengths Distribution

There are not many studies on link length distributions. Schumm [38] reported from his measurements in Badlands Basins at Perth Amboy, New Jersey, that the distribution of first order stream lengths, that is, exterior link lengths is log-normal. Smart [39] concluded from a goodness-of-fit test of measurements from maps of basins in Missouri, Virginia, and Arizona that the distribution of link lengths could be exponential as suggested by his computer simulation [40]. Krumbein and Shreve [27] measured 10 basins in Marion County in Eastern Kentucky. They concluded that the exterior links and the interior links must be considered separately. They also suggested a family of gamma distributions.

This study does not intend to find some probability distribution of the link lengths, but intends to find parameters to quantify the basin characteristics. Therefore, means and standard deviations of link lengths were chosen to illustrate these properties. Fig. 4-6 shows that the mean link length varies with the link magnitude. Half standard deviations on the higher and the lower sides are also shown. For most of the basins, the exterior links have larger mean link lengths than the interior links. The means of interior links show a general trend to decrease as the link magnitudes increase in most basins. The standard deviations vary little with the link magnitudes. This information illustrates the conclusion that the mean exterior links are larger than the mean interior links.

4.4.5 Summary Table of Watershed Characteristics

The summary of the watershed characteristics of these fourteen basins is given in Table 4-4. From this table, a few watershed characteristics relationships may be found as follows:

1) Relationship between drainage areas and mean stream lengths:

This is the basic relationship between lengths of basins and basin areas. It is apparent that the geometric similarity of the basin will yield an average relationship between area and length of basin. Each individual case will vary from this mean. The catchment length is usually taken to be the length of the main stream. Gray [41] showed in his report using his data, and those of Taylor and Schwartz [42] that:

$$L_0 = 1.40\ A_0^{0.568} \qquad (4.4.4)$$

where L_0 = main stream length, in miles

A_0 = drainage area, in square miles

The data from the Indiana basins plotted in log-log scales are shown in Fig. 4-7. A straight line may be fitted to the data. A least square fit gave the regression equation:

$$L_0 = 1.64\ A_0^{0.55} \qquad (4.4.5)$$

The regression coefficients have similar values as those reported by Gray [41].

2) Relationship between drainage area and watershed slope:

The drainage areas plotted vs. watershed slopes as shown in Fig. 4-8 exhibit the general trend that smaller watersheds have steeper slopes. This point might be verified by examining the main stream profiles. The stream profiles generally have concave upward tendency. The upper land areas have steeper slopes than the low land areas.

3) Relationship between drainage density and watershed slope:

The plot of drainage density and watershed slope in Fig. 4-9, shows that watersheds with steeper slope have a higher drainage density. It illustrates that the slope is one of the major factors for the land erosion to generate the drainage networks. However, the data show much scatter. The influence of other factors is still an unanswered question.

4) Relationship between drainage density and texture ratio:

Figure 4-10 shows that the drainage density tends to increase as the texture ratio increases, but the scatter is considerable. The drainage density and texture ratio are dominated by the total number of stream segments, because the stream segment length does not vary appreciably in this set of data from Indiana watersheds.

5) Relationship between Elongation Ratio and Drainage Area:

Schumm [38] reported that the elongation ratio tends to increase with increasing catchment area. This means that the larger drainage areas tend to becomenearly circular,and smaller drainage areas have a higher probability to have irregular shapes. However, Fig. 4-11 shows that watersheds under 200 square miles in Indiana have no consistent trend in elongation ratio.

6) Relationship between basin link length and areal factor:

Shreve [37] had reported two important parameters relating the linear and areal dimensions. Let the total stream length, L_T, of channels in a basin of magnitude μ be $L_T = \ell(2\mu-1)$ where ℓ is basin mean link length and $(2\mu-1)$ is the total number of links in a basin. ℓ is a good measurement to relate the linear aspect to the link-magnitude system. Similarly the area A_0 of the basin may be written:

$$A_0 = K\ell^2 (2\mu-1) \tag{4.4.6}$$

where $K\ell$ is the average width which the stream link can cover. Therefore, K is the relative ratio of the average width to basin average link length. Table 4-4 shows the ℓ values of these fourteen basins in Indiana varying from 0.084 to 0.28. The K values range from 0.887 to 1.99. It is important to point out here that the drainage density D_d is defined as:

$$D_d = \frac{T_L}{A_0} = \frac{\ell(2\mu-1)}{K\ell^2(2\mu-1)} = \frac{1}{K\ell} \tag{4.4.7}$$

where T_L is total stream length. It is obvious that drainage density is the combination of these two parameters.

The identification of ℓ and K values can be done as follows. ℓ can be expressed as

$$\ell = \frac{L_T}{T_{MN}} \tag{4.4.8}$$

where L_T is total stream length and T_{MN} is total link number. They can be measured from maps. In general, ℓ does not have a near constant value. The K value can be obtained in two ways. First, it can be obtained from the relationship of basin average link length (ℓ) and drainage density (D_d). Drainage density is expressed as

$$D_d = \frac{1}{K\ell} \quad \text{or} \quad \frac{1}{\ell} = KD_d \tag{4.4.9}$$

A plot of $1/\ell$ versus D_d in Fig. 4-12 shows that there is an approximately straight line for drainage density below 8 miles per square mile. It shows a K value of approximately 5/3. The other way to identify the K value is by introducing the link frequency F_L. By definition, F_L is expressed as:

$$F_L = \frac{T_{MN}}{A_0} = \frac{(2\mu-1)}{A_0} \qquad (4.4.10)$$

where T_{MN} is the total link number, A_0 is drainage area. If link frequency, F_L, is divided by drainage density square (D_d^2), then

$$\frac{F_L}{D_d^2} = \frac{(2\mu-1)}{A_0}\frac{A_0^2}{T_L} = \frac{(2\mu-1)^2}{(2\mu-1)^2}\frac{K\ell^2}{\ell^2} \qquad (4.4.11)$$

Therefore,

$$\frac{F_L}{D_D^2} = K \qquad (4.4.12)$$

The plot of F_L versus D_d^2 will yield the estimated K value which is shown in Fig. 4-13. K value is about 5/3.

It was noted that Strahler's basin order gives a wide range of drainage areas. For instance, sixth order basins range from 18.2 to 205.7 square miles in the data shown in Table 4-4. The Shreve magnitude system gives a better description of the drainage area. The drainage areas were plotted against basin magnitudes for the fourteen watersheds in Fig. 4-14. The drainage density of each basin was labelled on the same plot. It indicates that the relationship between basin magnitude and drainage area varies with the drainage density. For the same basin magnitude, a smaller drainage density yields a larger drainage area. In other words, with the same drainage area, a higher drainage density yields a larger basin magnitude. The precise relationship needs more data to define the regression equation.

4.5 Summary and Conclusions

The study of the watershed characteristics in Indiana leads to the following conclusions:

1) Laws of stream number and stream length, in general, are valid in the Indiana area. However, the presence of "incomplete drainage networks" is one of the key factors for the deviations.
2) The average bifurcation ratio of 12 watersheds for each stream order has a nearly constant value of about 4.5, almost equal to the ideal network value.
3) The mean first order stream length ranges from 0.08 to 0.13 miles.

This is due to the large detail of the county drainage maps compared to U.S.G.S. quadrangle maps. From the stream length point of view, in the U.S.G.S. quadrangle maps, a first order stream is about equivalent to a 3rd or 4th order stream in Indiana County drainage maps.

4) The combination of effects in watershed characteristics is dominated by the drainage area in Indiana. The drainage area has a strong correlation with the stream length, and is inversely related with the watershed slope. Because the drainage density is affected by the slope, the drainage area is indirectly related to the drainage density. And since the texture ratio has the same trend as the drainage density, then the drainage area is indirectly related with the texture ratio. These relationships are only general trends in Indiana. The exact quantitative relationships require more data and further verification.

5) Shreve's link magnitude concept is a newly developed concept. For a large basin, it is known to have a definite relationship with the Strahler ordering system. It has the advantage of detecting the same order basin with different basin characteristics, in particular for higher orders. There are three basic measurements that portray the planform of the basins: The basin magnitude, the basin average link length ℓ and the width covering factor K.

Table 4-4 Watershed Statistics

Item No.	Item	Unit	WS 1	WS 2	WS 3	WS 10	WS 16	WS 19	WS 24
1	Basin order	Dimensionless	4	5	6	6	6	5	6
2	No. of seg.	Dimensionless	115	332	990	4113	815	1119	1091
3	Basin magn.	Dimensionless	97	259	785	3066	624	894	817
4	No. of link	Dimensionless	193	517	1569	6138	1247	1787	1633
5	Length of all channel	miles	16.15	57.03	149.9	809.66	120.6	116.7	192.6
6	Main st. length	miles	2.30	4.17	7.2	29.75	9.8	7.5	12.5
7	Basin perimeter	miles	7.42	11.39	18.7	71.94	19.4	18.27	33.32
8	Basin length	miles	2.170	3.66	5.22	26.39	4.83	6.63	9.72
9	Basin Azimuth	degree	28.34	205.72	212.9	225.23	86.9	231.48	280.2
10	Texture ratio	1/miles	15.49	29.14	52.9	42.62	41.9	61.23	32.73
11	Link ratio	1/miles	25.99	45.38	83.8	85.32	64.2	97.77	49.00
12	area	sq. miles	2.64	5.80	13.4	169.72	18.2	10.31	33.84
13	Drainage dens.	mi/sq. mi.	6.10	9.8	11.8	4.88	6.62	11.31	5.69
14	Const. channel maintenance	sq. ft/ft	865.14	537.8	472.12	1219.47	797.3	466.5	927.9
15	Channel freq.	1/sq. mi.	43.47	57.15	73.86	21.99	44.7	108.5	32.23
16	Link freq.	1/sq. mi.	72.95	88.99	117.06	32.82	68.4	173.3	48.24
17	Area with basin perimeter	sq. mi.	4.38	10.33	27.8	411.92	30.02	26.6	88.37
18	Diameter of circle	mile	1.84	2.72	4.13	14.70	4.81	3.62	6.56
19	Basin circularity	Dimensionless	0.603	0.562	0.48	0.412	0.61	0.38	0.382
20	Elongation ratio	Dimensionless	0.846	0.742	0.79	0.557	0.99	0.54	0.675
21	Watershed shape factor	Dimensionless	1.25	1.53	1.74	2.024	2.04	2.07	1.01
22	Unity shape ratio	Dimensionless	1.334	1.52	1.43	2.026	1.13	2.06	1.67

Table 4-4 continued

Item No.	Item	Unit	WS 1	WS 2	WS 3	WS 10	WS 16	WS 19	WS 24
23	$KS = (15)/(13)^2$	Dimensionless	1.168	0.595	0.530	1.172	1.019	0.848	0.995
24	$K = 2\mu-1/LD$	Dimensionless	1.95	0.925	0.887	1.748	1.561	1.353	1.490
25	$FL/D^2 = K$	Dimensionless	1.96	0.926	0.841	1.751	1.561	1.354	1.489
26	Mean link length	miles	0.0836	0.1103	0.0955	0.1319	0.0967	0.0653	0.1179
27	Relative relief	Feet	120.9	310.0	373.6	240.67	110.0	207.8	45.3
28	Basin slope	ft/mi	52.1	44.7	22.1	8.07	8.01	26.4	7.39

Item No.	Item	Unit	WS 35	WS 37	WS 39	WS 42	WS 43	WS 44	WS 22
1	Basin order	Dimensionless	7	5	6	6	5	6	6
2	No. of seg.	Dimensionless	2820	294	1304	1216	647	167	3928
3	Basin magn. (μ)	Dimensionless	2159	226	1003	933	490	129	3066
4	No. of link	Dimensionless	4282	451	2005	1865	979	257	631
5	Length of all channel	miles	469.00	75.40	195.4	386.0	196.6	72.53	885.722
6	Main st. length	miles	17.0	11.17	15.75	23.0	15.5	10.45	42.0
7	Basin perimeter	miles	40.27	25.31	36.07	68.45	50.42	26.31	68.12
8	Basin length	miles	12.03	7.38	9.68	16.68	11.52	8.82	18.40
9	Basin Azimuth	degree	291.0	3.34	76.51	58.41	273.08	263.94	156.04
10	Texture ratio	1/miles	70.03	11.61	36.07	17.76	12.83	6.35	12.771
11	Link ratio	1/miles	106.33	17.82	55.57	27.24	19.41	9.77	19.304
12	Area	sq. miles	80.55	22.03	42.06	138.2	78.85	33.43	205.738
13	Drainage dens.	mi/sq. mi.	5.82	3.42	4.64	2.79	2.49	2.17	4.305

Table 4-4 continued

Item No.	Item	Unit	WS 35	WS 37	WS 39	WS 42	WS 43	WS 44	WS 22
14	Const. channel maintenance	sq. ft/ft	906.57	1542.4	1136.6	1890.5	2116.9	2433.6	1226.5
15	Channel freq.	1/sq. mi.	35.01	13.34	30.9	8.79	8.20	4.99	19.092
16	Link freq.	1/sq. mi.	53.16	20.47	47.6	13.49	12.41	7.68	29.800
17	Area with basin perimeter	sq. mi.	129.04	50.97	103.6	372.9	202.34	55.06	369.286
18	Diameter of circle	mile	10.12	5.29	7.32	13.2	10.02	6.52	16.185
19	Basin circularity	Dimensionless	0.624	0.432	0.406	0.371	0.389	0.607	.557
20	Elongation ratio	Dimensionless	0.839	0.717	0.755	0.795	0.870	0.739	.879
21	Watershed shape factor	Dimensionless	1.68	2.11	2.15	1.74	1.55	1.60	2.593
22	Unity shape ratio	Dimensionless	1.343	1.57	1.493	1.42	1.29	1.52	1.283
23	$KS = (15)/(13)^2$	Dimensionless	1.033	1.14	1.43	1.12	1.32	1.05	1.030
24	$K = 2\mu\text{-}1/LD_d$	Dimensionless	1.581	1.748	2.211	1.732	1.999	1.632	1.608
25	$FL/D^2 = K$	Dimensionless	1.569	1.750	2.210	1.733	2.001	1.631	1.608
26	Mean link length	miles	0.1095	0.1671	0.0976	0.2069	0.2008	0.2822	0.140
27	Relative relief	Feet	182.4	81.7	110.0	80.0	95.3	77.3	200.
28	Basin slope	ft/mi	10.73	7.31	6.98	3.47	6.10	7.39	4.762

CHAPTER V

FORMULATION OF THE HYDROLOGIC MODEL

5.1 The Natural Watershed as a System

As defined by the Indiana Flood Control and Water Resources Act of 1959, a watershed is an area from which water drains to a common point [43]. From a system point of view a watershed is defined as an open physical system. Matter is imported into and exported out of this system. The outlet of this system is the gaging station which is used in this report for watershed identification purposes. The import matter (or the input function) is the rainfall and the export matter (or the output function) is the runoff. Fig. 5-1 shows a simplified natural watershed system.

The area of a watershed usually is determined from topographic maps and this definition is used in this study. The drainage area can also be obtained from detailed drainage maps. These two methods of determining watershed area do not necessarily yield the same results, nevertheless, the discrepancy is generally small. The lineswhich divide surface water and the groundwater basins do not necessarily coincide. Only the surface water basin is considered in this study as it addresses itself primarily to the modeling of direct runoff. All the characteristics within the watershed boundary form the system basic properties. As far as the hydrograph is concerned, these properties have the function of attentuating and translating the rainfall input and yield the runoff output.

The runoff time series (output function) in this system generally is divided into two portions: the direct runoff and the base flow. As the experience of a previous study [44] indicated, the base flow portion of the runoff hydrograph does not vary significantly with the several methods of base flow separation and that the base flow is only a small portion of the total hydrograph. Table 5-1 shows the mean and the standard deviation of the ratio of the average base flow to the peak runoff for several storms in six watersheds. It confirms that the average base flow is generally a small but not negligible percentage of the peak flow in single storm events. In view of the importance of the direct runoff this study concentrates on the modeling of the two principal parts of the rainfall-runoff process.

Table 5-1 Comparison of Peak and Base Flows Testing Data Set

Watershed No.	Watershed Name	Drainage Area (sq.mi.)	Main Stream Length (mi)	No. of Storms	Avg. Base Flow / Peak of Runoff Hydrograph (%)	
					mean	st.dev
1	Lawrence Cr. at Ft. Benjamin Harrison	2.86	2.3	13	0.95	.609
2	Bear Cr. near Trevlac	7.00	4.17	15	6.39	6.61
3	Bean Blossom Cr. at Bean Blossom	14.6	7.2	16	2.37	2.068
10	Big Blue River at Carthage	187.	29.75	24	11.2	7.31
16	Hinkle Cr. near Cicero	16.3	9.8	10	3.85	2.32
19	Brush Cr. near Nebraska	11.7	7.5	24	2.01	2.51

First is the determination of the contributing rainfall volume in both space and time. The second portion is the routing of these rainfall excesses to the direct runoff. Before modeling the rainfall-runoff process, the simplifying of watershed geometry is necessary to lead to a practical solution.

5.2 Areal Distribution Along Stream Reach

The geometry of a watershed is three dimensional. It is impractical to discretize and to tabulate the coordinates of this three dimensional geometry even with the aid of a large memory and high speed computer because of the vast amount of data required. Therefore, some idealization or simplification of the physical system which constitutes the watershed must be sought, keeping in mind that this simplified watershed geometry is for the estimation of runoff hydrographs. This estimation includes the identification of the portion of the rainfall which becomes runoff and the routing of these rainfall excesses from the different parts of the watershed through the stream network to the watershed outlet.

Hydrologists define isochrone line as the locus of the points in the watershed for which the runoff travel time to the outlet is a constant. Surkan [45] utilized the channel network to synthesize hydrographs. He assumes that the velocity of flow along the network is effectively uniform. Chorley [46] cites that the downstream channel slope of most rivers tends to decrease from the source to the mouth, giving to the longitudinal profile a concave-upward form. Nevertheless, the downstream channel has a higher hydraulic efficiency. Leopold's study [47] in the midwest U.S. of the combined effects of the relief distribution and of the runoff characteristics indicates there is no definite tendency for the velocity to have a great change along the length of the stream system. It has been observed in this study of Indiana watersheds that the stream links which have the same travel distances in the same basin are subject to similar relief and hydraulic constraints. Based on these two observations, the simplifying assumption will be made that locations having equal distances measured along the stream network to the outlet, have the same runoff travel time to the outlet. This makes it possible to simplify the two-dimensional planform of the drainage network to a one-dimensional representation.

The observation of Indiana drainage networks further showed that the streams were approximately uniformly distributed over the watersheds.

Table 5-2 shows as an example the drainage density of each sub-basin of the Big Blue River at Carthage, Indiana (watershed no. 10) and of each sub-basin of the Salamonie River at Portland, Indiana (watershed no. 35). Watersheds 10 and 35 have an average drainage density of 4.876 and 5.822 miles per square mile respectively and standard deviations of 0.950 and 1.249 respectively. These data confirm that the drainage density is approximately uniform within each watershed. Therefore, the assumption was made that the total stream length upstream of a particular point on a stream is proportional to the tributary drainage area at that point.

Based on the two simplifying assumptions that locations having equal distances along the stream network to the outlet have the same runoff travel time and that the total stream length upstream of a point on a stream is proportional to the tributary drainage area at that particular point, it is now possible to estimate the distribution of travel time along the stream reaches. The distribution of the travel time is thus proportional to the distribution of the drainage area along the watershed reaches, and only the latter needs to be considered.

The method of estimating the distribution of tributary drainage areas along the stream reaches is illustrated in Fig. 5-2. The upper part of the figure shows an idealized stream network. The central portion of the figure shows the distribution of the number of stream links along the main stream. The area under this line is the total stream length of the watershed. The longest stream reach is the main stream length. Dividing the ordinates of the stream link distribution by the drainage density, or stream link length per unit area, the distribution of drainage area along the stream reaches is obtained as shown in the lower part of Fig. 5-2. The area under the drainage area distribution must be equal to the watershed area. Within a constant the latter diagram is also a time-area diagram. Fig. 5-3 shows, as an example, a) the CALCOMP plot of the discretized stream network of Bean Blossom Creek (watershed no. 3), b) the distribution of the number of stream links and c) the distribution of drainage areas along the stream reaches. The following sections discuss the physical response of a watershed.

Table 5-2 Drainage Density and Source Distribution of Sub-basins of the Big Blue River at Carthage, Indiana (watershed no. 10) and of the Salamonie River at Portland, Indiana (watershed no. 35)

Sub-basin No.	Sub-basin Area (SQ.MI)	Total Stream Length in Sub-basin (MI)	Drainage Density (MI/SQ.MI)	Number of Stream Source or 1st order Stream	Source / Area (1/SQ.MI)	Source / Stream Length (1/MI)
10-1	24.85	100.056	4.026	353	14.203	3.528
10-2	28.07	136.584	4.864	471	16.779	3.448
10-3	33.56	163.133	4.861	570	16.984	3.494
10-4	20.90	117.820	5.636	481	23.014	4.082
10-5	17.46	75.948	4.349	280	16.037	3.687
10-6	21.47	140.850	6.558	519	28.830	4.395
10-7	6.77	37.654	5.561	136	20.090	3.612
10-8	16.65	55.635	3.342	163	9.793	2.929
	Σ=169.73	Σ=827.680	AVG.=4.876	Σ=3073	AVG.=18.105	AVG.=3.713
			ST.DEV.=0.950		ST.DEV.= 5.415	ST.DEV.=0.410
35-1	7.64	47.095	6.167	214	28.025	4.544
35-2	5.78	46.204	7.996	237	41.017	5.129
35-3	10.97	65.268	5.948	313	28.529	4.795
35-4	4.99	36.194	7.249	174	34.856	4.807
35-5	7.37	54.420	4.387	258	35.026	4.741
35-6	19.63	76.010	3.872	285	14.520	3.740
35-7	12.16	81.819	6.728	398	32.732	4.860
35-8	12.02	61.990	5.156	266	22.129	4.290
	Σ= 80.56	Σ=469.000	AVG.=5.822	Σ=2145	AVG.=26.626	AVG.=4.574
			ST.DEV.=1.249		ST.DEV.= 7.779	ST.DEV.=0.401

5.3 Fixed Response Area and Varied Response Area

In the last decade, hydrologists [3, 4, 5, 6] have found more evidences that the traditional methods of separation of the rainfall excess have their weaknesses. As a result a number of hydrologists [4,6,8,9] have proposed a spatial variation, or a space-time variation of rainfall excess rather than a time separation of the rainfall time series.

The traditional method of rainfall excess separation is based on the relationship

$$X_R(t) = \frac{d}{dt} P_0(t) - \frac{d}{dt} G(t) \qquad (5.3.1)$$

where $P_0(t)$ is the total precipitation distribution, and

$G(t)$ is the loss function, including interception, evapotranspiration, depression and detention storages and infiltration,

$X_R(t)$ is the excess precipitation time distribution.

As $G(t)$ is unknown, various empirical methods are used to obtain the excess precipitation. A summary of these methods can be found in Van De Leur [1].

One of the most common approaches is that of the infiltration capacity which was proposed by Horton [2]. It was defined as the maximum rate at which a given soil in a given condition can absorb water. It was expressed as:

$$f = f_c + (f_o - f_c)e^{-kt} \qquad (5.3.2)$$

where f_c = infiltration rate which represents the fairly steady rate of water absorption reached after water has been applied continuously for a long period of time.

e = base of natural logarithms

f_o = the initial infiltration rate at $t = 0$, and

k = parameter

After the infiltration rate is determined, the rainfall excess $X(t)$ can be obtained by subtracting the infiltration rate from the rainfall hyetograph.

The boundary condition associated with the differential equation (5.3.1) may be expressed in terms of the response area, A_0, taken as the watershed area:

$$\int_{t_s}^{t_f} Q(t)dt = \int_{t_s}^{t_f} A_0 \cdot X_R(t)dt \qquad (5.3.3)$$

or discrete form

$$\sum_{i=o}^{T} Q(i\Delta t)\Delta t = \sum_{i=o}^{T} A_0 \cdot X_R(i\Delta t)\Delta t \qquad (5.3.4)$$

where t_s is the starting time of the rainfall,
t_f is the time at the end of the storm event,
$Q(t)$ is the time series of direct runoff,
$X_R(t)$ is the time series of rainfall excess,
A_0 is the response area, and
T is the total number of sampling points of the direct runoff.

In the traditional method of rainfall excess separation the response area A_0 is considered to be fixed and equal to total drainage area. This assumption is generally used for lumped linear systems analysis which excludes the spatial variation of the input function. The input function is then lumped as $I(t) = A_0 \cdot X_R(t)$. The effects of the response area concept was absorbed and mixed with the rainfall excess separation procedure which forces the total volume of rainfall excess to be equal to the total volume of direct runoff.

If a distributed system is considered, it is necessary to know the time and space distribution of the input. Thus, it becomes necessary to know the time and space distribution of the response area (which is the area on which rainfall excess occurs) and which may include only part of the drainage area. The time and space distribution of the response area affects the rainfall excess routing into the direct runoff at the basin outlet.

Freeze [12,14] made a theoretical analysis of the runoff process by using three runoff mechanisms. They were: (1) overland flow due to surface saturation from above, (2) subsurface stormflow, (3) overland flow from near-channel partial areas due to surface saturation from below. He concluded that on concave slopes with lower permeabilities, and on all convex slopes, hydrographs are dominated by direct runoff with a very short overland flow path from precipitation on transient, near-channel wetlands. He also cited that the classic Horton type of overland flow is a rare occur-

rence in time and space. His simulation confirmed that the varying response area in a basin is the basic runoff generating mechanism in the rainfall-runoff process.

The TVA [3] made an experiment at Bradshaw Creek and Elk River, Tennessee. It was concluded that a new concept of a dynamic watershed was needed to simulate the field condition. It was cited that the watershed is dynamic in the sense that when rainfall starts after a dry period, this dynamic watershed is very small; only the bottom lands and stream channels contribute runoff. But as rain continues and the slope gets wet, the watershed expands and more area contributes runoff. The difference between the new concept and the classical Horton method is illustrated in Figure 5-4. The upper portion of Figure 5-4 shows the Horton approach. The response area is fixed and the key problem is to estimate the rainfall excess, $X_R(t)$. On the other hand, the lower portion of Figure 5-4 shows the dynamic watershed. The major problem is to estimate the response area $a(L,t)$. Then this dynamic area times the rainfall time series in excess of "B" horizon permeability was utilized as input for channel routing process.

These field experiments and theoretical simulations illustrate that the stream runoff originates from a rather fixed, consistent portion of the watershed along the stream channels [11]. However, the application of the coupling of the channel flow and saturated-unsaturated subsurface flow on the entire watershed is laborious and impractical in engineering design. In fact, it is beyond the capabilities of the present generation of digital computers [12] without considering the problems associated with the necessary data acquisition. A simplified version of the dynamic source area model is urgently needed for practical engineering application.

For the simplified watershed idealized in the previous section, with its one dimensional distribution of the drainage area along the main stream, equation (5.3.3) may be modified as:

$$\int_{t_s}^{t_f} Q(t)dt = \int_{t_s}^{t_f} \int_{o}^{L_0} a(L,t)R_B(t)dL\,dt \qquad (5.3.5)$$

where L_0 is the main stream length and $a(L,t)$ is the variable response area at stream reach L and at time t. In discrete form Eq. (5.3.5) may be rewritten as

$$\sum_{i=o}^{T} Q(i\Delta t) = \sum_{i=o}^{T} \sum_{j=o}^{S} a(j\Delta L, i\Delta t) R_B(i\Delta t) \Delta L \, \Delta t, \qquad (5.3.6)$$

where T is total number of sampling points in the runoff time series, and
S is total number of stream reach sampling points in the idealized one dimensional watershed,
ΔL is the stream link length,
$a(j\Delta L, i\Delta t)$ is the variable response area at stream reach $j\Delta L$ and at time $i\Delta t$,
i is the running index for counting the time intervals and
j is the running index for counting the number of links.

The concept of a dynamic response area of a watershed, $A(i\Delta t)$, was reported by TVA et al. [48] and the following conceptual model was proposed to simulate the dynamic hydrological behavior of watersheds, in discrete form:

$$A(i\Delta t) = \alpha + \beta[S_{RF}(i\Delta t)]^{\gamma} \qquad (5.3.7)$$

where $A(i\Delta t)$ is the response area of a basin at time $i\Delta t$, and α, β, γ are the parameters and $S_{RF}(i\Delta t)$ is the accumulated rainfall in excess of the "B" horizon infiltration given by

$$S_{RF}(i\Delta t) = \left[\sum_{k=o}^{i-1} R(k\Delta t) \right] + R(i\Delta t) - B \qquad (5.3.8)$$

where B = "B" horizon permeability
$R(k\Delta t)$ = rainfall at time $k\Delta t$
i,k = the running indexes to count the time sampling points, $o \leq k < i$

Eq. (5.3.7) expresses the response area as a function of the accumulated rainfall over time in a storm event. This accumulated rainfall, however, includes only that volume of rainfall for each time increment that is in excess of the "B" horizon permeability. The study of Ragan [5] suggested that the contributing area was a function of the storm duration and intensity. TVA [13] made a diagrammatic sketch as shown in Fig. 5-5 in which a watershed responds to rainfall under the dynamic watershed concept. At the beginning of a storm the runoff producing area is relatively small and

is located near the low wet land. As a storm progresses the contributing area generally increases, although the rate of increase or decrease is a function of the intensity of storm rainfall. Hewlett and Nutter [6], Nutter and Hewlett [10] have depicted the expansion of the source area and the channel system during a storm, as shown in Fig. 5-6. Dunne and Black [8] reported that the area contributing to overland flow is dynamic in the sense that it may vary seasonally or throughout a storm. The fluctuation of this partial area can be rationally related to topography, soils, antecedent moisture, and rainfall characteristics.

Based on these preceding reviews, the following two modified models are proposed. In discrete form, the first model is expressed as:

$$A(i\Delta t) = A_0 \left[\frac{D \sum_{k=o}^{i-1} [R(k\Delta t) - B]\Delta t + [R(i\Delta t) - B]\Delta t}{\sum_{k=o}^{T} [R(k\Delta t) - B]\Delta t} \right]^N \qquad (5.3.9)$$

where $A(i\Delta t)$ = the contributing (response) area at time $i\Delta t$

A_0 = total drainage area

$R(k\Delta t)$ = the rainfall intensity at time $k\Delta t$

B = "B" horizon permeability

D = fraction of the antecedent rainfall contributing to the response area

N = parameter

T = the total number of sampling points of runoff hydrograph

k = index to count time of antecedent rainfall excess, $k < i$

i = index indicating current time

In the second model it is assumed that the fraction of the antecedent rainfall excess contributing to the response area decreases exponentially with the elapsed time. The model in discrete form is expressed as:

$$A(i\Delta t) = A_0 \left[\frac{\sum_{k=o}^{i-1} D^{(i-k)} [R(k\Delta t) - B]\Delta t + [R(i\Delta t) - B]\Delta t}{\sum_{k=o}^{T} [R(k\Delta t) - B]\Delta t} \right]^N \qquad (5.3.10)$$

As the volume of rainfall excess should be equal to that of the direct runoff, the following continuity equation may be written:

$$\sum_{I=o}^{T} A(I\Delta t)\,[R(I\Delta t) - B] = \sum_{I=o}^{T} Q(I\Delta t) \qquad (5.3.11)$$

where $Q(I\Delta t)$ = the direct runoff at time $I\Delta t$. By using the continuity equation one of the unknown parameters B, D, or N can be eliminated. In this study, D was considered as model parameter and N was determined to satisfy the continuity equation at the end of the storm events, B was estimated from the soils map. The estimation of B and D will be discussed in the next chapter.

Further investigation is needed in connection with the response area for the one-dimensional simplified areal distribution. The study of the Tennessee Valley Authority [3] cited that the lower portions of the watersheds would have higher soil moisture levels. These lower portions could be expected to produce runoff early in the storm period, while the initial losses were still being satisfied on the slopes and on the ridges.

The observation of drainage maps of Indiana small watersheds, for example Fig. 5-3 of Bean Blossom Creek (watershed no. 3), indicated that stream sources (first order streams) are approximately uniformly distributed over the basin. Table 5-2 shows the quantitative description of the source distribution in the Big Blue River watershed (no. 10) and in the Salamonie River watershed (no. 35). The average numbers of sources (first order streams) per unit area are 3073 ÷ 169.73 = 18.105 and 2145 ÷ 80.56 = 26.626 sources per square mile respectively. Their standard deviations are 5.42 and 7.78 sources per square mile.

Another method of investigating the sources distribution is by calculating the number of sources per unit stream length in each sub-basin. It was found that the mean numbers of sources per unit stream length for watersheds 10 and 35 are 3073 ÷ 827.68 = 3.713 and 2145 ÷ 469 = 4.574 sources per mile respectively. The corresponding standard deviations are 0.41 and 0.40 sources per mile. For the reason of comparison in the same unit, the standard deviations of the latter method are multiplied by drainage density. They yield 1.9991 and 2.352 sources per square mile which are smaller than the standard deviations for the previous method. The latter method is more logical for the present study because it ties with the previous distribution of tributary

area along the stream reaches.

The analysis of stream classification (Chapter IV) indicated that the number of the streams varies with stream orders approximately in an inverse geometric progression (law of stream number of Horton's law). This taxonomic hierarchy utilizes stream sources as the basis and emerges into higher order streams. The uniform distribution of stream sources ensures the uniform scatter of the successively higher order segments along the main stream. The expansion of the source area and the channel system suggested by Nutter and Hewlett [10] (Fig. 5-6) starts from the higher order streams in the early stage of a storm and gradually extends to lower order streams. Because of these response characteristics, the stream sources are considered as the late response portion of the basin and at an early stage of the storm, the stream sources are considered as nonresponse areas. The uniform distribution of the stream sources reduces uniformly the ratio of drainage area to the response area along the stream reach. Therefore, it is further assumed that the ratio of the response area of a stream reach interval to the drainage area at a stream reach interval is equal to the ratio of the response area of the whole basin to the total watershed area. This is expressed as:

$$\frac{a(j\Delta L, i\Delta t)}{a_0(j\Delta L)} = \frac{A(i\Delta t)}{A_0} \quad \text{or} \quad a(j\Delta L, i\Delta t) = \frac{A(i\Delta t)}{A_0}\, a_0(j\Delta L) \qquad (5.3.12)$$

where A_0 is the total drainage area.

$A(i\Delta t)$ is the dynamic response area of whole basin.

$a_0(j\Delta L)$ is the drainage area per unit reach at stream reach $s = j\Delta L$, and

$a(j\Delta L, i\Delta t)$ is the response area of stream reach $j\Delta L$ at time $i\Delta t$.

Substituting (5.3.12) into (5.3.6), it yields

$$\sum_{i=o}^{T} Q(i\Delta t)\Delta t = \sum_{i=o}^{T} \sum_{j=o}^{S} \frac{a_0(j\Delta L)A(i\Delta t)}{A_0} R_B(i\Delta t)\Delta L\, \Delta t \qquad (5.3.13)$$

This is the continuity equation applied to the distributed varied response model.

In summary, the study of the stream networks lead to the following simplifying assumptions used in the formulation of the partial area concept:

1) The locations having equal distance along the stream network to the outlet have the same runoff travel time, i.e. the velocity of flow along stream network is uniform.

2) The total stream length upstream of a point on a stream network is proportional to the tributary drainage area at that particular point, i.e., the drainage density is a constant within a watershed.
3) At any given time, the ratio of the response area to the drainage area at a stream reach interval is equal to the ratio of the response area of the whole basin to the total watershed area. This implies that the late response areas, i.e. stream sources (first order streams) are uniformly distributed along the stream reaches.

After the response areas are determined, the rainfall excesses from these areas are routed through the stream network to obtain the direct runoffs at the outlet of the basin.

5.4 Flood Routing Technique

The dynamic and kinematic approaches have been used in solving a single stream reach problem, but are laborious to apply to the stream network of a watershed. The diffusion analogy is a simplified version of a linear complete solution. It was shown [17] to give a better simulation of the flood wave propagation than the two parameters model such as the Muskingum method [49], the lag and Route method [50] and the diffusion analogy [51] or other three-parameter models such as the lagged diffusion method [16], three parameter gamma method [50] and multiple reach Muskingum method [52]. It is noted that most of the models which were compared with the complete linear routing method were derived from the simple storage concept. Harley showed that the models which are based on the unsteady flow equation give better perspective simulation than those based on the simple storage concept. It is observed that the parameters in the complete linear routing method represent some of the physical characteristics of the drainage basin such as the slope of the stream reaches, and the coefficients of certain physical formulas such as the Chezy constant and the reference discharge. These parameters have their measured values for comparison purpose in the identification stage. Therefore, the linearized complete solution was pursued further and employed to route the rainfall excess to direct runoff.

Following Harley for the purpose of hydrograph prediction it is desirable to rewrite the St. Venant equations:

$$\frac{\partial q}{\partial x} + \frac{\partial y}{\partial t} = q_L$$

$$\frac{\partial y}{\partial x} + \frac{u}{g}\frac{\partial u}{\partial x} + \frac{1}{g}\frac{\partial u}{\partial t} = S_0 - S_f + \frac{u}{g} q_L$$

in terms of q and y. They are expressed as:

$$\frac{\partial q}{\partial x} + \frac{\partial y}{\partial t} = q_L \qquad (5.4.1)$$

$$(qy^3 - q^2)\frac{\partial y}{\partial x} + 2qy\frac{\partial q}{\partial x} + y^2\frac{\partial q}{\partial t} = gy^3 S_0 - gq^2/C_z^2 \qquad (5.4.2)$$

where $S_f = \frac{q^2}{C_z^2 y^3}$, $q = yu$ and C_z is a roughness coefficient.

It is assumed furthermore that a perturbation occurs about some reference discharge q_o and reference depth y_o. Thus

$$q = q_o + q' \qquad (5.4.3)$$

$$y = y_o + y' \qquad (5.4.4)$$

where q' = deviation from the reference discharge

y' = deviation from the reference depth

A linearized partial differential equation is obtained by substituting Eq. (5.4.3) and Eq. (5.4.4) into Eq. (5.4.1) and (5.4.2) and neglecting the second order differential terms based on the assumption that the perturbations are small. It is expressed as:

$$(qy_0^3 - q_0^2)\frac{\partial^2 q}{\partial x^2} - 2q_0 y_0 \frac{\partial^2 q}{\partial x \partial t} - y_0^2 \frac{\partial^2 q}{\partial t^2} - 3qS_0 y_0^2 \frac{\partial q}{\partial x} - 2qy_0^3 \frac{S_0}{q_0}\frac{\partial q}{\partial t} =$$

$$= (gy_0^3 - q_0^2)\frac{\partial}{\partial x}(q_L(x,t)) - 3gS_0 y_0^2 q_L(x,L) \qquad (5.4.5)$$

Consider first the case of an upstream inflow instantaneous unit hydrograph without lateral inflow. The imposed boundary conditions are:

$$q(o,t) = \delta(t) \qquad (5.4.6)$$

$$q(x,o) = 0 \qquad (5.4.7)$$

$$q_L(x,t) = 0 \qquad (5.4.8)$$

The impulsive response of this system was derived by Harley [16]. It is expressed as:

$$H_u(x,t) = \delta(t - \frac{x}{c_1}) \exp(-px)$$

$$+ h(\frac{x}{c_1} - \frac{x}{c_2}) \exp(-rt + sx) \frac{I_1[\sqrt{2h(t - \frac{x}{c_1})(t - \frac{x}{c_2})}]}{\sqrt{(t - \frac{x}{c_1})(t - \frac{x}{c_2})}} \quad (5.4.9)$$

where $u_o = C_z\sqrt{y_o S_o}$ $\qquad p = \frac{S_o}{2y_o} \frac{2-F}{F(1+F)}$

$F = \frac{u_o}{\sqrt{gy_o}}$ $\qquad r = \frac{S_o u_o}{2y_o} \frac{2+F^2}{F^2}$

$c_1 = u_o + \sqrt{gy_o}$ $\qquad S = \frac{S_o}{2y_o}$

$c_2 = u_o - \sqrt{gy_o}$ $\qquad h = \frac{S_o u_o}{2y_o} \frac{\sqrt{(4-F^2)(1-F^2)}}{2F^2}$

$I_1[\cdot]$ = first order modified Bessel function of the first kind

where u_o, q_o, and y_o are the reference steady state conditions. This impulse response consists of two portions. The first term including the delta function represents the head of the wave. As a matter of fact, it can be stated to represent the propagation of a decaying delta function at the wave celerity along the forward characteristics. The second term represents the main body of the wave which is traveling at a slower rate and which can be shown to be $3/2u_o$ on the average, a propagation velocity often referred to as Seddon's Law [53].

The response $H_u(x,t; S_o, q_o, C_z)$ is a three-parameter model of the flood wave propagation. Harley calls it the Linear Channel Routing (LCR) method.

The Upstream Inflow Instantaneous Unit Hydrograph $H_u(x,t)$ (in abbreviation as UIIUH) has the function of translating and attenuating the rainfall excess. The storage and decay effects are quantified by parameters q_o, C_z, and S_o. Fig. 5-7 illustrates the physical expression of the upstream inflow instantaneous unit hydrograph. In the upper portion of the Figure 5-7, a stream reach with distance L is considered. If a delta function, $\delta(t)$, is applied at time $t = 0$ at the upstream end, the response at the downstream end can be expressed by $H_u(L,t)$ as shown at Fig. 5-7(c). In other words,

this stream segment can be considered as a linear system as shown in Fig. 5-7(b). The upstream inflow, $q(o,t) = x(o,t)$ is the input into the system and the output at the downstream end is the routed outflow $q(L,t) = Y(L,t)$ as shown in Fig. 5-7(e). The response at the downstream end may be obtained by the standard techniques of linear system analysis, namely by performing the convolution operation as shown in Fig. 5-7(e). The mathematical expression is given as:

$$Y(L,t) = \int_o^t H_u(L,t-\tau)X(o,\tau) \qquad (5.4.10)$$

where $Y(L,t)$ is the runoff contribution at stream reach L due to the input $X(o,t)$. In discrete form, it is expressed, for a reach of the simplified watershed model described in section 5-2, as:

$$Y(j\Delta L,i\Delta t) = \sum_{k=o}^{i} H_u(j\Delta L,(i-k)\Delta t)X(j\Delta L,k\Delta t)\Delta t \qquad (5.4.11)$$

where $X(j\Delta L,k\Delta t) = a(j\Delta L,k\Delta t)\ R_B(k\Delta t)$

where $a(j\Delta L,i\Delta t)$ = the response area of the simplified watershed at time $i\Delta t$ and at stream reach $j\Delta L$

$R_B(i\Delta t)$ = the rainfall at time $i\Delta t$ in excess of the B horizon permeability

i = the running index for time

j = the running index for stream reach

For whole stream network represented by the simplified watershed model, the calculated direct runoff is then given by:

$$Q_c(t) = \int_o^{L_o} Y(\ell,t)d\ell$$

or

$$Q_c(t) = \int_o^{L_o}\int_o^t H_u(\ell,t-\tau)a(\ell,\tau)R_B(\tau)d\tau d\ell \qquad (5.4.12)$$

In discrete form, it is expressed as:

$$Q_c(i\Delta t) = \sum_{j=0}^{s}\sum_{k=0}^{i} H_u(j\Delta L,(i-k)\Delta t)a(j\Delta L,k\Delta t)\cdot R_B(k\Delta t)\cdot \Delta t\Delta L \qquad (5.4.13)$$

where s = the total number of sampling points in the idealized network

i = the index for present time

k = the running index for time array

j = the running index for one-dimensional watershed area distribution

In summary, Eq. (5.3.13) of the previous section is used to identify the portion of rainfall which becomes direct runoff. Eq. (5.4.13) has the function of translating and attenuating the rainfall excess into direct runoff based on the watershed characteristics.

The formulation of model elements in previous sections is the preparation for an integrated system. The complete description of the proposed system is discussed in the following sections.

5.5 Formulation of the Model

The decomposition of the hydrograph and the utilization of the geomorphologic characteristics in the hydrograph model lead to the integrated system shown in Fig. 5-8. It illustrates the total system in the identification mode. The prediction mode is shown inside the dotted line box of Fig. 5-8. The input information in this model is as follows:

(1) The rainfall time series, R(t)

(2) The soils map (to estimate the parameters B and D)

(3) The response area parameters, N

(4) The map of the drainage network of the basin

(5) The topographic map of the watershed (to estimate S_o)

(6) The routing parameters q_o and C_z (reference discharge and roughness)

In the identification stage the direct runoff time series is also needed, and only the parameters B, D, q_o and C_z are necessary. The rainfall time series is used to develop the contributing (response) area which requires the previous rainfall weighted by a factor D and the B horizon permeability. The parameter N in the identification stage is determined by satisfying the conservation of mass between the effective rainfall and direct runoff.

The output of block (1) in Fig. 5-8 is the response area time series, A(t). Using the simplified watershed area distribution along the main stream reaches $a_o(L)$, and the response area A(t), the contributing area, a(L,t), for the stream reach L is determined as shown in the output of block (2). The

rainfall imposed on the response area a(L,t) is considered as the input to block (3). The output of block (3) is the rainfall excess time distribution, X(t,L), produced at stream reach L. The watershed mean slope and the two linear routing parameters q_o and C_z, are used to form the upstream inflow instantaneous unit hydrograph as shown in block (4). Considering the runoff producing rainfall as the input, and the supstream inflow instantaneous unit hydrograph as the transfer function the convolution operation shown in block (5) is performed to calculate the runoff, Y(L,t), contributed by stream reach L. This operation is repeated for all the stream reach intervals of the simplified watershed. The block (6) shows the accumulation of the runoffs from all the stream reaches up to the main stream total length L_o.

For the runoff estimation, the parameters B, D, q_o, and C_z are estimated from the watershed characteristics and the rainfall pattern. The output of block (6) is the calculated direct runoff hydrograph, Q(t). In the identification stage, the parameters B, D, q_o, and C_z are adjusted so that the calculated hydrograph matches the observed hydrograph within a tolerance ε. The parameter identification is discussed further in the next section.

5.6 Estimation of Parameters

In the parameter estimation mode, the calculated direct runoff hydrograph is compared to the observed direct runoff hydrograph. A criterion is needed to estimate the error function shown in block (7). At present, there are two criteria commonly used. The first one is based on a comparison of the direct runoff hydrographs. The sum of the absolute values of the differences between the ordinates of the calculated and the observed hydrographs is expressed as a percentage of the sum of the observed hydrograph ordinates:

$$E_1(\%) = \frac{\sum_{i=1}^{T} |Q_{ci} - Q_{ci}|}{\sum_{i=1}^{T} Q_{oi}} \qquad (5.6.1)$$

where the Q_{ci} are the ordinates of the calculated direct runoff hydrograph and Q_{oi} are the ordinates of the observed direct runoff hydrograph. The second criterion is based on the difference between the observed and cal-

culated peak discharges and the time to the peak discharge. It is defined [54] as follows:

$$E_2(\%) = \left\{ \left[\frac{Q_{po} - Q_{pc}}{Q_{po}} \right]^2 + \left[\frac{T_{po} - T_{pc}}{T_{po}} \right]^2 \right\}^{1/2} \cdot 100 \qquad (5.6.2)$$

where Q_{po} is the peak of the observed hydrograph
Q_{pc} is the peak of the calculated hydrograph
T_{po} is the time to peak of the observed hydrograph
T_{pc} is the time to peak of the calculated hydrograph

The error detected is compared with the allowable error as shown in block (8). At this stage, there are two possible ways to proceed. If the error is acceptable, then the parameter estimation procedure is completed. Otherwise readjusting of the pre-assigned parameters is needed. In order to seek the minimum error function, an optimization technique is required. The next section discusses the optimization method used and shown in block (9).

5.7 The Unit-Variate Search Method

There are numerous optimization methods which are widely used in system analysis. In order to limit the computer time consumed in the evaluation of the error function, it was decided to find the optimum grid point in the error space. The unit-variate search [55] method was used. It is easily visualized in the case of two-variables. The method involves alternating only one variable at a time, holding the other variable constant. After the error values at two neighboring points are calculated, the direction towards the optimum point is determined. The procedure is repeated until there is no further improvement in that variable. Then this variable is held as a constant and the other variable is changed. The same procedure is repeated until the error function is within allowable limit. Fig. 5-9 illustrates the path in the error space. In this study, only C_z and q_o were considered as independent variables. B and D were pre-assigned to relate watershed soil class and the rainfall pattern.

In general, it is easier to locate the optimum grid point in problems with error contours characterized by little interaction between the variables. However, it should be pointed out that the grid point with the minimum error value is not the exact optimum point, but it locates the closest

neighborhood for the selected grid size. After the parameters C_z and q_o are optimized the calculation returns to block (4) to evaluate a new calculated direct runoff hydrograph. When the error function is within the acceptable limit, then the identification procedure is completed.

This procedure can handle one storm at a time. The same procedure can be used to test a set of storms in the same watershed. Storms of different watersheds were analyzed and the model parameters can be compared. The correlations among the geomorphological parameters, rainfall pattern and the estimated parameters in this model are pursued further in the next chapter.

CHAPTER VI

RESULTS AND DISCUSSIONS

6.1 Introduction

The results obtained with the proposed model using observed rainfall, runoff and watershed characteristics are presented in this chapter. Fourteen watersheds and about 200 storms were analyzed. The summary of the data was shown in Table 4-2. The results are presented in the following sequence. Section 6.2 discusses the drainage area distribution. Section 6.3 gives the estimation of "B" horizon loss and the weight factor D for the antecedent rainfall effect in the varied source area model. Section 6.4 and 6.5 give some justifications and sensitivity analysis of the Upstream Inflow Instantaneous Unit Hydrograph (in abbreviation as UIIUH). Section 6.6 presents the sample results of the parameter estimation. Section 6.7 discusses the correlation of estimated model parameters with climatologic and geomorphologic parameters. Section 6.8 presents the proposed simulation model. Finally, section 6.9 presents some regeneration performance and comparison.

6.2 Contributing Area Distribution Curve

The calculation of the contributing drainage area distribution curve may be thought of as a simplified or integrated watershed network and was obtained by means of the basic assumptions of Chapter V. Two examples of drainage area distribution curves are illustrated in Figure 6-1 and 6-2. The method used to calculate the contributing area distribution curve was illustrated in an ideal network with equal link lengths. Hence, it is necessary to set up a sampling procedure to handle these field stream networks. For the convenience of the calculations an equal interval sampling was utilized. The sampling interval was used as a tool to measure the network. In this study, 0.05 mile was used as the sampling interval. The measurement of the fractional value was treated by the following method. The residual link lengths which are less than one half sampling interval are neglected. It is considered as a whole sampling unit if the residual value is greater than or equal to one half of a sampling unit. For later calculation purposes, a larger sampling value can be achieved by averaging neighboring

sampling values. For example in Figures 6-1 and 6-2, the 0.25 mile sampling interval is the average of five sampling values of the 0.05 mile basic interval. Three examples of the contributed area distribution are presented in Figure 6-3. The sampling intervals are 0.05 mile. The 0.25 mile sample interval was obtained by averaging the neighborhood five values.

Based on the geometric similarity, it was found that the main stream length (the longest stream length in the stream network) was correlated with the drainage area. The Figure 4-7 shows the regression analysis result as:

$$L_0 = 1.64\ A_0^{0.55} \qquad (6.2.1)$$

where L_0 = main stream length, miles

A_0 = drainage area, square miles

The maximal ordinates of the drainage area distribution curves are plotted in Figure 6-4, which shows, on the average, an increase of the maximal ordinates as the drainage area increases. Nevertheless, the rate of increase of the maximal ordinates of the drainage area distribution curves is smaller than the rate of increase of the main stream length as a function of the drainage area. The location of maximum ordinates in the drainage area distribution curve depends upon the characteristics of the stream network. The possible quantitative characteristic parameter is the stream length ratio of the highest stream order. Table 6-1 shows the stream length ratios of highest stream orders of watersheds number 1, 2, 3 and 16. It indicates watershed no. 1 has the smallest stream length ratio for the highest stream order. Its drainage area distribution curve, shown in Figure 6-3, indicates that it has the maximal ordinate located near the basin outlet. On the other hand, the watershed no. 16 has the highest stream length ratio for the highest stream order. As a result, the maximal ordinate of the drainage area distribution curve is located at the far end from the basin outlet as shown in Figure 6-2. Watersheds no. 2 and 3 are somewhere between these two extreme cases.

It is also noted that the shapes of the watershed boundaries do not always give the right information regarding the paths of the runoff, expecially for meandering channels. Table 6-1 indicates that watersheds no. 1 and 16 have very similar basin circularities; they are 0.603 and 0.610 respectively. However, the drainage area distribution curves are completely different as

Table 6-1 Stream Length Ratio and Some Basin Shape Characteristics

Watershed No.	Highest	Stream Length Ratios of Highest Orders	Basin Circularity	Elongation Ratio	Shape Factor
1	3-4	0.483	.603	.846	1.25
2	4-5	2.354	.562	.742	1.53
3	5-6	2.187	.480	.790	1.74
16	5-6	4.517	.610	.990	2.04

shown previously. These indicate that the basin circularity, that is the ratio between the basin area to the area of a circle having a circumference equal to the perimeter of the basin is not a good indicator for the paths of the runoff. Similarily, both the elongation ratio and shape factor quantify the departures of basin shapes from a circle. They do not indicate the drainage area distribution characteristics.

The following section discusses the dynamic response area parameters.

6.3 The Determination of "B" Horizon Loss and Weight Factor D

The "B" horizon loss is based on the properties of the subsoil. There are several sources of information available for the soil permeability. The general soil mapping and classification in Indiana was reported by Purdue University [56] and by Bushnell [57]. The general soil regions are shown in Figure 6-5. The broad classification is divided into 16 categories labeled A to P as shown in Fig. 6-5. The U.S.G.S. Indianapolis Office [58,59] made an estimation of the soil permeability index which is shown in Table 6-2.

Table 6-2 Estimation of Soil Permeability in Indiana

Soil Type (Fig. 6-5	Permeability Index
1. A, (H)*, (O)	20
2. (A), B, (C), D, H	10
3. C, E, G, I, J, L, M. N, O, P	5
4. (L)	1
5. F, K	0.5

*The minor group

The study of Betcher et al. [60] showed the sublayer soil permeabilities given in Table 6-3.

Table 6-3 indicates that the measured subsoil permeability is low compared to the usual rainfall intensities. The estimation by U.S.G.S. Indianapolis [59] indicates only the relative values. Therefore, the Table 6-3 values were utilized in this study. Because their values are very small, the B value was taken as zero based on the present available data.

The next parameter to be estimated is the weighing factor D. This factor indicates the influence of the previous rainfall on the behavior of the source

Table 6-3 Soil Results Permeability After Betcher et al.
Ref. No. 60

Soil Name	County	Soil Classification	Depth (IN)	Permeability (IN/HR)
1. Brookston	Tipton	E	40	0.00005
2. Brookston	Tipton	E	40	0.00006
3. Cincinnati	Switzerland	E,J	36	0.0040
4. Clermont	Jennings	J	72	0.0020
5. Crosby	Jennings	J	72	0.0004
6. Crosby	Tipton	E	15	0.0002
7. Crosby	Tippecanoe	H,C,J	21	0.00009
8. Crosby	Tippecanoe	H,C,J	21	0.00003
9. Crosby	Tippecanoe	H,C,J	21	0.00007
10. Crosby	Tippecanoe	H,C,J	40	0.00005
11. Crosby	Tippecanoe	H,C,J	40	0.0001
12. Crosby	Tippecanoe	H,C,J	40	0.0001
13. Frederick	Washington	M	24	0.002
14. Maumee	Pulaski	A	30	0.003
15. Miami	Tippecanoe	H	25	0.002
16. Miami	Tippecanoe	H	40	0.00003
17. Miami	Tippecanoe	H	40	0.00001
18. Newton	Pulaski	A	20	-
19. Plainfield	Pulaski	A	20	-
20. Robertsville	Gibson	H	18	0.002
21. Warsaw	Vermillion	J	24	-

area. The weighing factor D was defined between 0 and 1. The sensitivity of the response area to changes in D was tested by giving D values of 0.5, 0.65 and 0.80 and keeping B = 0. Figure 6-6 shows that the response area curve does not exhibit a sensitive variation. However, it should be pointed out that the N values increase as the values of D increase. It indicates that both D and N have the function of quantifying the expansion of dynamic source area. Due to the insensitivity of the factor D and for simplification the D value was chosen as a fixed value and N was utilized to quantify the expansion of the dynamic source areas.

The testing of the proposed dynamic response area model showed that the value of N has a close relationship with the runoff ratio. Figure 6-7 shows the results of six watersheds in which several storms were tested. Therefore, further study was done to find the factors affecting the runoff ratio or N value. That study is given in section 6.7.

The previous study by Wu et al. [61] utilized the soil types to determine the runoff ratio (or runoff coefficient). The storm data of the fourteen watersheds were used to test Wu's method of finding the estimated runoff ratio. The soil type of each watershed was labeled according to the general soil classification [56]. If there was more than one soil type occurring in a basin, the soil type of low land areas was chosen, because it was illustrated that the runoff production area was located in those areas. Then the method proposed by Wu et al. [61] was applied. The results of the observed and estimated runoff ratios are listed in Table 6-4 and displayed in Figure 6-8. The results obtained by the method of Wu et. al. [61] are higher than those calculated from the actual storm data. Nevertheless, it appears that the Wu et al. [61] method is safe and yields an over estimation for engineering design. The spread of the estimated values was also larger than that suggested by Wu et al. [61]. The mean runoff ratios of watersheds do not have a definite trend as the soil types change. The conclusion is that the runoff ratio is not a function of soil type only.

In summary, the estimation of B is based on the soil properties. It appears to be very small compared to the rainfall intensity normally observed in Indiana. The dynamic response area function appears insensitive to the the D value. Therefore, the N value was utiilized to quantify the dynamic source area.

Table 6-4 Runoff Ratio of Testing Watersheds

No.	Watershed Name	Soil Class	No. of Storm	Estimated Runoff Coefficient after Wu et al. [61]	Observed Runoff Ratio mean	Observed Runoff Ratio st.dev	Range of Rainfall Volume (IN)
1	Lawrence Cr. at Ft. Benjamin	E*	13	.70	.599	.275	2.21 -0.378
2	Bear Cr. near Trevlac	L	15	.80	.472	.225	1.84 - .330
3	Bean Blossom Cr. at Bean Blossom	H	17	.50	.439	.229	2.660-0.410
10	Big Blue River at Carthage	H	23	.50	.252	.121	2.960- .671
16	Hinkle Cr. near Cicero	E	10	.70	.526	.246	2.560-0.571
19	Brush Cr. near Nebraska	J	25	1.00	.575	.254	1.800- .460
22	Cicero Cr. at Noblesville	H	22	.50	.314	.222	2.310- .321
24	Buck Cr. at Muncie	E	21	.70	.172	.102	2.130-0.150
35	Salamonie River at Portland	F	20	.5-.8	.408	.253	2.460- .430
37	Bice Ditch near South Marion	A	17	.30	.427	.260	3.847- .195

Table 6-4 continued

No.	Watershed Name	Soil Class	No. of Storm	Estimated Runoff Coefficient after Wu et al. [61]	Observed Runoff Ratio mean	Observed Runoff Ratio st.dev	Range of Rainfall Volume (IN)
39	Little Cicero Cr. near Arcadia	E	14	.70	.372	.181	5.665- .100
42	Wildcat Cr. near Jerome	E	15	.70	.397	.224	3.640- .265
43	Slough Cr. near Collegeville	A	12	.30	.195	.101	2.470- .468
44	Little Indian Cr. near Royal Center	D	6	.50	.258	.178	1.800- .720

*The soil classification emphasizes stream low land.

The next section discusses the transfer function of the contributing rainfall into direct runoff in space and time.

6.4 Verification of Computer Programs Used in the Analysis of Upstream Inflow Instantaneous Unit Hydrograph (UIIUH)

The UIIUH was derived by Harley [16]. The previous studies based on the Linear Channel Routing (abbreviated as LCR) were reported in [17,62,63]. This section intends to compare the results of the present computer programs evaluating the UIIUH to those of the previous studies. The sensitivity of the parameters of the cited model was also investigated.

The UIIUH was expressed as:

$$H_u(L,t;\ q_o,C_z,S_o) = q_1 + q_2 \qquad (6.4.1)$$

The UIIUH consists of two portions, q_1 and q_2. The first term including the delta function represents the head of the wave. The second term represents the main body of the wave. The relative magnitudes of these two portions are dependent on the parameters L, q_o, C_z and S_o. It should be noted that the sum of these two portions is equal to unity. An understanding of the magnitude of the first term is very important for the calculation scheme of the total direct runoff. A special computation procedure is necessary for handling the delta function. Figure 6-9a illustrates the variation of the magnitudes of q_1 with varying roughness coefficient C_z and stream reach, L, but holding the reference discharge q_o at 50 cfs and the basin slope S_o at 1 foot per mile. It shows that q_1 is almost negligible when L is larger than 10 miles. The magnitude of q_1 decreases as the roughness coefficient C_z decreases. By the same token, Figure 6-9b illustrates the variation of q_1 as the stream slope S_o and stream reach L vary but holding C_z and q_o fixed. It shows that as the stream slope increases, the q_1 decreases quite rapidly. The magnitude of q_1 becomes negligible when L is longer than 3 miles and stream slope is larger than 5 feet per mile.

The computer program was coded to display the UIIUH. The verification of the UIIUH calculation was done by displaying some of the results from previous studies [17,63]. Harley and Dooge [17] used two dimensionless parameters to quantify the UIIUH. These two parameters are: Froude number $F_N = u_o/\sqrt{gy_o}$ and $D_N = \frac{S_o L}{y_o}$. Figure 6-10 shows six cases of UIIUH with

F_N = 0.1, D_N = .25, 1.0, 5.0 and F_N = 0.9; D_N = 5., 15. and 50.. The dimensionless forms in time axes were calculated by dividing the real time by the time to the wave head, $T_o = L/(u_o+\sqrt{gy_o})$. The UIIUH of these six cases are the same as those reported by Harley and Dooge [17].

Another verification consisted of comparing the UIIUH with q_o = 50 cfs, C_z = 50 $ft^{1/2}$/sec, S_o = 1 ft/mile with L = 50, 100 and 200 miles as calculated by Bravo et al. [63] and by the program developed in this research. The results of this comparison are shown in Fig. 6-11. These two comparisons confirm that the computer program of UIIUH has the same performance as previously reported [17,63]. Next is the verification of the convolution technique. The numerical convolution used in this study is a discrete convolution with equal time interval sampling whereas Bravo et al. [63] used a Gaussian quadrature method of integration with a variable sampling interval. The equal interval sampling of UIIUH is very straight forward for the second term because it is continuous. The treatment for the first term in the UIIUH is described as follows: First, the time to the wave head, L/c_1 and the magnitude of q_1 are calculated. Then the sampling values which appear before the wave head are set equal to zero except the sampling point just before the wave head. The sampling value of q_2 at the wave head, h_y, is then computed. In order to conserve the constant sampling interval a new value h(i) is chosen as shown in Figure 6-13 located just before the wave head and is defined such that the following relationship is satisfied: (i.e. the total area between these two sampling values is the same as the trapezoidal area using these two sampling values as two parallel sides and the sampling interval as height.)

$$[h(i) + h(i+1)]\frac{\Delta t}{2} = q_1 + \frac{1}{2}[h_y + h(i+1)][t(i+1) - \frac{L}{c_1}] \qquad (6.4.2)$$

The Thomas-96-hours wave was used as input which was used by Harley and Dooge [17] and which is expressed as:

$$q(o,t) = 125 - 75\cos(\pi t/48) \qquad (6.4.3)$$

It was used for the purpose of comparison. The transfer functions or UIIUH were calculated with Q_o = 150 cfs, C_z = 50 $ft^{1/2}$/sec, S_o = 1 ft/mile and L = 5, 50, 200 and 500 miles. The convolution operations were performed. The results are shown in Figure 6-12. The results are very close to those

which were reported by Harley and Dooge [17]. This comparison confirms that the convolution scheme used in this study yields essentially the same results as reported in the previous study.

6.5 Sensitivity Analysis of Model Parameters

After the verification of the computer programs, the sensitivity analysis of the model parameters is needed for a better understanding of the model behavior. The geomorphologic data analysis in this study indicated that the main stream lengths range from 3 to 42 miles. The 5 and 20 miles stream reaches were chosen to represent the typical cases. Figures 6-14 (A), (B) and (C) refer to 5 mile stream reaches and Figures 6-14 (D), (E), and (F) refer to the 20 mile stream reaches. Figure 6-14 (A) shows the variation of UIIUH due to a variation in Q_o by holding C_z = 50 $ft^{1/2}$/sec and S_o = 1 ft/mile. The peak of the UIIUH has a strong rate of attenuation and a weak rate of translation at large Q_o. When Q_o decreases, the rate of attenuation is reduced and the effect of the rate of translation becomes dominant. This phenomenon is the same for 20 mile stream reaches shown in Figure 6-14 (D). However, it was noted that for the 5 mile stream reach case, the attenuation effect is stronger than that of the 20 mile stream reach. Figure 6-14 (B) shows the variation of the UIIUH due to a slope S_o variation for a 5 mile stream, with Q_o = 50 cfs and C_z = 50 $ft^{1/2}$/sec held constant. It indicates that the slope has a very strong attenuation effect and very weak translation effect. A similar situation for a 20 mile stream is shown in Figure 6-14 (E). Figure 6-14 (C) shows the variation of UIIUH due to a variation in C_z for a 5 mile stream, with S_o = 10 ft/mile and Q_o = 50 cfs held constant. It indicates that the attenuation effect of C_z decreases as C_z decreases. A similar situation for a 20 mile stream reach is shown in Figure 6-14 (F). However, it should be noted that the slope increases to 10 ft/mile in Figure 6-14 (C) and (F).

In summary, the Q_o and C_z have a strong attenuation effect for large values. The translation effect becomes dominant for small values of Q_o and C_z. The slope has a strong attenuation effect and a very weak translation effect.

The next section discusses the results of utilizing the UIIUH as the transfer function, the simplified watershed as the drainage basin and the dynamic response area model as the tool to identify the runoff contributing portion in space and time.

6.6 The Sample Results of Identification Mode

A sample of the results obtained for watersheds which have been analyzed in the hydrologic and geomorphologic phases is presented in this section. The two dynamic response area models were compared. The two criteria of the optimization procedures were investigated.

The proposed model was tested by utilizing the rainfall as the input, the observed direct runoff as given output, and the drainage area distribution of the basin. The parameters B and D are pre-assigned. The parameters N, q_o, and C_z need to be estimated.

There are two dynamic response area models cited in Chapter V. The first one, eq. (5.3.9), assumes that the previous rainfalls have the same weight. In the second model, eq. (5.3.10), it is assumed that the fraction of the antecedent rainfall excess contributing to the response area decreases exponentially with the elapsed time. At Bean Blossom Creek near Bean Blossom (Watershed No. 3) the storm of February 27, 1955 (storm No. 4) was tested to compare the two response area models. Figure 6-15 indicates that the response areas during the rainfall period are similar. In this figure the left list of parameters corresponds to model 2 and the right list of parameters corresponds to model 1. However, after the rainfall stops, the response area of the second model decreases rapidly, while the response area of the first model remains constant. The same situation holds for D = 0.5, 0.65, and 0.80. The effects of these two dynamic response models on the runoff estimation were investigated. Figure 6-15 (D), (E), (F) indicate that these two models gave results very close to the observed hydrograph for D = 0.5, 0.65 and 0.80. The reason may be interpreted as follows: The rainfall vanishes after the end of the storm; the input into the system is thus zero and the magnitude of dynamic response area does not matter. This confirms that these two models give very similar results. For the convenience of data analysis, the first model was utilized.

When the response area is determined, the rainfall imposed on these areas was considered as input. The complete linear channel routing method was utilized to estimate the direct runoff. The observed and estimated direct runoffs were compared based on the two given criteria. The first one, eq. (5.6.1), is based on the sum of the absolute values of the differences between the ordinates of the calculated and the observed hydrographs. The second criterion,

eq. (5.6.2), is based on the difference between observed and calculated peak discharges and the time to the peak discharge. The experience in this study indicated that with the second criterion it is easier to obtain the optimized value. For some storms, two criteria yield very similar results. However, for some other storms, these two criteria yield two different "optimum" situations. Figure 6-16 (A) shows the matching of the observed and the computed direct runoff hydrograph based on the first criterion. Figure 6-16 (B) shows the case based on the second criterion. Figure 6-16 (A) indicates that the tail and rising limb of the direct runoff hydrograph are better matched than those of Figure 6-16 (B). However, the difference between observed and computed peak discharges is larger than that of Figure 6-16 (B). In this study, both criteria were tested. When the two criteria did not yield similar results, the second criterion was utilized, because the engineering applications are usually concerned with the peak flows and their time of occurrence.

Nine sample storms which belong to nine different watersheds are presented in Figure 6-17 to 19. These results indicate that the model can match the observed direct runoff hydrographs within a reasonable error limit. After the optimization of model parameters, the correlations of the identified model parameters, with geomorphologic characteristics and with measures of the rainfall pattern are pursued further in the next section.

6.7 The Correlation of Identified Parameters with Geomorphologic Characteristics and Rainfall Pattern

The analysis of a large sample of storms in these testing watersheds resulted in sets of identified parameters in each watershed. To study the nature of the differences and its implications for practical engineering design, three watersheds are presented below. A summary of the hydrologic parameters of these three watersheds is listed in Table 6-5. Six samples of the observed and calculated direct runoff hydrographs are presented in Figure 6-20.

Table 6-5 indicates that the values of C_z corresponding to the several storms in the same watersheds were not constant. The C_z values were plotted against the rainfall volume of each storm. Figure 6-21 shows that C_z does not vary with the rainfall volume of the storms. However, it indicates that watershed no. 10 has a larger C_z value than those of water-

Table 6-5 Summary Information of Watershed No. 3, 10 and 24

Watershed & Storm No.	Date	N	q_o (cfs)	C_z ($\sqrt{ft}$/sec)	R_r	Peak (cfs)	P_{max} (IN/HR)	P_t (IN)	$T_{max}-T_{min}$ (F°)	B_f (cfs)	D_r (HR)	S_I
W 3- 1	12/04/51	.725	50	7.0	.522	1153	.280	1.78	63-43	2.1	18.	0.06
W 3- 2	3/19/53	1.00	50	1.5	.436	429	.165	.88	63-37	16.0	11.	0.06
W 3- 3	1/27/54	2.55	50	2.0	.200	361	.370	1.35	56-30	3.7	15.	0.06
W 3- 4	2/27/55	1.18	50	2.5	.407	522	.250	.88	55-47	35.0	7.	0.06
W 3- 5	11/17/55	.637	55	3.0	.613	748	.260	.63	51-21	2.6	4.	0.06
W 3- 6	11/27/55	1.81	55	5.0	.298	413	.220	0.72	54-22	11.4	5.	0.06
W 3- 7	6/29/57	1.42	45	2.5	.366	760	.285	1.30	75-62	28.5	7.	0.06
W 3- 8	7/05/57	2.68	60	3.0	.256	605	.650	1.20	90-62	5.9	5.	0.06
W 3- 9	12/26/57	.54	50	3.0	.604	889	.220	1.40	54-36	35.0	15.	0.06
W 3-10	8/17/58	.80	55	7.0	.584	672	.240	.41	85-54	3.8	4.	0.06
W 3-11	2/15/59	.22	60	2.5	.799	725	.160	.80	42-31	32.3	12.	0.06
W 3-12	2/10/60	1.34	50	2.5	.364	661	.370	1.26	58-33	40.3	16.	0.06
W 3-13	7/14/60	5.22	60	5.0	.850	363	1.04	1.34	78-56	7.6	3.	0.06
W 3-15	7/20/63	5.93	50	5.0	.067	235	.80	1.79	91-66	20.0	5.	0.06
W 3-16	5/05/64	1.68	50	1.5	.276	767	.26	2.67	85-52	1.0	17.	0.06
W10- 1	3/10/52	1.47	55	5.0	.314	2643	.240	1.93	60-48	151.8	18.	3.00
W10- 2	3/31/52	2.06	50	9.0	.244	1015	1.40	.67	69-50	213.5	10.	3.00
W10- 3	4/04/52	1.04	40	5.0	.409	1718	.138	1.11	57-44	281.0	21.	3.00
W10- 4	3/02/53	1.14	50	7.0	.394	3467	.310	1.76	33-22	122.0	19.	3.00
W10- 5	3/17/53	1.90	55	7.0	.264	890	.173	.72	58-40	237.9	12.	3.00
W10- 6	1/26/54	3.08	50	1.0	.151	1598	.330	1.72	53-44	80.9	15.	3.00

Table 6-5 continued

Watershed & Storm No.	Date	N	q_o (cfs)	C_z ($\sqrt{ft}$/sec)	R_r	Peak (cfs)	P_{max} (IN/HR)	P_t (IN)	T_{max}-T_{min} (F°)	B_f (cfs)	D_r (HR)	S_I
W10- 7	7/05/54	.94	40	13.0	.463	4729	.463	1.18	59-35	152.1	9.	3.00
W10- 8	9/29/55	2.85	50	7.0	.164	1072	.508	1.56	72-52	83.8	10.	3.00
W10- 9	11/15/55	1.25	65	7.0	.376	5708	.688	2.97	70-46	228.0	13.	3.00
W10-10	6/11/57	5.24	40	1.0	.124	1185	.693	1.99	85-65	194.9	4.	3.00
W24- 2	7/03/55	1.04	175	4.0	.609	333	.125	.15	96-69	25.3	4.	6.0
W24- 3	9/23/55	3.84	70	4.0	.106	450	.155	1.65	66-64	19.5	11.	6.0
W24- 4	9/29/55	3.42	45	2.0	.128	293	.495	1.41	72-51	20.5	10.	6.0
W24- 6	11/13/55	3.17	35	4.0	.341	217	.230	.50	75-57	33.0	4.	6.0
W24- 7	5/22/56	3.04	90	1.5	.159	173	.120	.53	85-61	33.5	9.	6.0
W24- 8	7/03/56	6.82	30	4.0	.046	139	.435	1.03	89-66	87.8	9.	6.0
W24- 9	6/11/57	11.5	35	3.5	.059	224	1.015	1.46	85-67	43.5	5.	6.0
W24-10	12/25/57	2.33	115	.5	.203	272	.150	.85	58-30	66.3	15.	6.0
W24-11	1/20/58	2.72	75	2.5	.168	212	.110	.62	40-28	36.6	12.	6.0
W24-12	6/25/58	2.51	60	2.5	.209	508	.503	1.07	17-66	52.2	8.	6.0
W24-13	7/31/58	6.05	45	2.5	.108	286	.650	1.10	75-67	41.3	6.	6.0
W24-14	5/22/59	2.37	50	2.5	.268	434	.330	.72	81-62	34.6	6.	6.0
W24-15	5/29/59	1.48	70	2.5	.402	545	.230	.43	88-65	38.9	5.	6.0
W24-16	7/27/59	6.32	35	5.0	.066	175	.630	.84	85-67	18.8	8.	6.0
W24-17	10/10/59	7.63	50	3.0	.082	202	.310	1.25	75-36	88.8	10.	6.0
W24-18	4/21/61	1.52	30	3.5	.323	677	.375	0.90	69-55	69.8	7.	6.0
W24-19	4/22/63	2.76	25	3.5	.244	166	.130	.27	66-40	44.1	3.	6.0
W24-20	6/04/63	1.37	50	5.5	.367	184	.075	.30	83-61	32.8	5.	6.0
W24-21	3/03/64	3.91	20	2.1	.100	217	.290	2.18	56-44	26.5	15.	6.0

sheds no. 3 and no. 24. The drainage area of watershed no. 10 is 187 square miles which is much larger than the areas of watersheds no.3 and no. 24. (Their drainage areas are 14.6 and 36.7 square miles respectively.). The geomorphologic data analysis showed that the drainage area is the primary factor in watershed characteristics. This may indicate that C_z is related to the geomorphologic parameters or antecedent conditions rather than to the storm pattern.

For finding the relation between geomorphologic parameters, antecedent conditions and C_z, more watershed data are needed. It is noticed that the data bank for the several watersheds does not contain the same number of storm events for each watershed. In order to weigh equally each watershed, the three best matched storms were selected to represent that particular watershed. Table 6-6 shows the representative storms and the geomorphologic parameters of thirteen watersheds. The selected parameters are: drainage area, drainage density, mean link length and basin slope. The base flow per unit drainage area is selected to represent the watershed antecedent condition. The stepwise multiple regression analysis [64] was utilized to find the correlation. The results are shown in the following equations (see Table 6-7):

Table 6-7 Regression Equations of C_z

Step	Multiple Correlation coefficient	Regression Equation
1	.242	$C_z = 1.21 \left(\frac{B_f}{A_0}\right)^{-.230}$
2	.311	$C_z = .677\ A^{.175} \left(\frac{B_f}{A_0}\right)^{-.232}$
3	.637	$C_z = 0.00141\ A_0^{.995} S_o^{1.42} \left(\frac{B_f}{A_0}\right)^{-.208}$
4	.640	$C_z = .00134\ A_0^{.983}\ S_o^{1.44} \left(\frac{B_f}{A_0}\right)^{-.227} S_I^{.070}$
5	.643	$C_z = .00098\ A_o^{.976}\ \ell^{-.238} S_o^{1.37} \left(\frac{B_f}{A_0}\right)^{-.236}\ S_I^{.092}$
6	.644	$C_z = 0.00082\ S_I^{.073}\ A_0^{.987}\ D_d^{-.206}\ \ell^{-.416}\ S_o^{1.41} \left(\frac{B_f}{A_0}\right)^{-.239}$

Table 6-6 Storms Selected for Regression Analysis of C_z

No.	Watershed Name	Storm No.	Date	Drainage Area (mi^2)	Drainage Density (mi/mi^2)	Mean Link Length (mi)	Basin Mean Slope (ft/mi)	q_o (CFS)	C_z ($\sqrt{FT}$/SEC)	Base Flow B_f (CFS)	Soil Index S_I
1	Lawrence Cr. at Benjamin Harrison	1	June 12, 52	2.86	6.10	0.836	52.1	55	3.0	1.10	1.25
		2	June 22, 52					50	0.2	6.18	
		5	July 10, 58					45	1.5	3.15	
2	Bear Cr. near Treviac	7	May 29, 55	7.00	9.80	.1103	44.7	55	0.4	3.31	2.25
		8	Feb. 25, 56					50	0.7	52.60	
		9	June 21, 57					50	3.0	0.19	
3	Bean Blossom Cr. at Bean Blossom	12	Feb. 10, 60	14.6	11.80	.0955	22.1	50	2.5	43.05	.06
		15	July 20, 63					50	5.0	0.26	
		16	May 6, 64					50	1.5	1.40	
10	Big Blue River at Carthage	4	March 2, 53	187.	4.33	.1319	8.07	50	7.0	123.00	3.00
		6	Jan. 26, 54					50	9.0	81.20	
		8	Sept.29, 55					50	7.0	84.00	
16	Hinkle Cr. near Nebraska	3	Feb. 26, 57	16.3	6.62	.0967	8.01	10	.15	14.53	1.25
		4	Nov. 13, 57					15	.15	16.60	
		6	July 12, 60					10	.15	4.74	
19	Brush Cr. at Noblesville	2	Nov. 15, 55	11.7	11.31	.0653	26.4	60	3.0	5.56	1.00
		12	May 2, 58					62	2.5	14.25	
		13	June 13, 58					32	3.5	4.55	
24	Buck Cr. at Muncie	6	Nov. 13, 55	36.7	5.69	0.1179	7.39	30	4.0	33.00	6.00
		11	May 22, 56					70	2.5	36.30	
		22	May 7, 61					20	2.1	55.10	
35	Salamonie Portland	11	July 20, 62	86.0	5.82	0.1095	10.7	20	2.5	16.66	3.00
		15	March18, 62					45	2.0	97.20	
		22	May 7, 61					50	2.0	92.50	

Table 6-6 continued

No.	Watershed Name	Storm No.	Date	Drainage Area (mi^2)	Drainage Density (mi/mi^2)	Mean Link Length (mi)	Basin Mean Slope (ft/mi)	q_o (CFS)	C_z ($\sqrt{FT}/SEC$)	Base Flow B_f (CFS)	Soil Index S_I
37	Bice Ditch near South Marion	6	Feb. 9, 60	22.6	3.42	0.1671	7.31	35	.65	40.43	2.50
		7	Jan. 29, 59					40	1.5	5.03	
		11	Aug. 11, 57					50	1.5	7.45	
39	Little Cicero Cr. near Arcadia	5	Feb. 5, 60	44.7	4.64	0.0976	6.98	30	1.6	24.30	1.00
		6	April 1, 59					35	1.1	41.50	
		10	Aug. 23, 57					40	1.1	9.88	
42	Wildcat Cr. near Jerome	2	Jan. 25, 62	148.0	3.79	0.2069	3.47	15	1.0	116.40	2.00
		9	March25, 64					30	.45	111.50	
		10	April 2, 64					30	.20	131.80	
43	Slough Cr. near Collegeville	1	March 5, 56	84.1	2.47	0.2008	6.10	35	1.6	84.00	2.75
		6	July 15, 57					35	1.1	50.50	
		9	Jan. 20, 58					40	2.1	27.65	
44	Little Indian Cr. near Royal Center	6	June 6, 60	35.0	2.17	0.2822	7.39	20	1.05	37.00	3.00
		7	Aug. 2, 60					20	1.05	11.40	
		14	April 17, 60					45	0.8	8.00	

where S_I = soil permeability index [39]

B_f = base flow when the storm occurs (cfs)

ℓ = mean link length (miles)

A_0 = drainage area (square miles)

D_d = drainage density (mi/square mi)

S_o = basin slope (ft/mi)

The lack of substantial improvement in the multiple correlation beyond the third step is probably due to the fact that few geomorphologic parameters are independent as was shown in the analysis of the geomorphologic data.

The next important parameter is the reference discharge. Table 6-5 shows values ranging from 20 to 175 cfs. Figure 6-22 shows that the reference discharges are apparently unrelated to the rainfall volume. The three watersheds' data do not indicate any separable groups. However, the values of q_o concentrate within the range of 40 to 70 cfs. The variations for small storms are larger than those for large storms. These results indicate that the reference discharge does not vary sensitively from storm to storm or from watershed to watershed.

The third major parameter is the exponential factor of the dynamic response area, N. A preliminary study showed that the N values and runoff ratios are closely correlated. Figure 6-23 illustrates the plot of N against the runoff ratio. It shows that N and the runoff ratio are approximately linearly related on semi-logarithmic paper. The regression analysis of $R_r = k_1 + k_2 \ln N$ was tested where k_1 and k_2 are the regression coefficients. The result of this regression analysis yields the following relationship:

$$R_r = .464 - .242 \ln N$$

or

$$N = \exp\left[\frac{.464 - R_r}{.242}\right] \quad \text{for} \quad D = .8 \text{ and } B = 0.0 \qquad (6.7.1)$$

To pursue further, it is necessary to find the factors governing the runoff ratio. It is noticed that the runoff ratio is measurable but is a variable collectively influenced by many factors. It depends primarily on the climatic condition, the rainfall pattern, the soil type, the watershed condition when the rainfall occurred, etc. As illustrated in the last section, the soil type is not the only indicator for the runoff ratio. Therefore it was

decided to select more factors to describe the runoff ratio. The following factors were selected.

(A) Rainfall pattern

(1) Rainfall volume (in inches), P_t

(2) Maximum rainfall intensity within the storm, in inches per hour, P_{max}

(3) Rainfall duration in hours, D_r

(B) Climatic condition

Daily temperature was selected. The available data in U.S. Weather Bureau Climatic data Indiana [65] are the daily maximum and minimum.

(C) Watershed Conditions

The average base flows when the storms occur were utilized to indicate the watershed condition. However, it was noted that the base flow is dependent on drainage area. Therefore, the average base flow per unit drainage area was used in the analysis.

(D) Soil type

A soil permeability index was developed by the U.S.G.S., Indianapolis Office [58]. It was expressed as a dimensionless number. These values were determined by assigning soil permeability values to major soil types occurring in the basins, and calculating the weighted average for each basin.

The regression analysis was performed for the data retrieved from three selected watersheds in Table 6-5. The stepwise multiple [64] regression analysis yields the following result (see Table 6-8).

Table 6-8 Regression Equations of Runoff Ratio

Step	Multiple Correlation Coefficient	Regression Equation
1	0.883	$R_r = T_{min}^{-.355}$
2	0.899	$R_r = T_{min}^{-.355} S_I^{-.123}$
3	0.909	$R_r = P_t^{-.221} T_{min}^{-.345} S_I^{-.154}$
4	0.914	$R_r = P_{max}^{-.245} P_t^{-.178} T_{min}^{-.422} S_I^{-.150}$

Table 6-8 (continued

Step	Multiple Correlation Coefficient	
5	0.915	$R_r = P_{max}^{-.252} P_t^{-.179} T_{min}^{-.425} (\frac{B_f}{A_0})^{.083} S_I^{-.150}$
6	0.916	$R_r = P_{max}^{-.289} P_t^{-.155} T_{min}^{-.386} (\frac{B_f}{A_0})^{.085} D_r^{-.093} S_I^{-.141}$

where R_r = runoff ratio

P_{max} = maximum rainfall intensity, (IN/HR)

P_t = rainfall volume, (INCHES)

T_{min} = minimal daily temperature when storm occurs (F°)

B_f = average base flow (CFS)

A_0 = drainage area (sq. mi.)

D_r = rainfall duration (HR)

S_I = soil permeability index

In summary, it was shown that two parameters were the dominant factors in this model. The N value is used to determine the runoff ratio which was correlated with the rainfall pattern such as rainfall volume, maximum rainfall intensity and rainfall duration, climatic condition such as daily minimal temperature when storm occurred, watershed condition such as average base flow per unit drainage area, and soil type such as soil permeability index. The second parameter is the roughness coefficient C_z. It is primarily a geomorphologic factor. It was correlated with the drainage area, the drainage density, the basin mean slope, and the watershed condition when storm occurs. With the results from these correlations, the prediction model is presented in next section.

6.8 Proposed Runoff Estimation Model

The correlation of geomorphologic parameters, rainfall pattern and identified parameters makes the estimation model possible, at least one based on regional data. The following runoff estimation model is based on the Indiana small watersheds data. The application for other regional areas requires the necessary data to define the regression equations. Nevertheless, the methodology still can be applied.

The runoff estimation model is shown in Figure 5-8 in a dotted box. The summary of the input information is listed in Table 6-9. The first input information is the rainfall hyetograph. This information may be obtained from the frequency analysis of the historical rainfall data or the historical storm events. The parameters which are retrieved from the rainfall hyetograph are rainfall volume, P_t, maximum rainfall intensity P_{max}, rainfall duration D_r. The second item is the base flow magnitude. This may be obtained from the U.S.G.S. surface water data [66]. The third item is the daily minimum temperatures. These temperatures can be obtained from the climatic data published by the Weather Bureau by state. The fourth item is the topographic maps. The mean basin slope and drainage area are retrieved from these maps. The fifth item is the drainage maps. The main parameters which can be retrieved are the contributed area distribution curve and the drainage density. These maps in Indiana were compiled by Purdue University [20]. The digitized data from drainage maps was reported in [19]. The sixth item is soil data. Two parameters, B and S_I, are determined from these soil data. The Indiana soil data [60] indicate that B is quite small. For runoff estimation purposes in Indiana, B is assumed to be zero. The S_I values can be obtained from [58].

The first six items are the fundamental information. The following items are the results of the regression analysis of identified systems parameters. The seventh item is the weighting factor D. It was found that D was not a sensitive factor as far as direct runoff is concerned. It ranges from 0.5 to 0.8. The value of D = 0.8 was used in this model. The eighth item is C_z. It was found that the drainage area, the mean basin slope, and the base flow are significantly correlated with C_z. For small Indiana watersheds, C_z was found to be

$$C_z = 0.00141\ A_0^{.995}\ S_o^{1.42}\ \left(\frac{B_f}{A}\right)^{-.208} \qquad (6.8.1)$$

The multiple correlation coefficient is 0.637. The nineth item is reference discharge. It's values were between 40 to 70 CFS in this study for storm volumes ranging from 0.1 to 5.6 inches, for small Indiana watersheds (3 to 200 square miles). The tenth item is the parameter N. It was found to be related with the runoff ratio. For Indiana watersheds, the following relationship was found

Table 6-9 Summary of Prediction Model Input Information

	Items	Parameters Retrieved	Data Source or Regression Equation for Indiana
(1)	Rainfall Hyetograph	P_t, P_{max}, D_r, $R(t)$	Design Rainfall Hyetograph
(2)	Base Flow	B_f	U.S.G.S. Data
(3)	Daily Temperature	T_{max}, T_{min}	Climatic Data
(4)	Topographic maps	S_o, A_0	Topograph maps
(5)	Drainage maps	Simplified Watershed and D_d	Drainage map
(6)	Soil maps	B, S_I	B = 0., U.S.G.S. Open file report [58]
(7)	D	D	D = 0.5 to 0.8
(8)	C_z	$C_z = C_z(B_f, A_0, S_o)$	$C_z = .00141\ A_0^{.995}\ S_o^{1.42}\ (\frac{B_f}{A_0})^{-.208}$
(9)	q_o	q_o	q_o = 40 to 70 cfs
(10)	N	$R_r = R_r(P_t, P_{max}, T_{min}, S_I)$	$R_r = P_{max}^{-.245}\ P_t^{-.178}\ T_{min}^{-.422}\ S_I^{-.150}$
		$N = N(R_r)$	$N = \exp(\frac{.464 - R_r}{.242})$

$$N = \exp\left[\frac{.464 - R_r}{.242}\right], \quad \text{for} \quad D = .8,\ B = 0 \qquad (6.8.2)$$

For defining the runoff ratio, the following regression equation may be utilized for Indiana small watersheds

$$R_r = P_{max}^{-.245}\ P_t^{-.178}\ T_{min}^{-.422}\ S_I^{-.150} \qquad (6.8.3)$$

where P_{max}, P_t, T_{min} and S_I could be retrieved from the fundamental information. The multiple correlation coefficient is .914.

After the parameters B, D, N, C_z and q_o are defined, then the estimated direct runoff hydrograph can be obtained as shown in Figure 5-8.

There are several limitations in this model. First the study used watersheds which have drainage areas ranging from 3 square miles to 200 square miles. Secondly, the storms which were analyzed have the rainfall volume ranging from 0.1 to 5.6 inches for each storm event. Thirdly, all the basins in this study are rural watersheds. The man-made disturbances are not included. Fourth, all the parameters are based on the presently available data in Indiana. Any new information could improve the parameter accuracy. However, the basic framework of this model still could be utilized. Finally, this model is designed for short term hydrologic prediction. The long term prediction is not valid.

6.9 Model Regeneration Performance and Comparison with Some Other Methods

In order to understand the regeneration performance of the proposed model, some storms and other given conditions were fed into the model to regenerate the predicted hydrographs. The summary results are listed in Table 6-10. The peak flows of the observed and regenerated direct runoff hydrographs are compared. They indicate the average error was about $\pm$ 20%. Table 6-9 also shows that the time to peak had better regeneration performance. The error of the regenerated hydrograph may be interpreted in terms of the estimation of the system parameters C_z and N. The N value is related to the runoff ratio. A good estimation of N indicates the total direct runoff volume close to that of the observed hydrograph. The C_z is the routing parameter which affects the shape of the hydrograph. The regenerated and identified C_z and N are listed in Table 6-10. The sample results of the observed and regenerated

Table 6-10 Summary Results of Regeneration Performance

Watershed No.	Storm No.	Peak Flow (CFS) Obs.	Reg.	Err. (%)	Time to Peak (HR) Obs.	Reg.	Err. (%)	C_z ($\sqrt{FT}$/SEC) Est.	Reg.	N Est.	Reg.
3	2	430	510	+18.6	8.5	9.5	+11.7	1.5	1.62	1.00	.766
3	4	420	650	+25.0	7.5	7.5	0.0	2.5	2.06	1.18	.788
3	5	748	480	-36.0	5.5	4.5	-18.1	3.0	2.06	.637	.915
3	8	605	570	- 5.7	4.5	5.5	+22.2	3.0	1.99	2.68	2.074
3	12	660	711	+ 7.7	15.5	15.5	0.0	2.5	2.06	1.34	1.084
10	5	890	675	-24.4	12.5	16.5	+32.0	7.0	4.74	1.90	2.041
10	6	1599	1280	-19.4	20.0	21.0	+ 5.0	1.0	5.93	3.08	2.921
10	8	1072	910	-15.1	18.0	17.0	- 5.5	7.0	5.89	2.85	2.921
10	10	1185	1080	- 8.6	13.5	15.0	+11.1	1.0	4.94	5.24	3.799
24	7	171	199	+16.4	7.0	7.5	+ 7.1	1.5	1.17	3.04	2.383
24	10	313	270	-13.7	13.0	14.0	7.6	0.5	.77	2.33	1.985
24	11	215	284	+31.6	10.5	11.5	9.5	2.5	.87	2.72	1.600
24	13	310	425	+37.1	19.0	16.5	13.1	2.5	.85	6.05	3.789

hydrographs are shown in Figure 6-24.

The proposed model was compared with some other methods. The storm of February 27, 1955 at Bean Blossom Creek near Bean Blossom (watershed no. 3) was selected to illustrate the differences. The methods selected for the comparison were: (1) the method of Wu et al. [61] and (2) the method of grouping the IUH suggested by Blank and Delleur [24]. The detailed calculations are shown in the appendix. The results of these three methods and the observed hydrograph are shown in Figure 6-25. It indicates that these three methods yield three different results. The IUH grouping method gives a late peak but the calculated peak flow is almost the same as the observed peak. Wu's method gives the highest peak flow. The dynamic area model gives the calculated hydrograph closest to the observed hydrograph. However, sets of storms and watersheds should be analyzed to obtain more definite conclusions. The following comparison is based on the characteristics of each method. It is shown in Table 6-11.

Table 6-II Comparison of Methods of Wu and of Grouping IUH's According to Peak Value and Time to Peak with Dynamic Area Model

Items	Wu's Method	Grouping of IUH	Dynamic Area Model
Type of System	Linear, lumped	Linear, lumped	Simplified distributed system
Determination of rainfall excess	By soil type	Not shown in prediction mode	Dynamic contributing area
Method of system identification	Preserve first and second moments of IUH	Fourier Transform	Optimization search (unit variable search)
IUH formulation	By parameters N, k_1 (Nash model)	Non-parametric	By UIIUH with parameters q_o, C_z, S_o (Harley and Dooge model)
Advantages	1. Easy to be applied 2. Less information needed	1. Not constrained to a particular model 2. Less computer time for system identification	1. Could be expanded to include spatial variations of rainfall, and ground surface conditions.
Disadvantages	1. Over estimate rainfall excess 2. Not coded in computer programs form yet	1. May require digital filtering of data 2. Difficult to be applied in ungaged watersheds.	1. Need more computer time for system identification. 2. Need digitized stream network data.

CHAPTER VII

SUMMARY AND CONCLUSIONS

The rainfall-runoff process in a watershed was simulated by two basic means, namely, a dynamic contributing area concept and a linear routing technique. The contributing area distribution curve which integrates the contributing areas along the stream network was developed for the purpose of hydrograph estimation. The model parameters were optimized to match the calculated and the observed direct runoff hydrographs. The rainfall characteristics, the climatic conditions expressed by the minimum daily temperature, the watershed conditions quantified by the base flow per unit area, the U.S.G.S. soil index and geomorphologic parameters were correlated with the system parameters. These results were utilized to estimate the stream flow of a watershed under varying climatic and watershed conditions.

The following conclusions are drawn, based on the application of this methodology to Indiana watersheds:

(I) The study of stream network geomorphology indicated that:

(a) The laws of stream number and stream length, in general, are valid in Indiana watersheds. The presence of incomplete networks is one of the key factors causing some deviations in these laws.

(b) The average bifurcation ratio for each stream order has a near constant value of about 4.5 which is almost equal to the ideal stream network value.

(c) The mean first order stream lengths range from 0.08 to 0.13 miles. This short length is due to the large detail of the county drainage maps used in this study compared with the U.S.G.S. quadrangle maps used by many others.

(d) In general, the drainage area, the drainage density, and the basin slope are the major geomorphologic parameters of hydrologic significance.

(e) The shreve magnitude system is portrayed by the mean link length, the link magnitude and the ratio of the basin area to the total stream length.

(2) The study of the dynamic response area model revealed that the "B" horizon infiltration and the weight of the antecedent rainfall, D, were not the primary parameters. The exponent N quantifying the rate of expansion of the response area was found to be correlated with the runoff ratio. The runoff ratio was, in turn, correlated with rainfall characteristics, the minimum daily temperature, the base flow per unit area and the U.S.G.S. soil index.

(3) The study of the three parameter linear routing method indicated that the watershed was characterized primarily by the contributing area distribution curve and by the roughness parameter. The latter was found to be correlated with geomorphologic parameters and the base flow per unit area. The reference discharge was found not to change significantly from storm to storm or from watershed to watershed and the slope was estimated from topographic maps.

(4) A comparison was made with Wu's method and that of grouping instantaneous unit hydrographs according to peak value and time to peak. This comparison indicated that each method has its advantages and disadvantages. A further systematic and quantitative comparison is suggested to evaluate the conditions for which each method is best suited.

BIBLIOGRAPHY

1. Van De Leur, D. A. K., Runoff Model with Linear Elements,Proc. of Tech. Meeting 21, Committee for Hydrol. Research, T.N.O. Netherland, 1966, pp. 31-64.

2. Horton, R. E., The Role of Infiltration in the Hydrologic Cycle, Trans. Am. Geophys. Union, Vol. 14, pp. 446-460, 1933.

3. Tennessee Valley Authority, Office of Tributary Area Development, Bradshaw Creek - Elk River a Pilot Study in Area-Stream Factor Correlation, Research Report No. 4, April, 1964.

4. Betson, R. P., What is Watershed Runoff?, Journ. of Geophy. Research, Vol. 69, No. 8, April 1964.

5. Ragan, R. M., An Experimental Investigation of Partial Area Contributions, Intl. Assoc. Sc. Hydrol.,Proc. Berne Sympsium, pp. 241-251, 1967.

6. Hewlett, J. D., and Nutter, W. L., The Relation of the Variable Source Area Concept to Hydrologic Modeling, Conference Proc. of Hydrologic Modeling Water Resources Management, Clemson Univ., pp. 95-117, March, 1970.

7. Carson, M. A., and Sutton, E. A., The Hydrologic Response of the Eaton River Basin, Quebec, Canadian Jour. of Earth Science, Vol. 8, pp. 102-115, 1971.

8. Dunne, T., and Black, R. D., Partial Area Contributions to Storm Runoff in a Small New England Watershed, Water Resources Research, Vol. 6, No. 5, pp. 1296-1311, 1970.

9. Betson, R. P., and Marius, J. B., Source Area of Storm Runoff, Water Resources Research, Vol. 5, No. 3, pp. 538-590, 1969.

10. Nutter, W. J., and Hewlett, J. D., Stream Flow Production from Permeable Upland Basin, Paper Presented to the Third International Seminar for Hydrology Professors, Purdue University, Lafayette, Indiana, July 18-30, 1971.

11. Hewlett, J. D., Surface Waters, Trans., American Geophys. Union, Vol. 52, No. 6, June, 1971.

12. Freeze, R. A., Role of Subsurface Flow in Generation Surface Runoff. 11. Upstream Source Areas, Water Resources Research, in press.

13. Tennessee Valley Authority, Area-Stream Factor Correlation, A Pilot Study in the Elk River System, Bull. Intern. Assoc. Sci. Hydrol., 10, 23-37, 1965.

14. Freeze, R. A., Role of Subsurface Flow in Generation Surface Runoff, 1. Baseflow Contribution to Channel Flow, Water Resources Research, Vol. 8, No. 3, pp. 609-623, June, 1972.

15. Chow, V. T., ed. Handbook of Applied Hydrology, McGraw-Hill Book Company, Inc., New York, N.Y., 1964.

16. Harley, M. B., Linear Routing in Uniform Open Channels, M. Eng. Science Thesis, National University of Ireland, Department of Civil Engineering, 1967.

17. Harley, M. B., Dooge, J. C. I., Systematic Comparison of Linear Flood Routing Procedures, Paper Represented at American Geophysics Union, 1971 Fall Meeting, San Francisco, California.

18. Coffman, D. M., Turner, A. K., Melhorn, W. N., The W.A.T.E.R. System Computer Programs for Stream Network Analysis, Purdue University, Water Resources Research Center, Technical Report 16, June 1971.

19. Lee, M. T., Blank, D., Delleur, J. W., Assembly of Hydrologic and Geomorphologic Data, Purdue University, Water Resources Research Center, Technical Report No. 23, May, 1972.

20. Purdue University Atlas of County Drainage Maps, Indiana Joint Highway Research Project, Engineering Bulletin, Extension Service No. 37, 1959.

21. Eagleson, P. S., Dynamic Hydrology, McGraw-Hill Book Company, Inc., New York, N.Y., 1970.

22. Chow, V. T., System Approaches in Hydrology and Water Resources, The Progress of Hydrology, Proceedings of the First International Seminar for Hydrology Professors, Vol. I, pp. 490-509.

23. Sherman, L. K., Stream Flow from Rainfall by Unit-Graph Method. Engineering News Record 108: 501-505, 1932.

24. Blank, D., and Delleur, J. W., A Program for Estimating Runoff from Indiana Watersheds - Part I. Linear System Analysis in Surface Hydrology and Its Application to Indiana Watersheds, Purdue Univ. , Water Resources Research Center, Lafayette, Indiana, August, 1968.

25. Delleur, J. W., and Rao, R. A., Linear System Analysis in Hydrology - The Transform Approach, The Kernel Oscillations and Effect of Noise, U.S.-Japan Bi-lateral Seminar in Hydrology, Honolulu, Jan. 1971 (Water Resources Publication)

26. Scheidegger, A. E., 1967 On the Topology of River Nets, Water Resources Research, Vol. 3(1), pp. 103-106, 1967.

27. Shreve, R. L., Stream Lengths and Basin Areas in Topologically Random Channel Networks, Jour. Geol., Vol. 77, pp. 397-414, 1969.

28. Horton, R. E., Erosional Development of Streams and Their Drainage Basins: Hydrophysical Approach to Quantitative Morphology, Geol. Soc. Am. Bull., Vol. 56, pp. 275-370, 1945.

29. Shreve, R. L., Statistical Law of Stream Number, Jour. Geol., Vol. 74, pp. 17-37, 1966.

30. Smart, J. S., A Comment on Horton's Law of Stream Number, Water Resources Res., Vol. 3, No. 3, pp. 773-776, 1967.

31. Morisawa, M. E., Quantitative Geomorphology of Some Watersheds in Appalachian Plateau, Bull. Geol. Soc. Am., Vol. 73, pp. 1025-1046, 1962.

32. Strahler, A. N., Hypsometric (Area-Altitude) Analysis of Erosional Topography, Geol. Soc. Am. Bull., Vol. 63, pp. 1117-1142, 1952.

33. Morisawa, M., Accuracy of Determination of Stream Lengths from Topographic Maps, Trans. Am. Geophy. Union, Vol. 38, No. 1, pp. 86-88, 1957.

34. Melton, M. A., A Derivation of Strahler's Channel Ordering System, Jour. Geol., Vol. 67, pp. 345-346, 1959.

35. Coates, D. R., Quantitative Geomorphology of Small Drainage Basins of Southern Indiana, Columbia Univ., Dept. Geol., Tech. Rept. 10, pp. 67, 1958.

36. Scheidegger, A. E., On the Theory of Evolution of River Nets, Bull. of Intern. Assoc. of Scientific Hydrology, Vol. 15, No. 1, pp. 109-115, 1970.

37. Shreve, R. L., Infinite Topologically Random Channel Networks, Jour. Geol., Vol. 75(2), pp. 178-186, 1967.

38. Schumm, S. A., Evolution of Drainage Systems and Slopes in Badlands at Perth Amboy, New Jersey, Bull. Geol. Soc. Am., Vol. 67, pp. 597-646, 1956.

39. Smart, J. S., Statistical Properties of Stream Lengths, Water Resources Research, Vol. 4, pp. 1001-1014, 1968.

40. Smart, J. S., Surban, A. J., Considine, J. P., Digital Simulation of Channel Networks, in Symposium on River Morphology, Inter. Assoc. Sci. Hydrol., Pub. 75, pp. 87-98, 1967.

41. Gray, D. M., Interrelationships of Watershed Characteristics, Jour. Geophy. Research, Vol. 66, No. 4, pp. 1215-1223, April, 1961.

42. Taylor, A. B., and Schwartz, H. E., Unit Hydrograph Lag and Peak Flow Related to Basic Characteristics, Trans. AGU, Vol. 33, pp. 235-246, 1952.

43. Indiana General Assembly, Indiana Water Resource Act, 1959, Annotated Indiana Statutes, Vol. 6, Part 2, pp. 330, The Bobbs-Merrill Co., Inc., Indianapolis, Indiana, 1970

44. Blank, D., and Delleur, J. W., A Program for Estimating Runoff from Indiana Watersheds, Part I. Linear System Analysis in Surface Hydrology and Its Application to Indiana Watersheds, Purdue University, Water Resources Research Center, Lafayette, Indiana, Technical Report No. 4, August, 1968.

45. Surkan, A. J., Synthetic Hydrographs: Effect of Network Geometry, Water Resources Research, Vol. 5, No. 1, pp. 112-128, February, 1969.

46. Chorley, R. J., (Ed.), Water, Earth, and Man, Methuen & Co., Ltd., London, pp. 325-326, 1969.

47. Leopold, L. B., Downstream Change of Velocity in Rivers, Am. Jour. of Science 25/, pp. 606-624, 1953.

48. Tennessee Valley Authority, and North Carolina State University, Watershed Research in Western North Carolina, A Study of the Effects of Agricultural Covers Upon the Hydrology of Small Watersheds, Final Report, June, 1970.

49. McCarthy, G. T., The Unit Hydrograph and Flood Routing, Unpublished Manuscript presented at a Conference of the North Atlantic Div., Corps of Engineers, War Department, 1938.

50. Meyer, O. H., Simplified Routing, Civil Eng., Vol. 11, No. 5, pp. 306-307, 1941.

51. Hayami, S., On the Propagation of Flood Waves, Kyoto University, Disaster Prevention Research Institute, Bull, 1, Kyoto, Japan, Dec., 1951.

52. Laurenson, E. M., Storage Analysis and Flood Routing in Long River Reaches, Jour. Geophy. Research, Vol. 64, No. 12, pp. 2423-2433, 1959.

53. Seddon, J. A., River Hydraulics, Trans. ASCE, Vol. 43, 179-243, 1900.

54. Sarma, P. B. S., Delleur, J. W., Rao, A. R., A Program in Urban Hydrology Part II. An Evaluation of Rainfall-Runoff Models for Small Urbanized Watersheds and the Effect of Urbanization on Runoff, Purdue University Water Resources Research Center, Lafayette, Indiana, Technical Report No. 9, October, 1969.

55. Copper, J., and Steinberg, D., Introduction to Methods of Optimization, W. B. Saunders Co., Philadelphia, 1970.

56. Purdue University, The Agronomy Handbook, Agricultural Extension Service, Nov. 1961.

57. Bushnell, T. M., A Story of Hoosier Soils and Ramblets in Pedological Fields, PEDA-Products, 1958.

58. Marie, J. R., and Swisshelm, R. V., Jr., Evaluation of and Recommendations for Surface Water Data Program in Indiana, U.S.G.S. Water Resources Division, Open File Report, Indianapolis, Indiana, 1970.

59. Marie, J. R., Personal Communication.

60. Betcher, D. J., Gregg, L. E., and Woods, K. B., The Formation Distribution and Engineering Characteristics of Soils, Joint Highway Research Project, Engineering Bulletin, Purdue University, Research Series No. 87, Highway Research Bulletin No. 10, January, 1943.

61. Wu, I. P., Delleur, J. W., Diskin, M. H., Determination of Peak Discharge and Design Hydrographs for Small Watersheds in Indiana, Indiana Flood Control and Water Resources Commission, Indiana State Highway Commission and Purdue University, October, 1964.

62. Harley, B. M., Perkins, F. E., and Eagleson, P. S., A Modular Distributed Model of Catchment Dynamics, Ralph M. Parsons Laboratory for Water Resources and Hydrodynamics, Report No. 133, Dec., 1970.

63. Bravo, C. A., Harley, B. M., Perkins, F. E., Eagleson, P. S., A Linear Distributed Model of Catchment Runoff, M.I.T., Hydrodynamics Laboratory, Report 123, June 1970.

64. Health Sciences Facility, UCLA, BMD2R-Multiple Regression - Version of May 2, 1966.

65. U. S. Department of Commerce, Weather Bureau, Climatic Data Indiana.

66. U. S. Department of the Interior, Geological Survey, Water Resources Data for Indiana, Published annually.

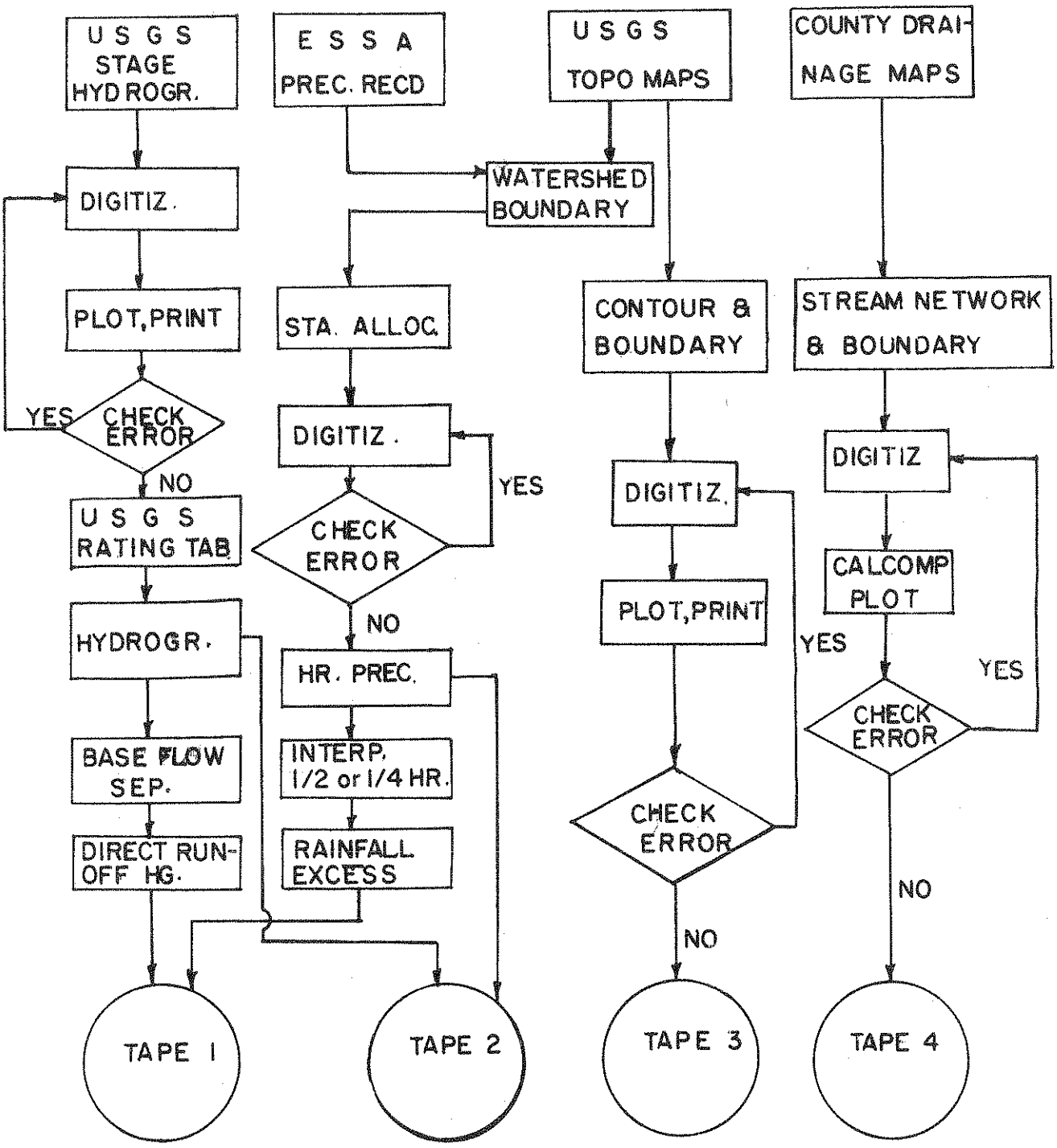

FIGURE 3-1 DATA ACQUISITION PROCEDURE

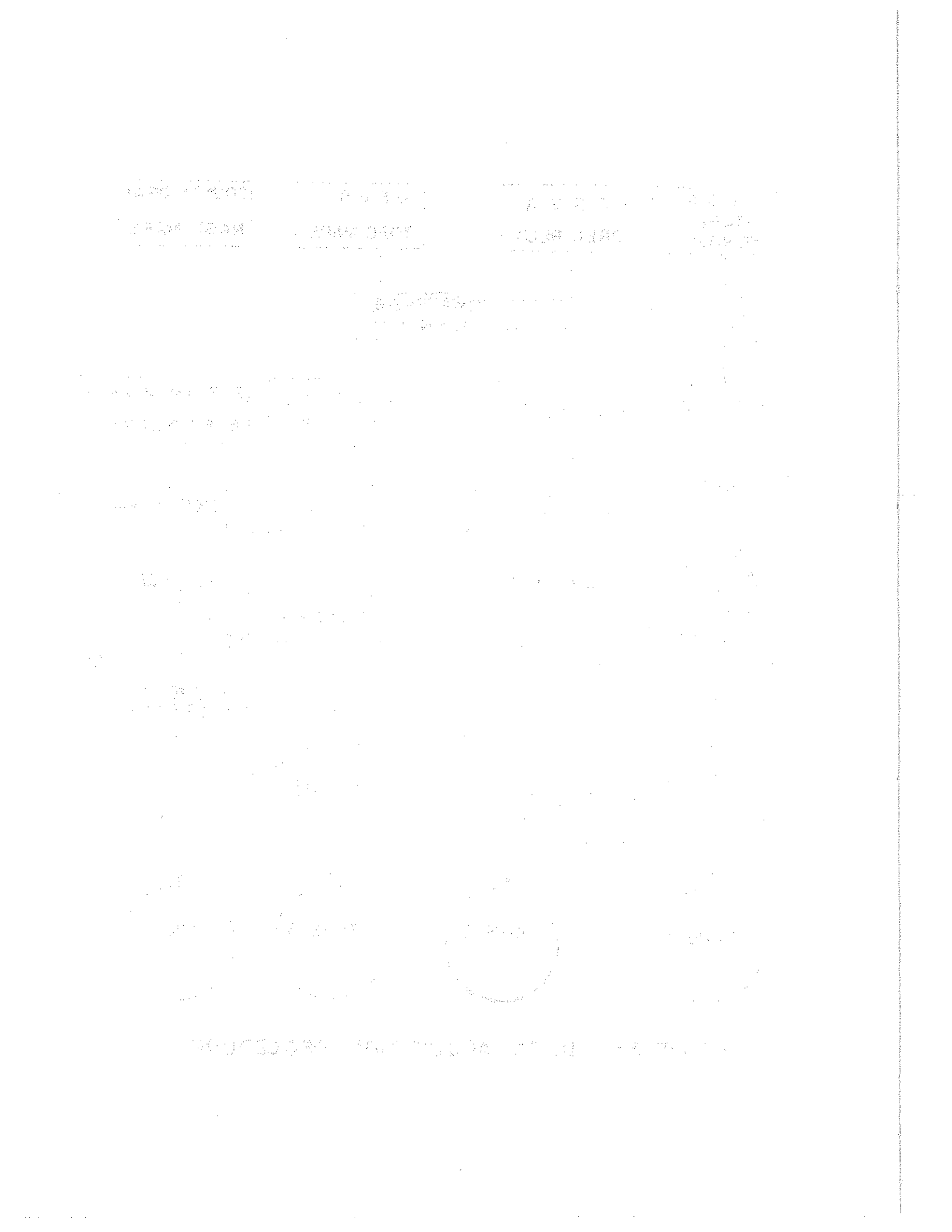

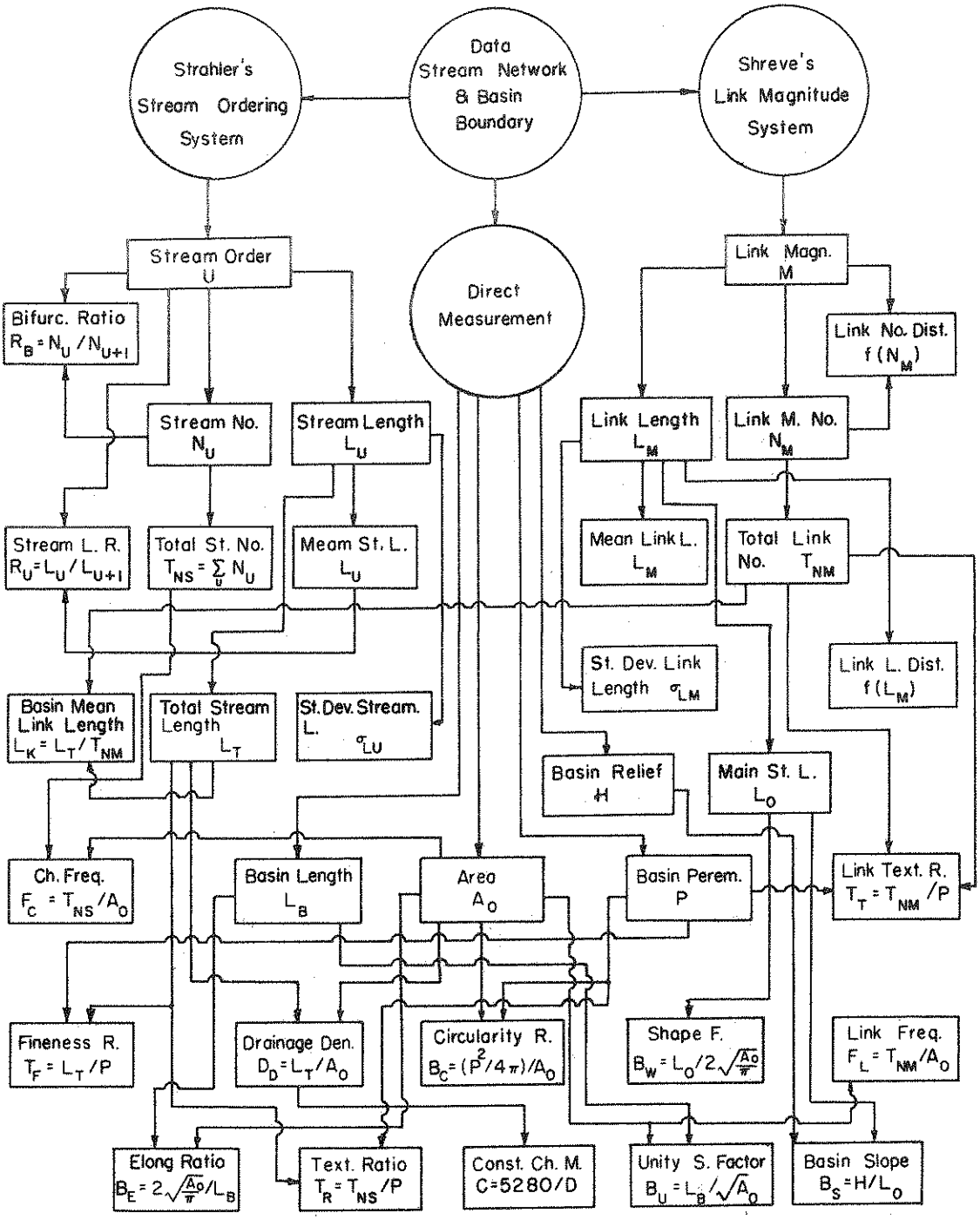

FIGURE 4-1 INTER-RELATED SCHEME OF GEOMORPHIC PARAMETERS

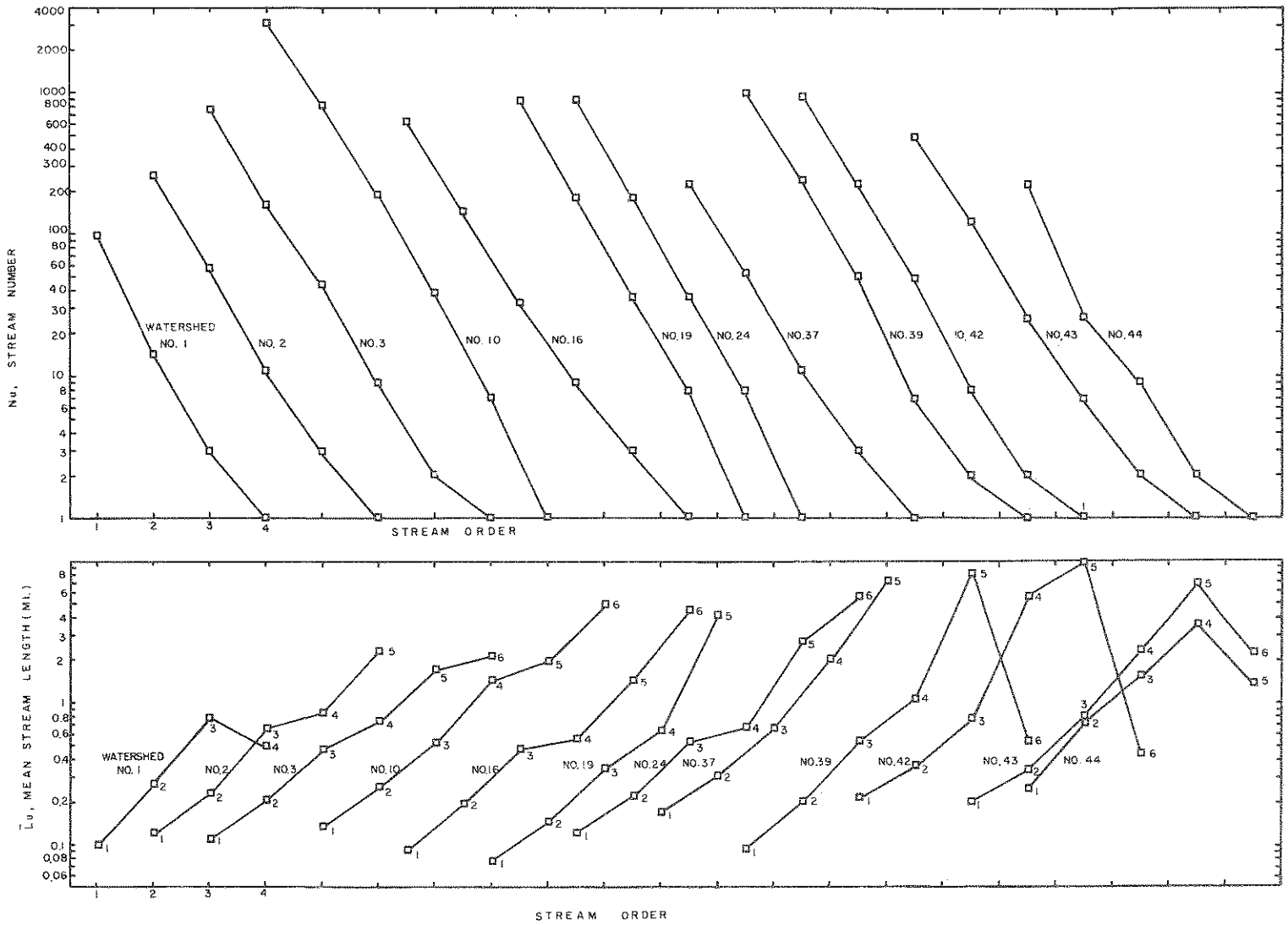

FIGURE 4-2 LAWS OF STREAM NUMBERS AND STREAM LENGTHS

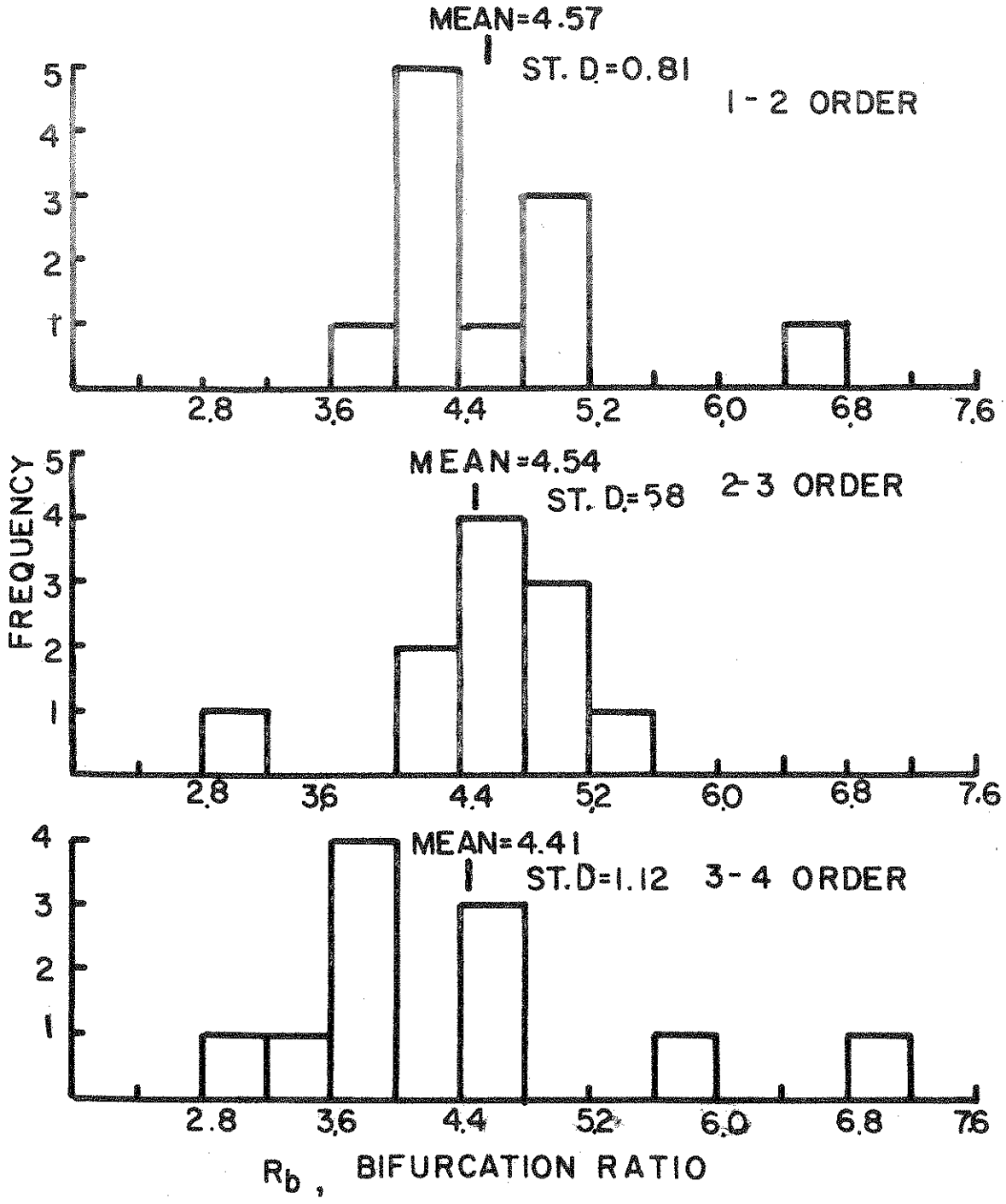

FIGURE 4-3. DISTRIBUTION OF BIFURCATION RATIO

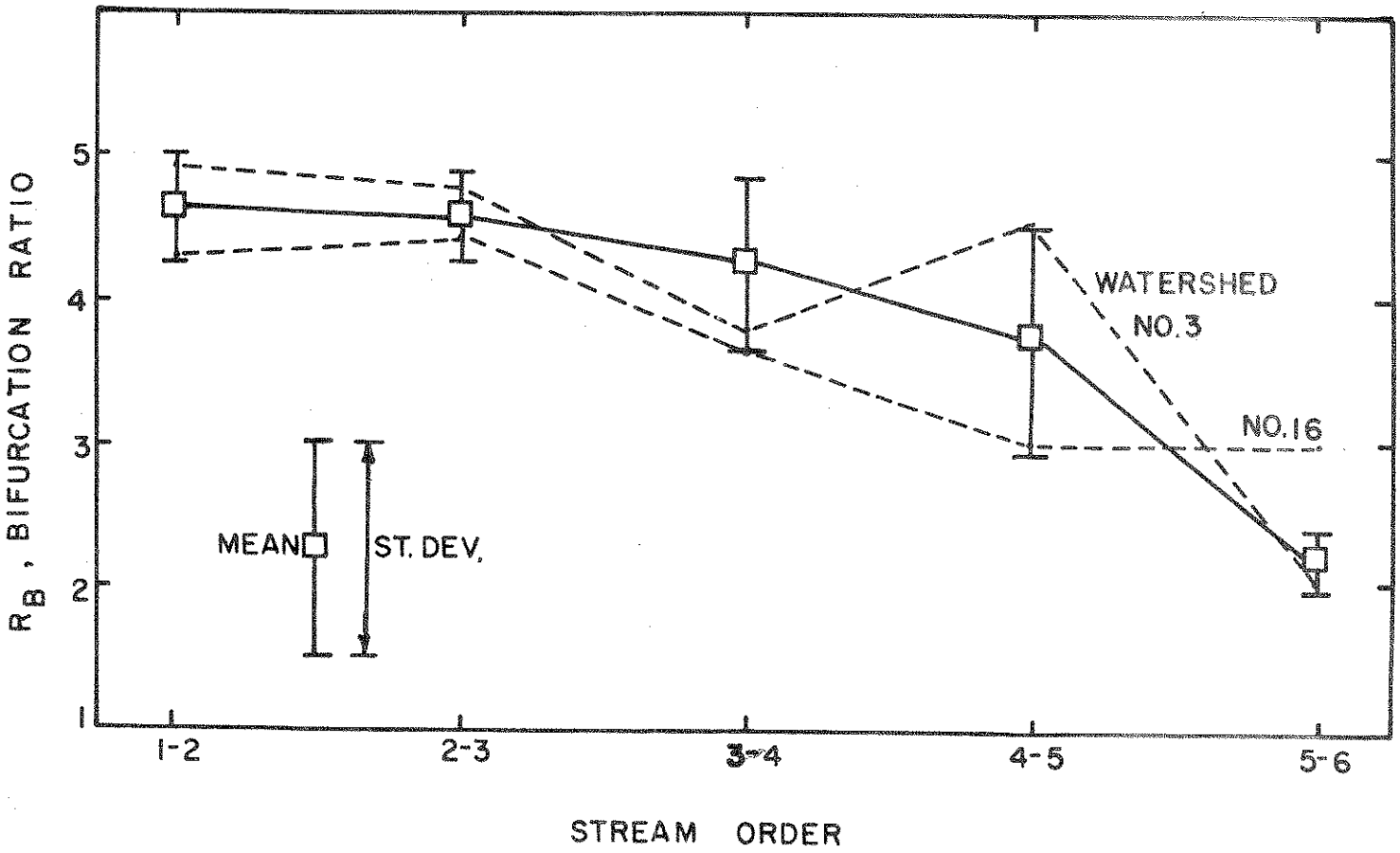

FIGURE 4-4a BIFURCATION RATIOS VS. STREAM ORDERS

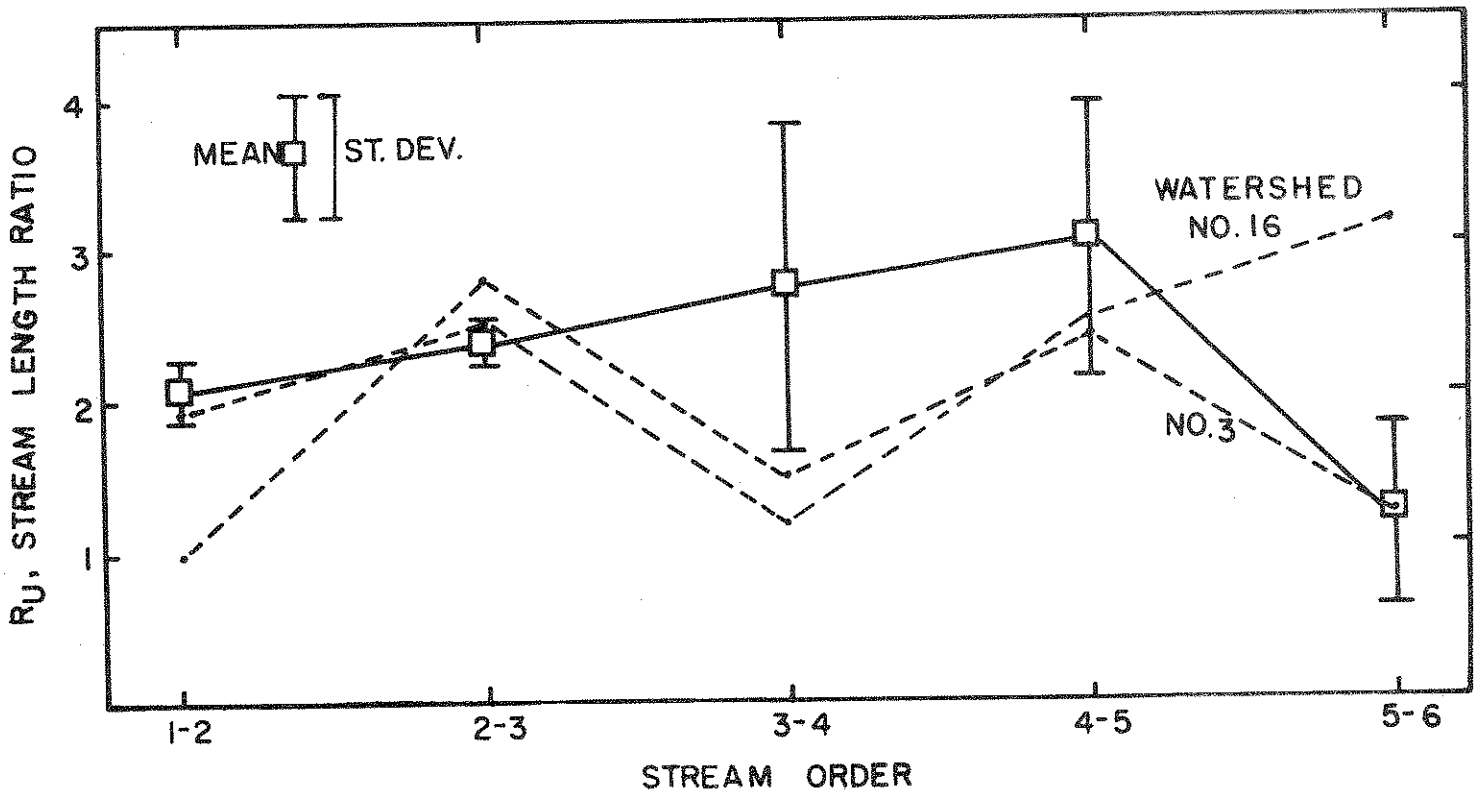

FIGURE 4-4b STREAM LENGTH RATIOS VS. STREAM ORDERS

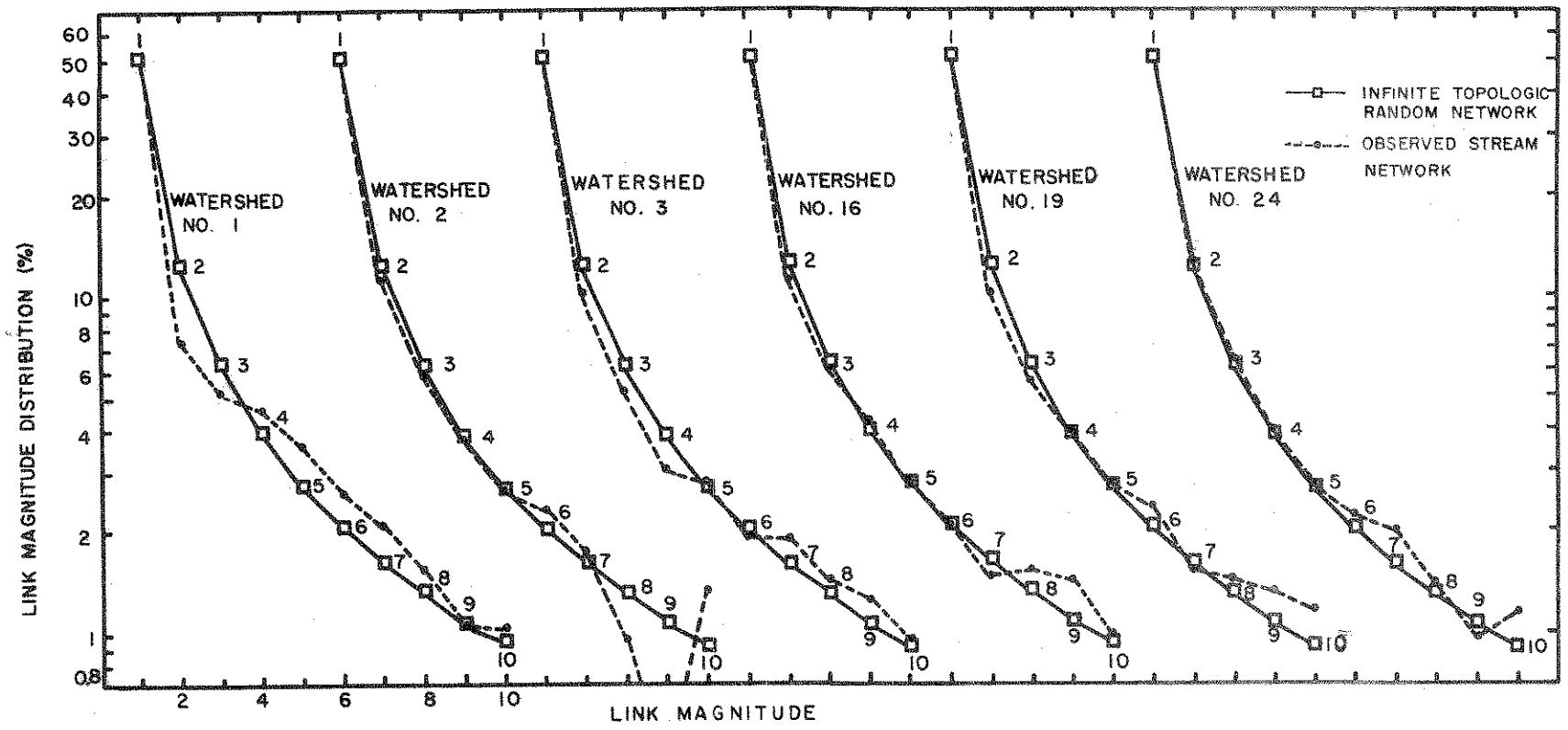

FIGURE 4-5 LINK NUMBER DISTRIBUTION

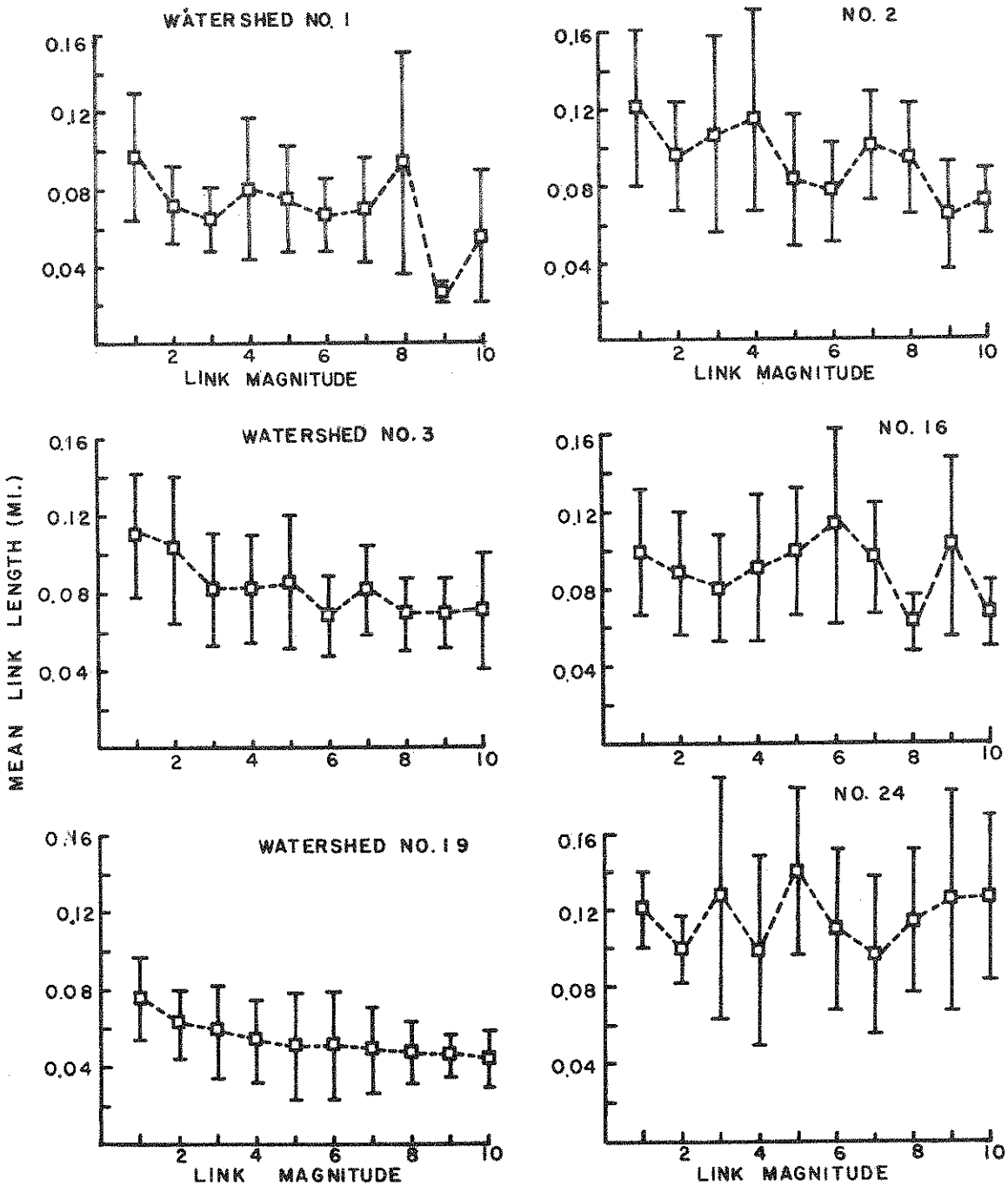

FIGURE 4-6 MEANS AND STANDARD DEVIATIONS OF LINK LENGTHS

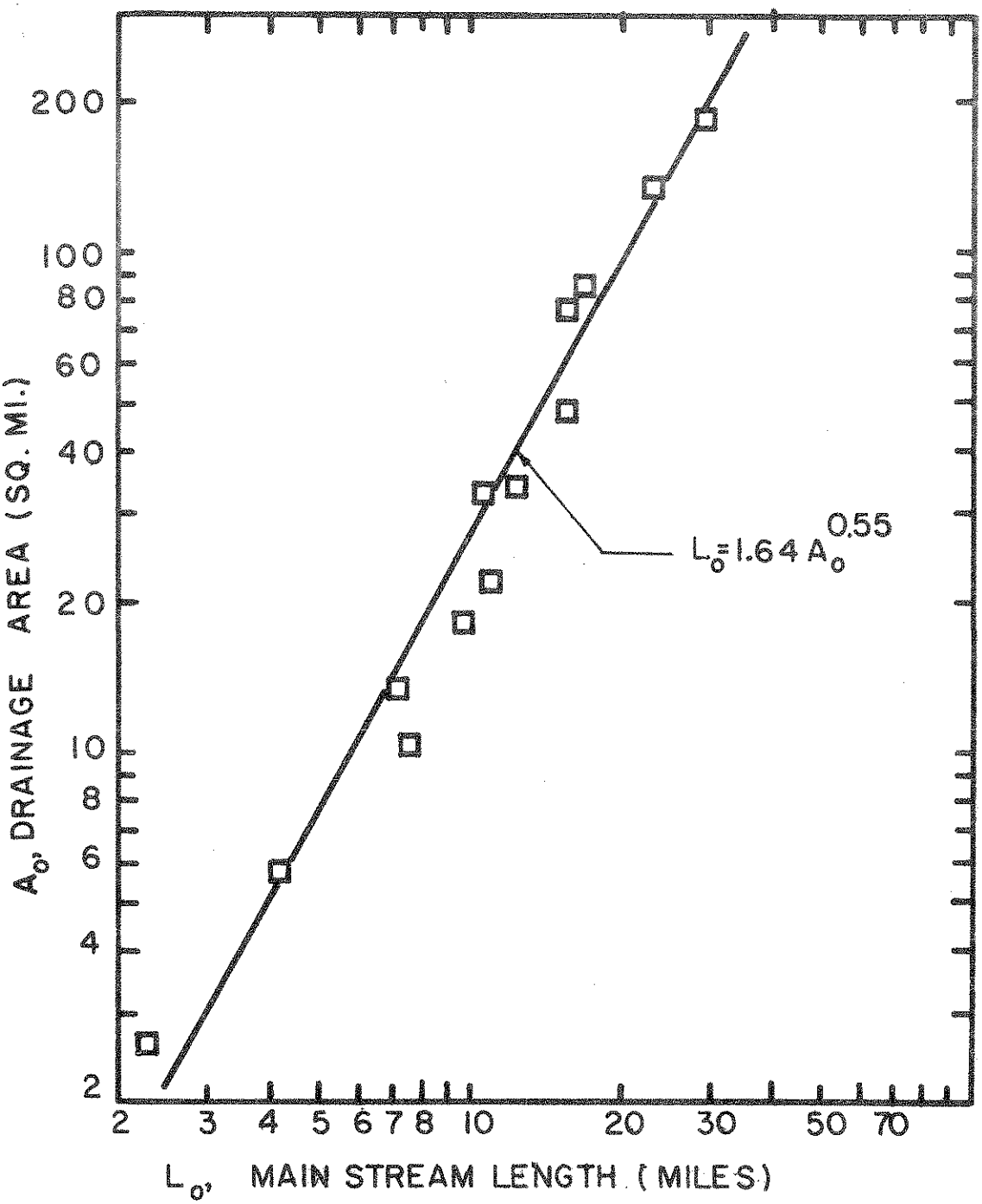

FIGURE 4-7 MAIN STREAM LENGTH AND DRAINAGE AREA

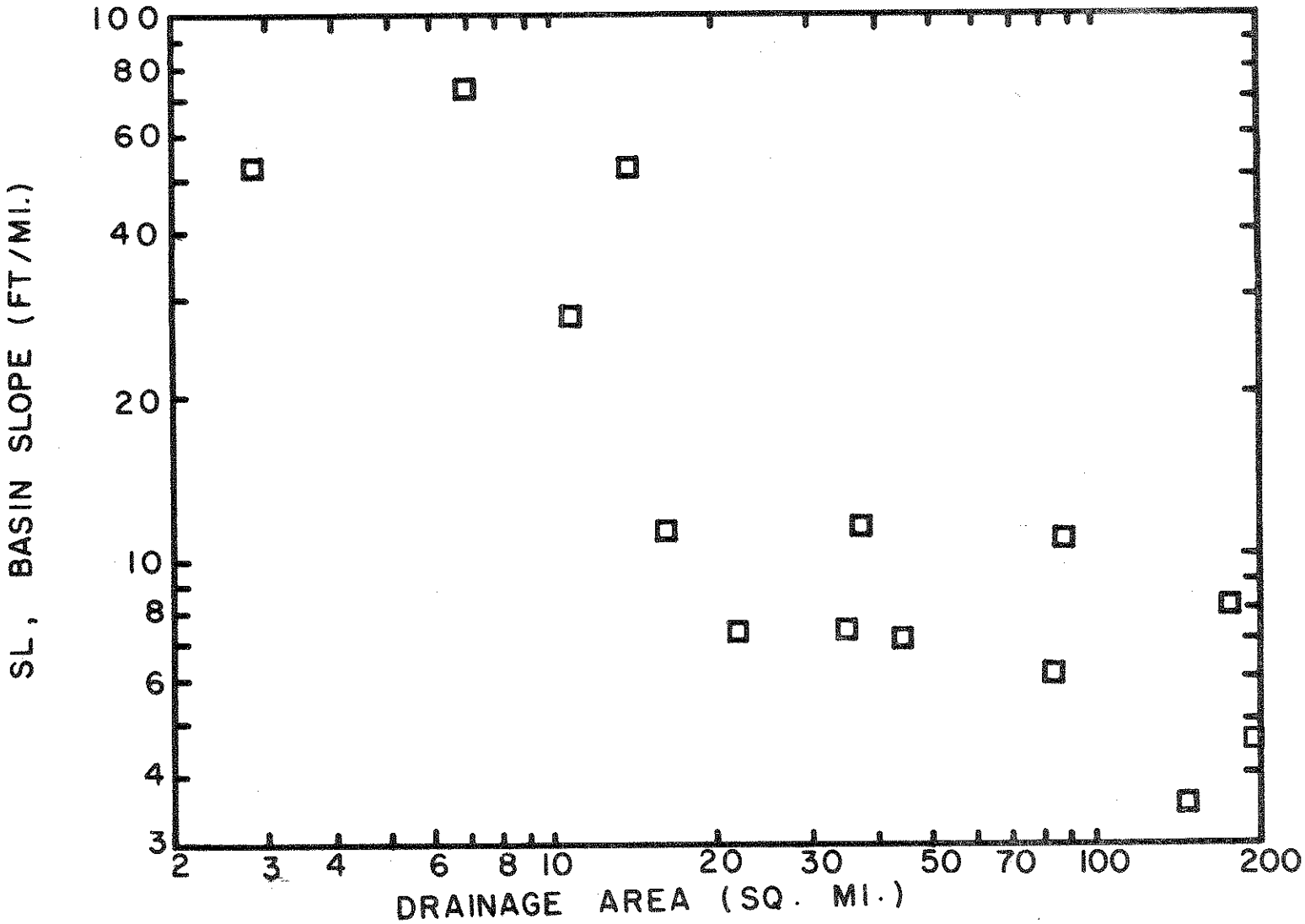

FIGURE 4-8 BASIN SLOPES VS. DRAINAGE AREAS

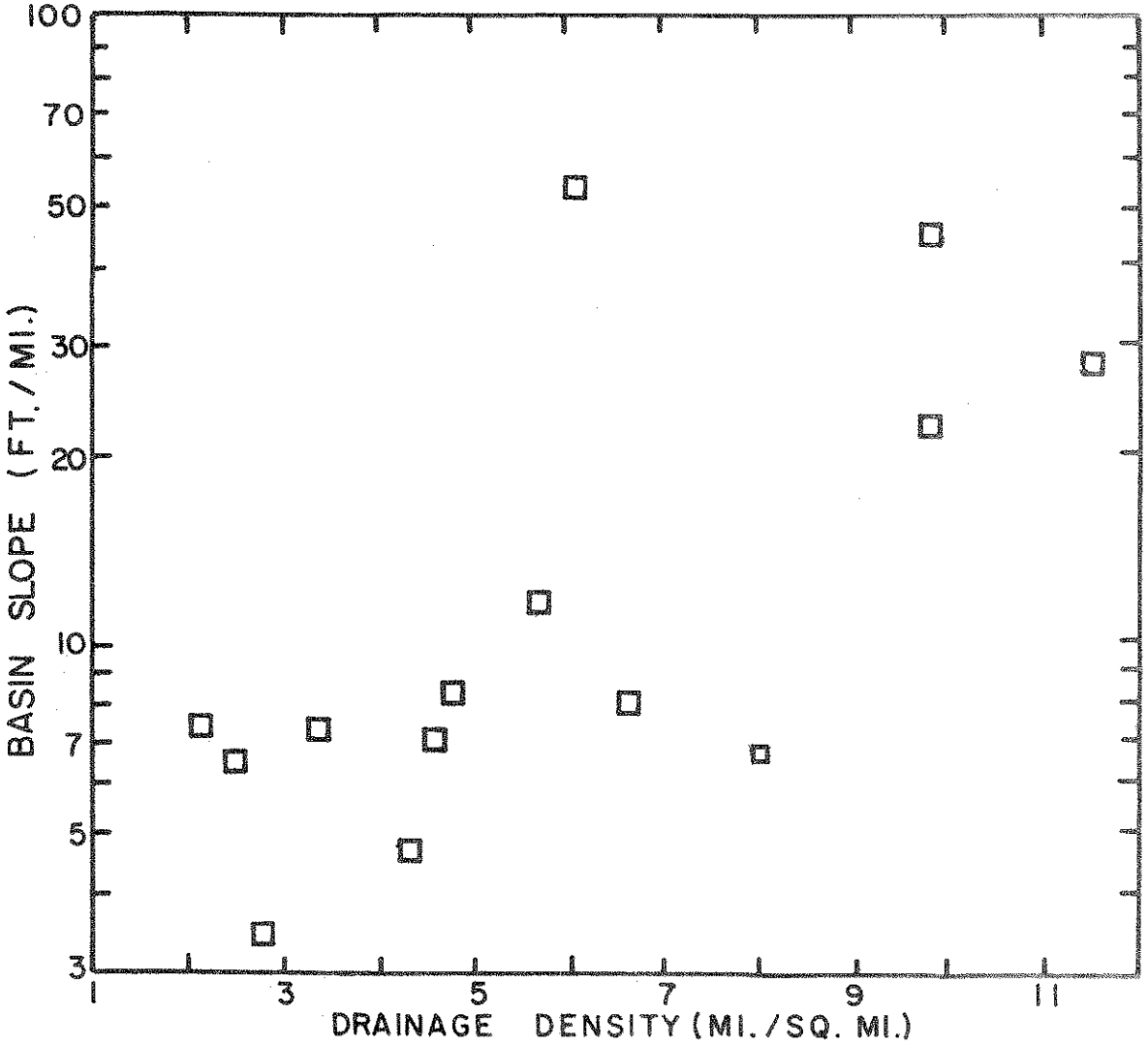

FIGURE 4-9 DRAINAGE DENSITY AND BASIN MEAN SLOPE

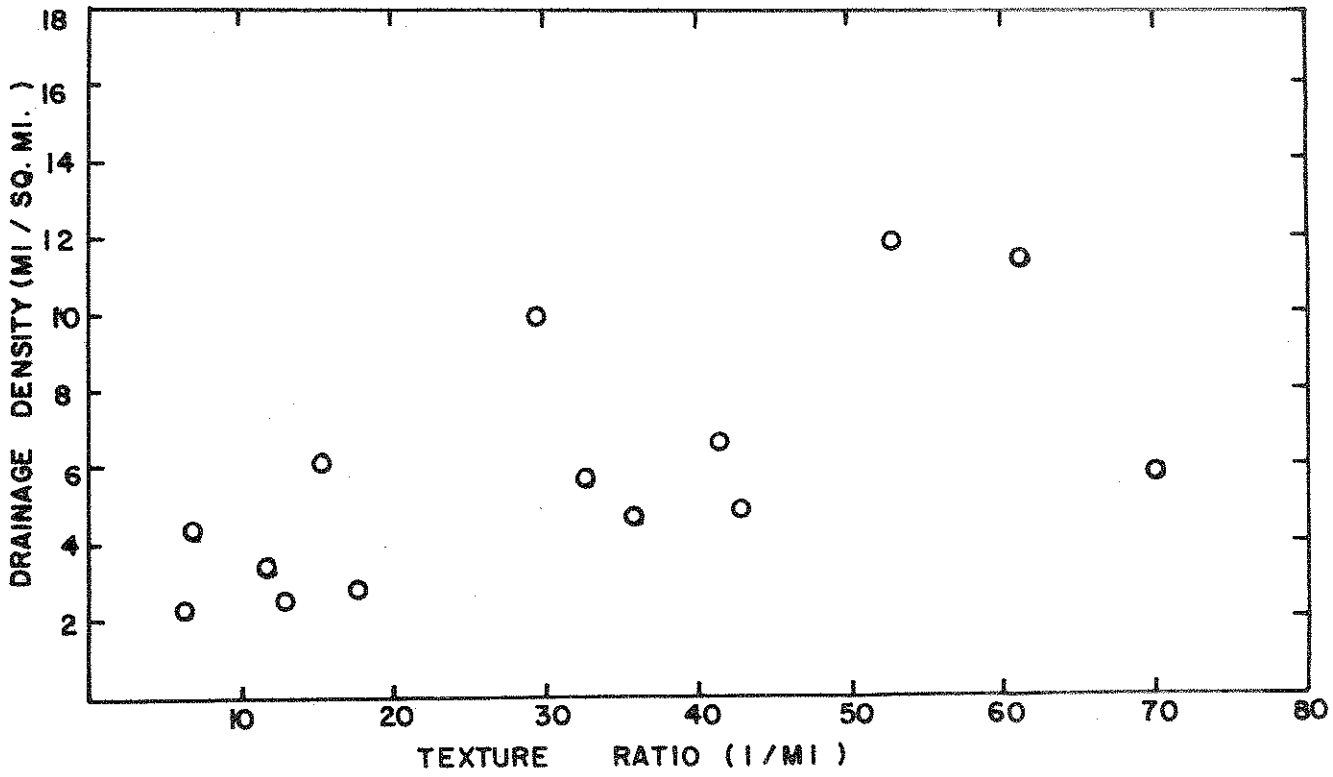

FIGURE 4-10 DRAINAGE DENSITY AND TEXTURE RATIO

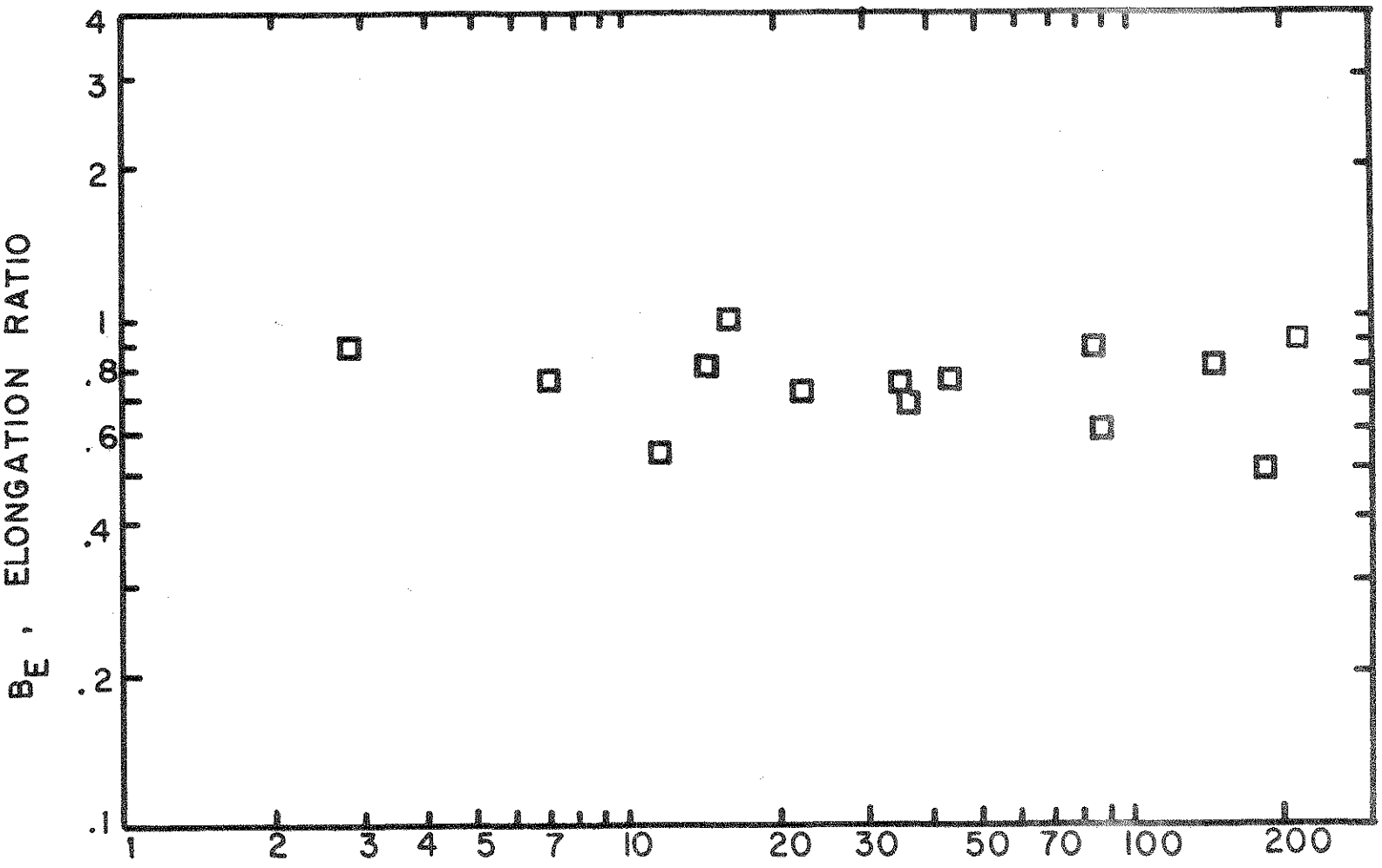

FIGURE 4-11 DRAINAGE AREA VS. ELONGATION RATIO

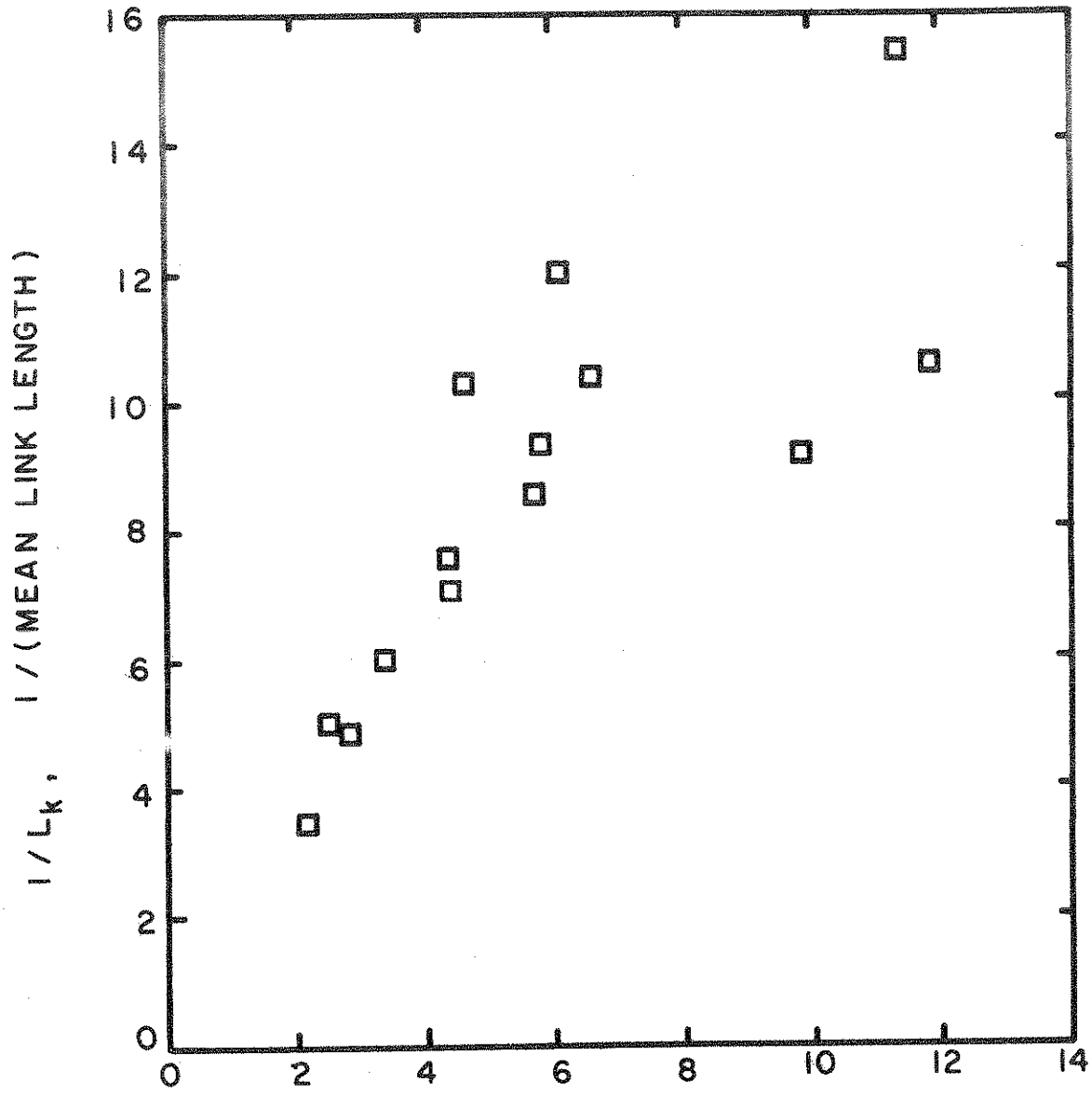

FIGURE 4-12 DRAINAGE DENSITY VS. MEAN LINK LENGTH

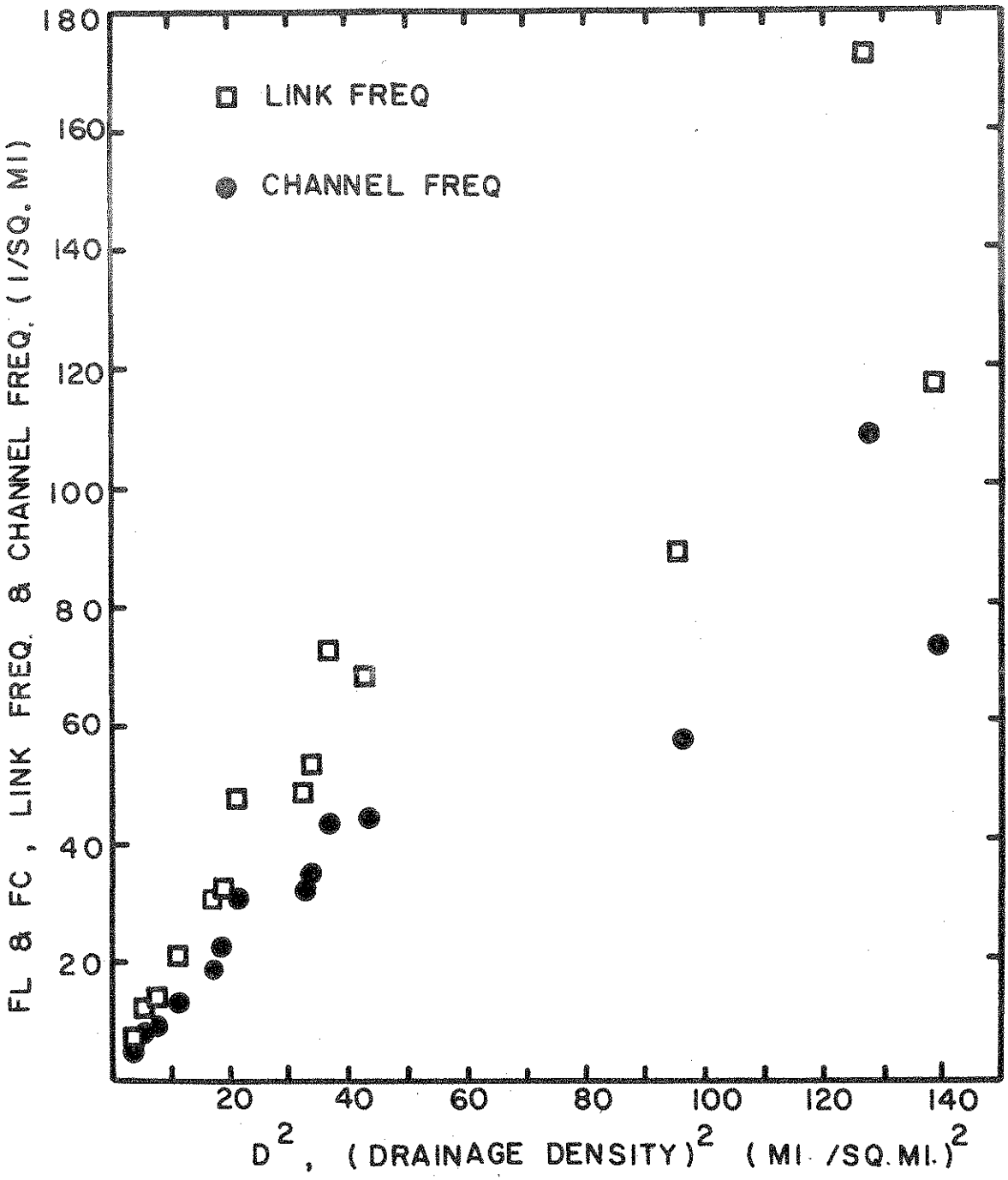

FIGURE 4-13 DRAINAGE DENSITY VS. LINK FREQUENCY AND CHANNEL FREQUENCY

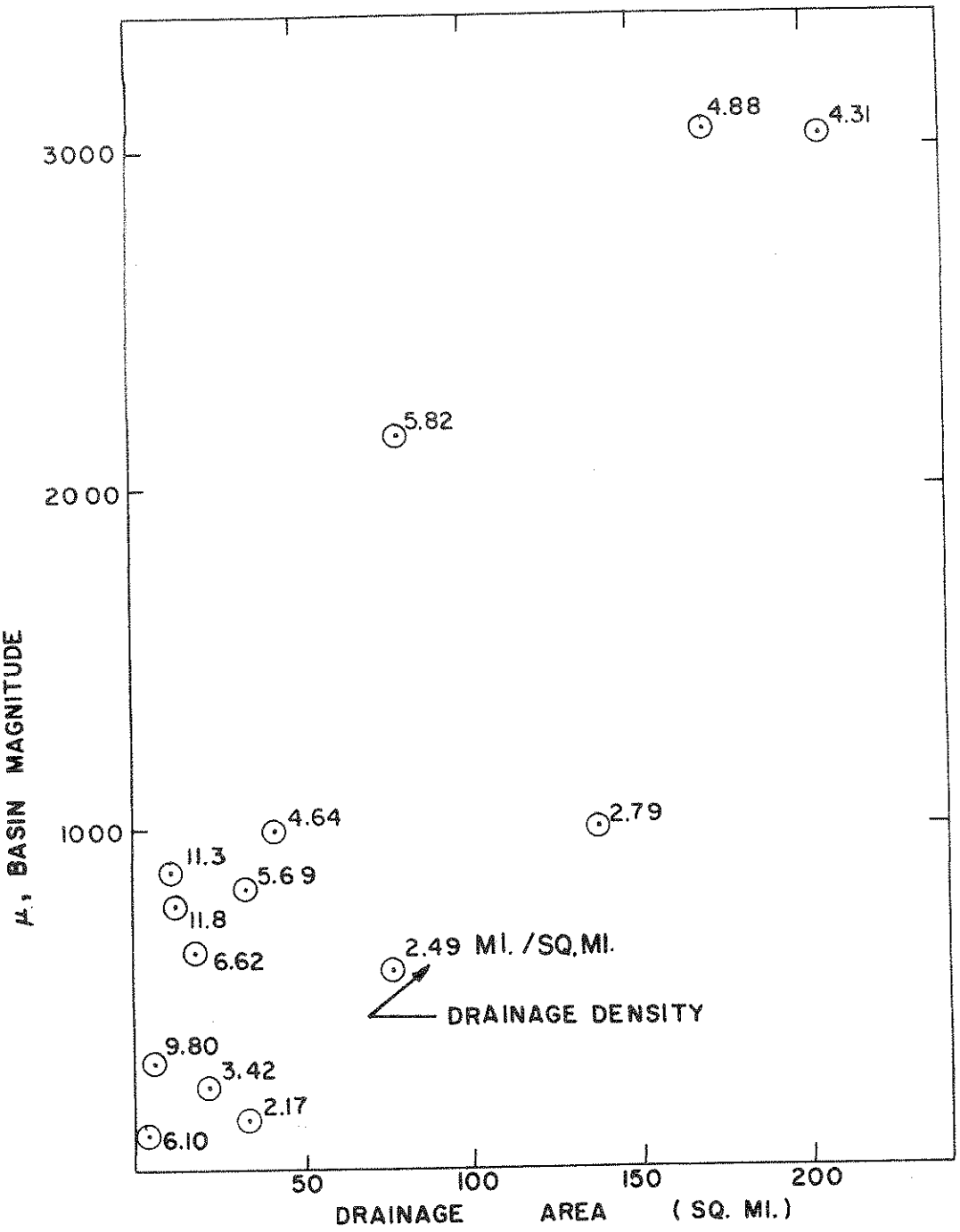

FIGURE 4-14 LINK MAGNITUDE VS. DRAINAGE AREA WITH DRAINAGE DENSITY AS PARAMETER

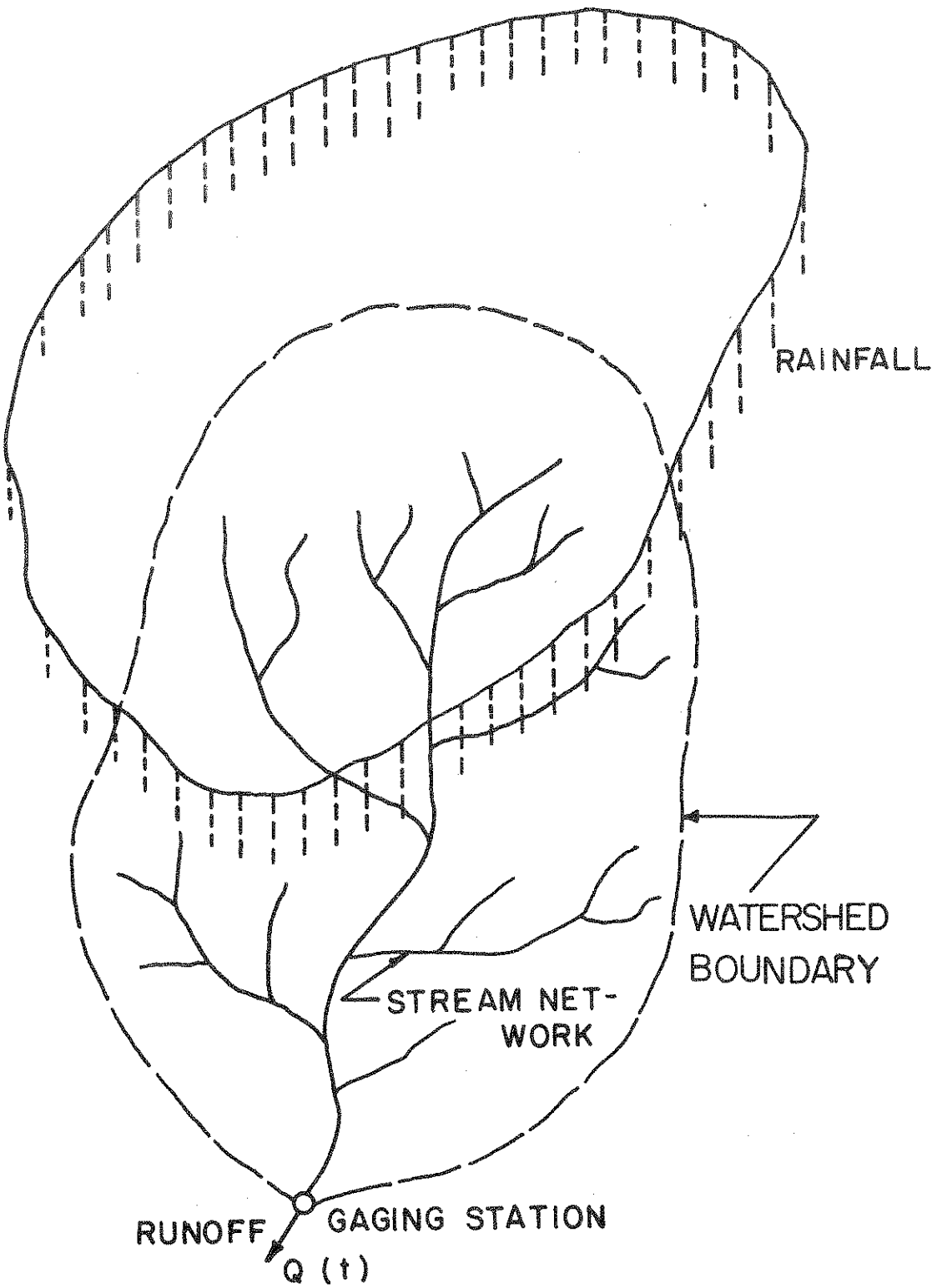

FIGURE 5-1 NATURAL WATERSHED SYSTEM

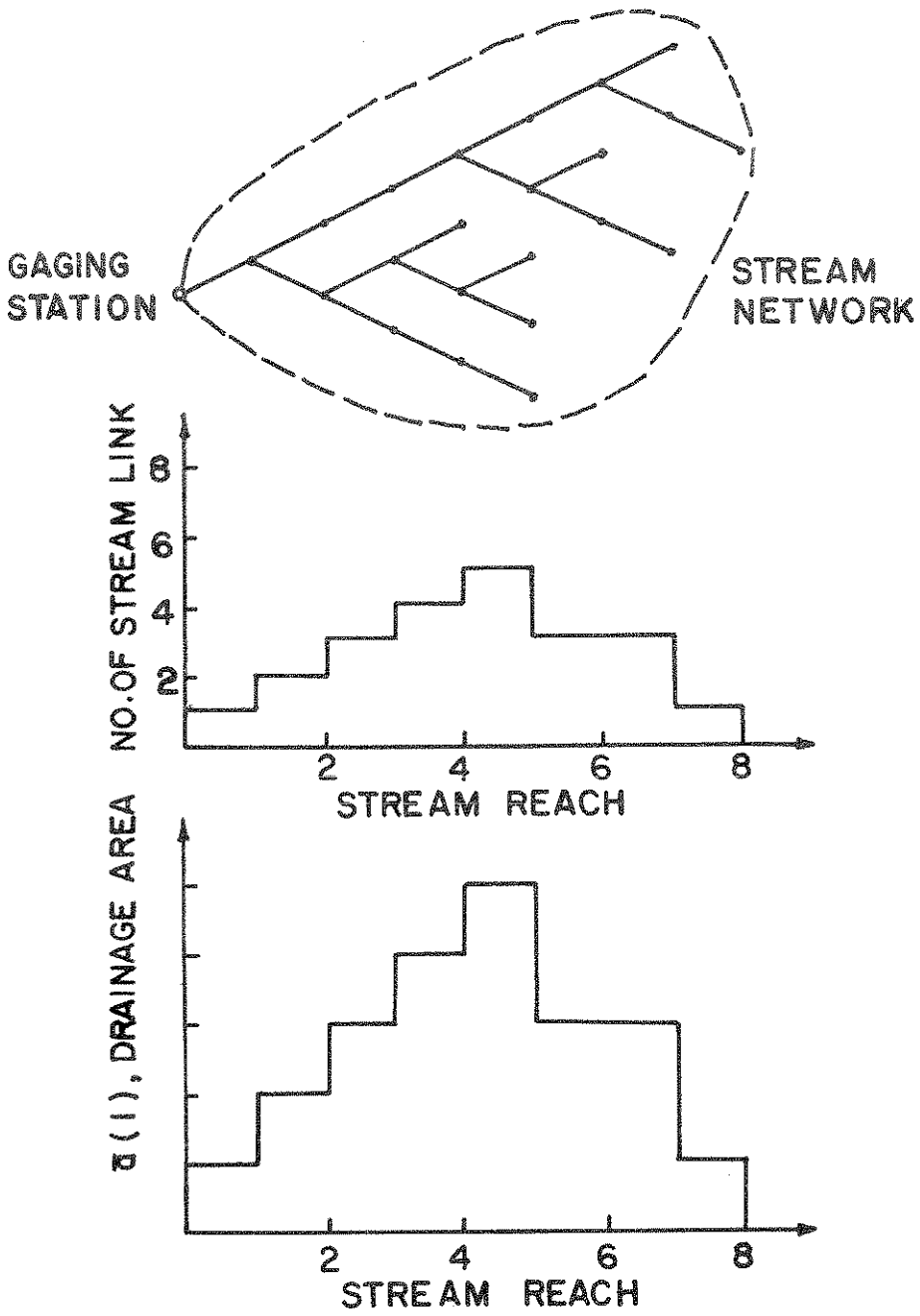

FIGURE 5-2 DRAINAGE AREA DISTRIBUTION ALONG THE STREAM REACHES

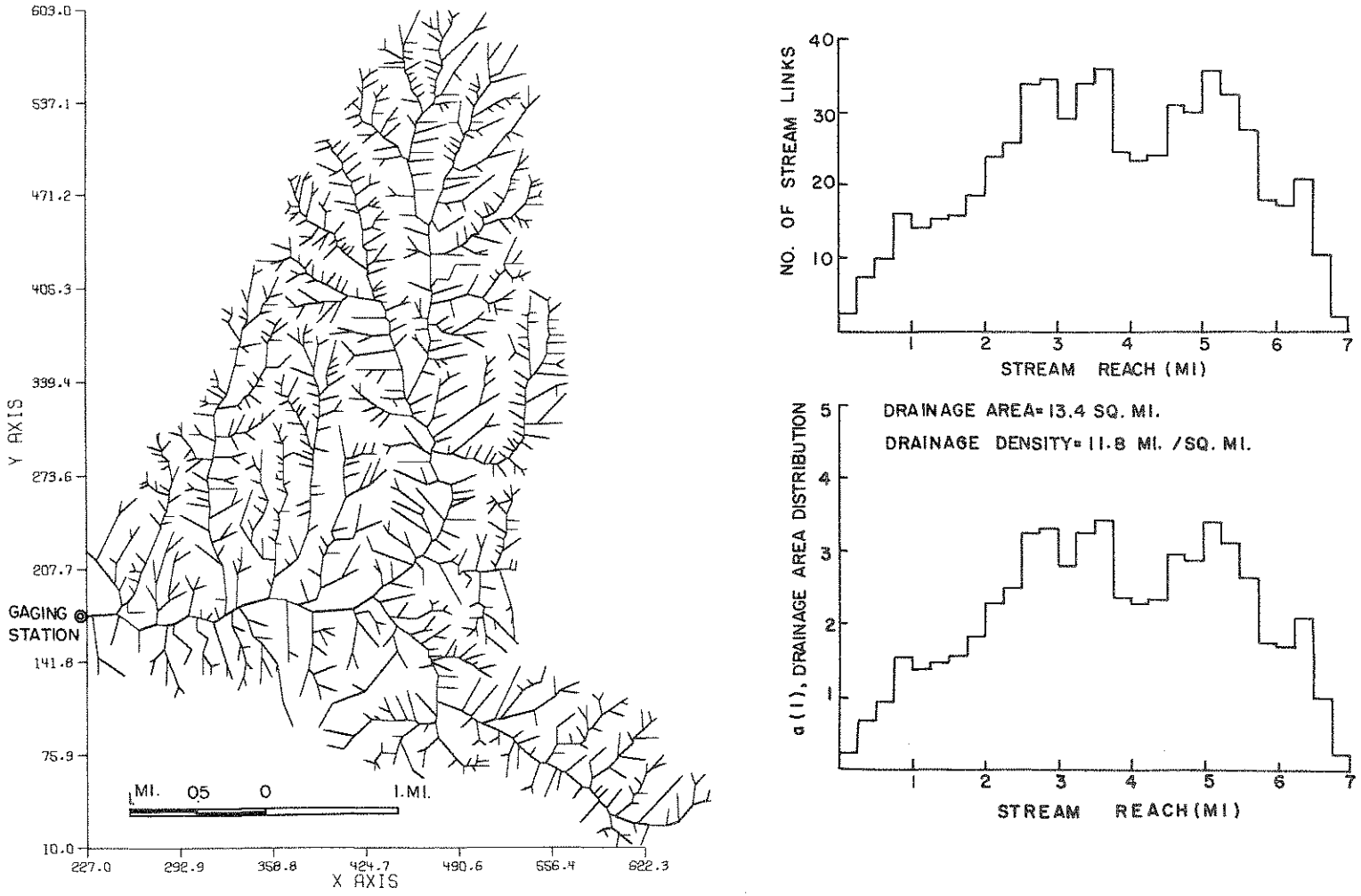

FIGURE 5-3 EXAMPLE OF DRAINAGE AREA DISTRIBUTION ALONG THE STREAM REACHES ; BEAN BLOSSOM CREEK AT BEAN BLOSSOM , INDIANA

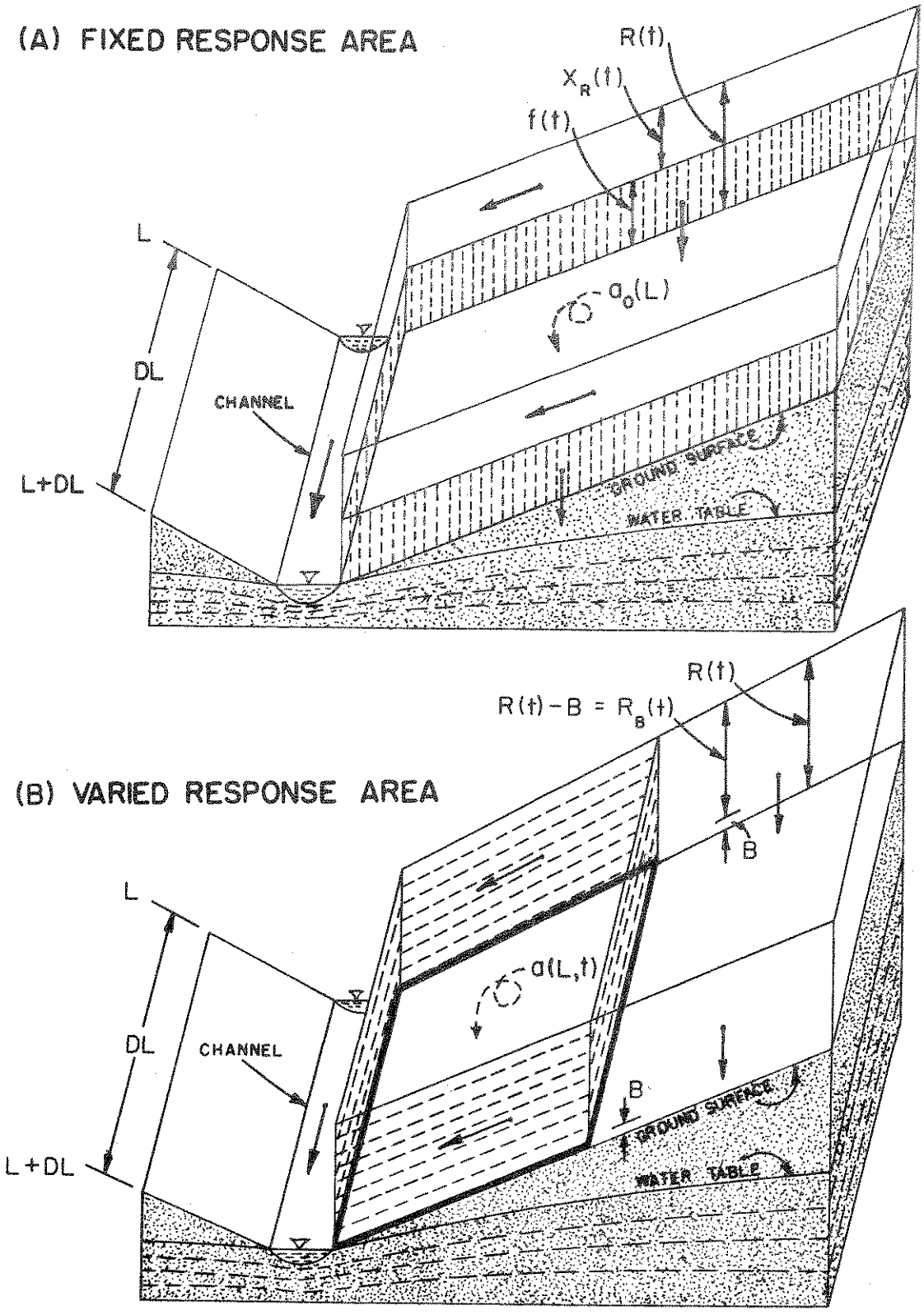

FIGURE 5-4 FIXED AND VARIED RESPONSE AREA CONCEPTS

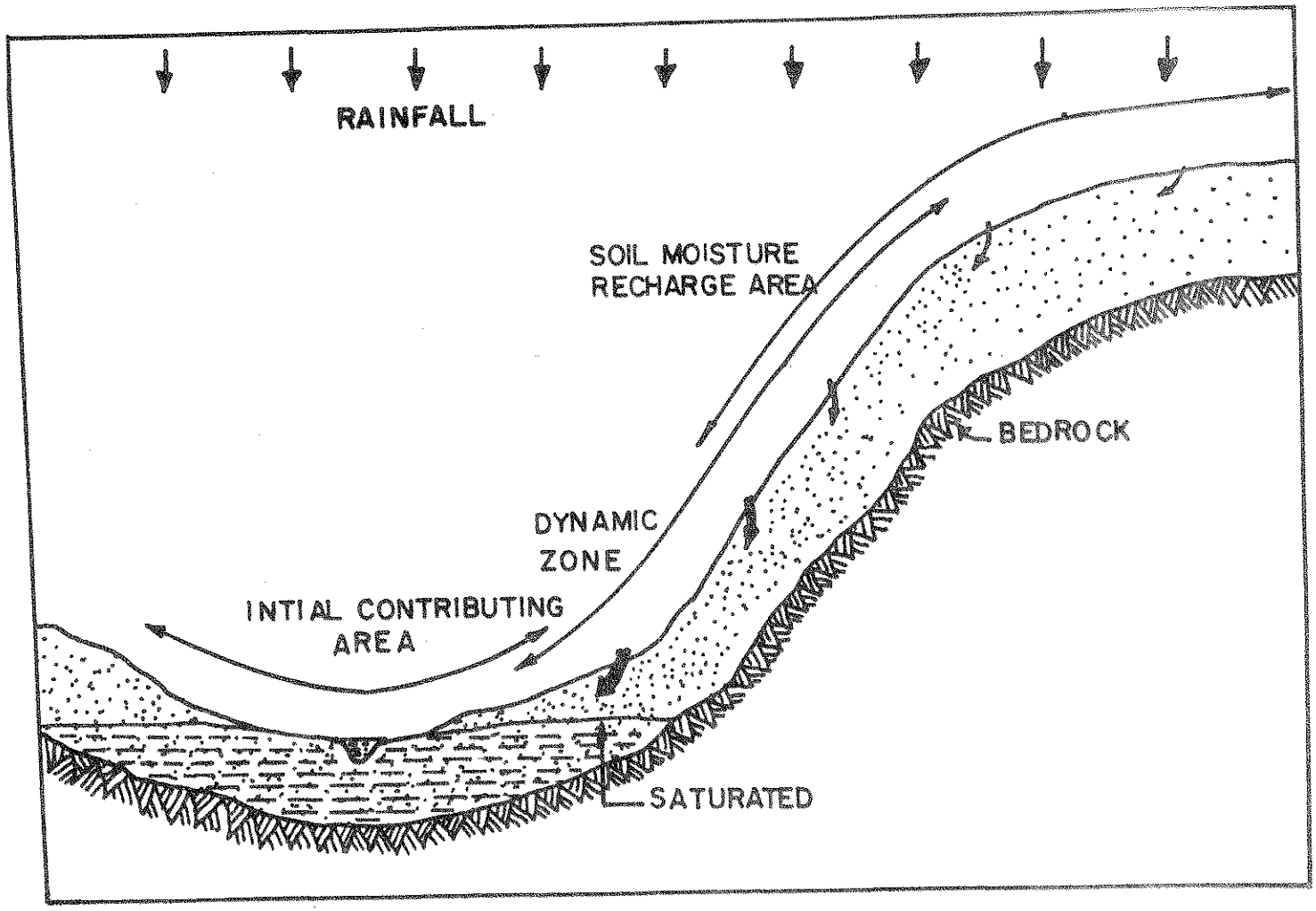

FIGURE 5-5 DYNAMIC WATERSHED CONCEPT (SOURCE : TVA, 1965)

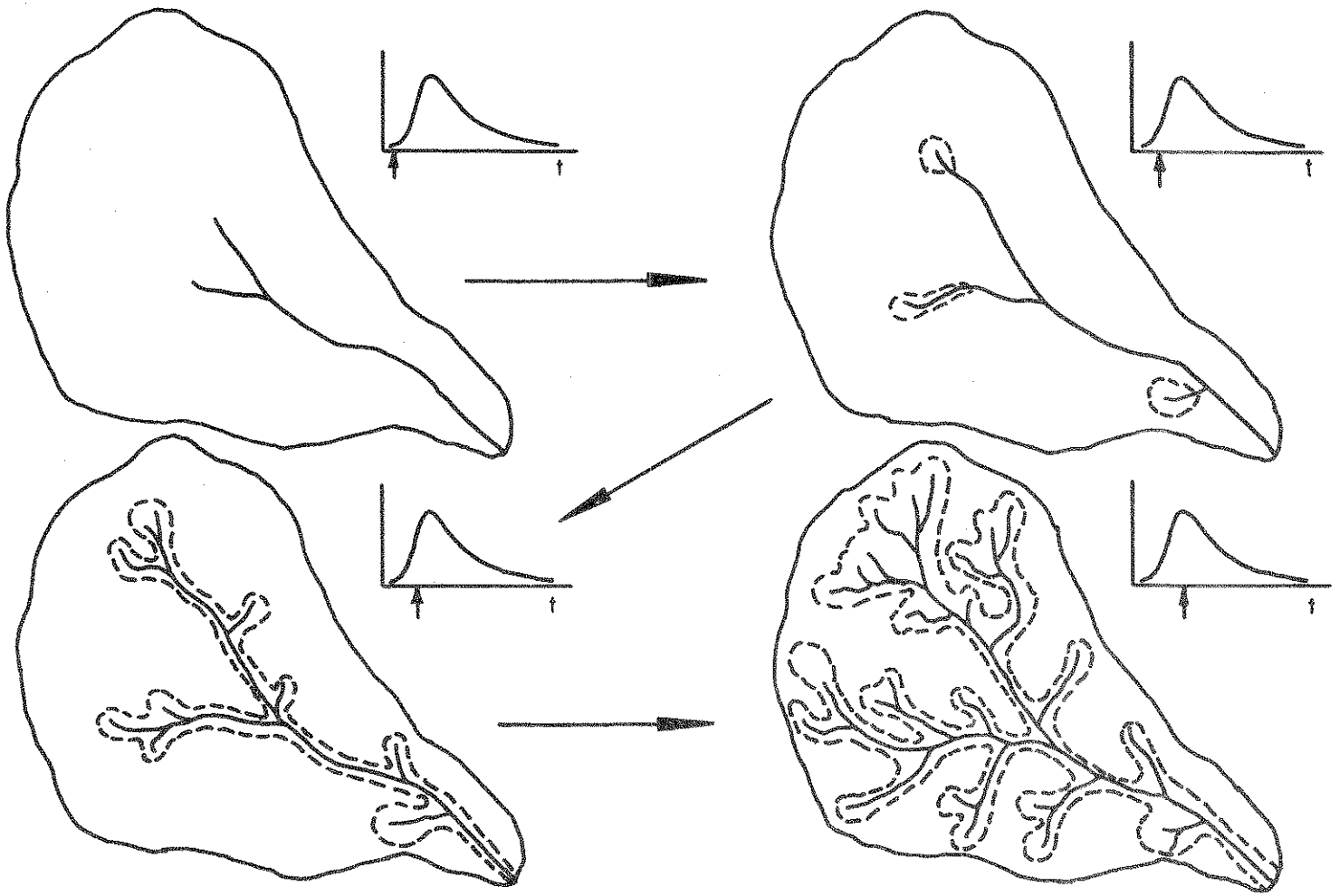

FIG. 5-6 A TIME-LAPSE VIEW OF A BASIN SHOWING EXPANSION OF THE SOURCE AREA AND THE CHANNEL SYSTEM DURING A STORM (SOURCE: NUTTER AND HEWLETT, 1971)

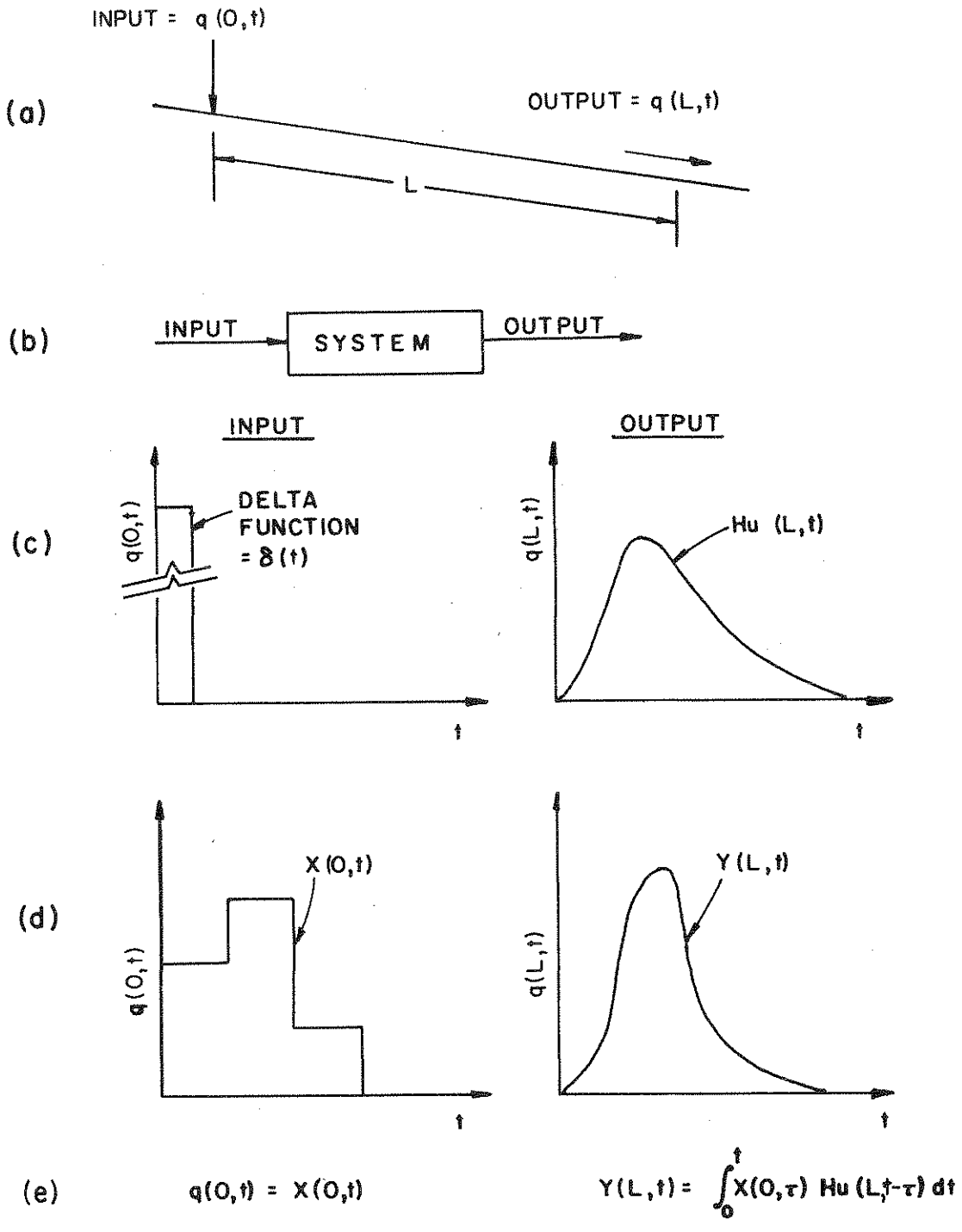

FIG. 5-7 PHYSICAL DIAGRAM OF UPSTREAM INFLOW INSTANTANEOUS UNIT HYDROGRAPH FOR SINGLE STREAM REACH

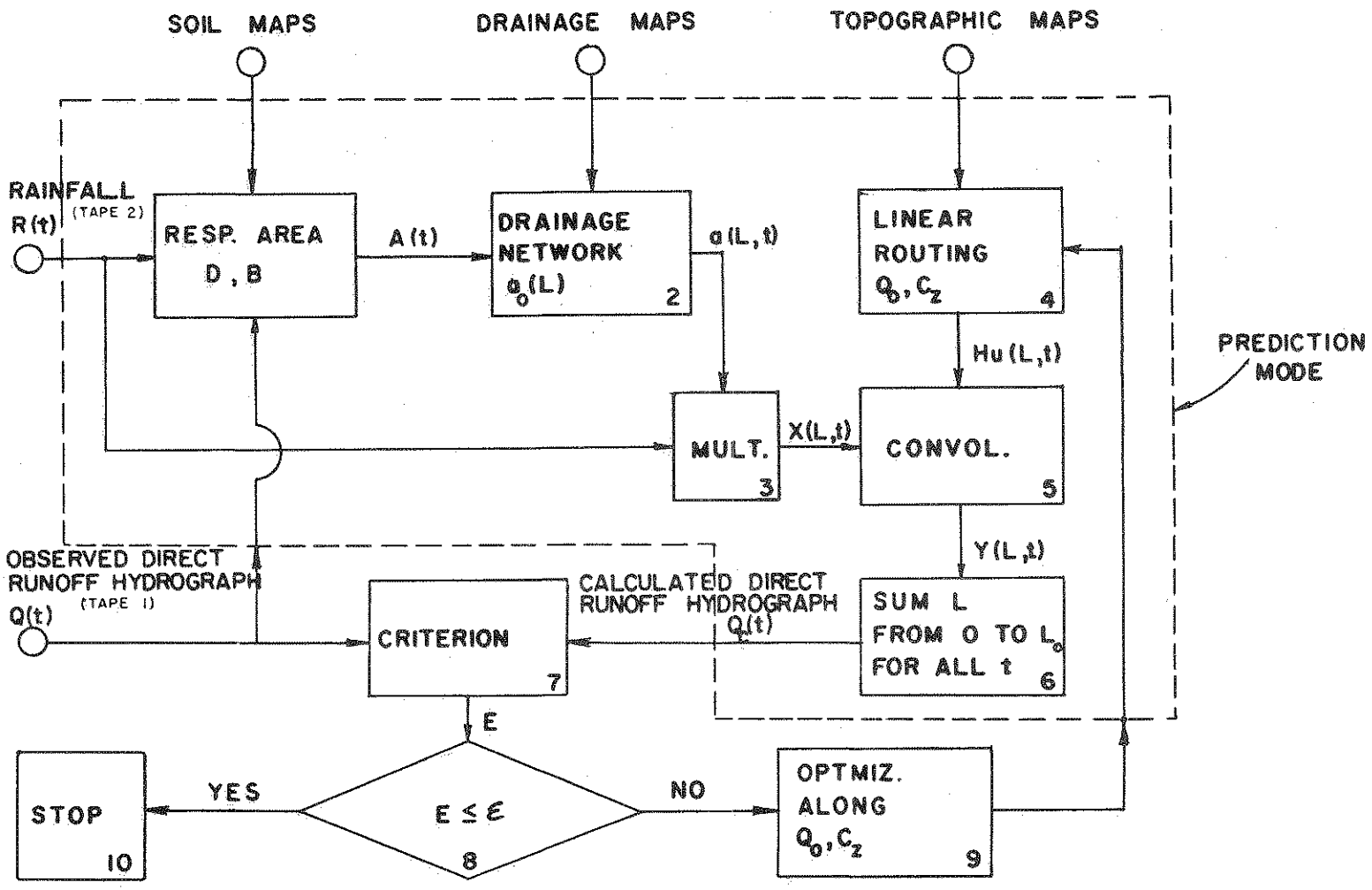

FIG. 5-8 FLOW DIAGRAM OF SYSTEM PARAMETERS AND RUNOFF ESTIMATIONS

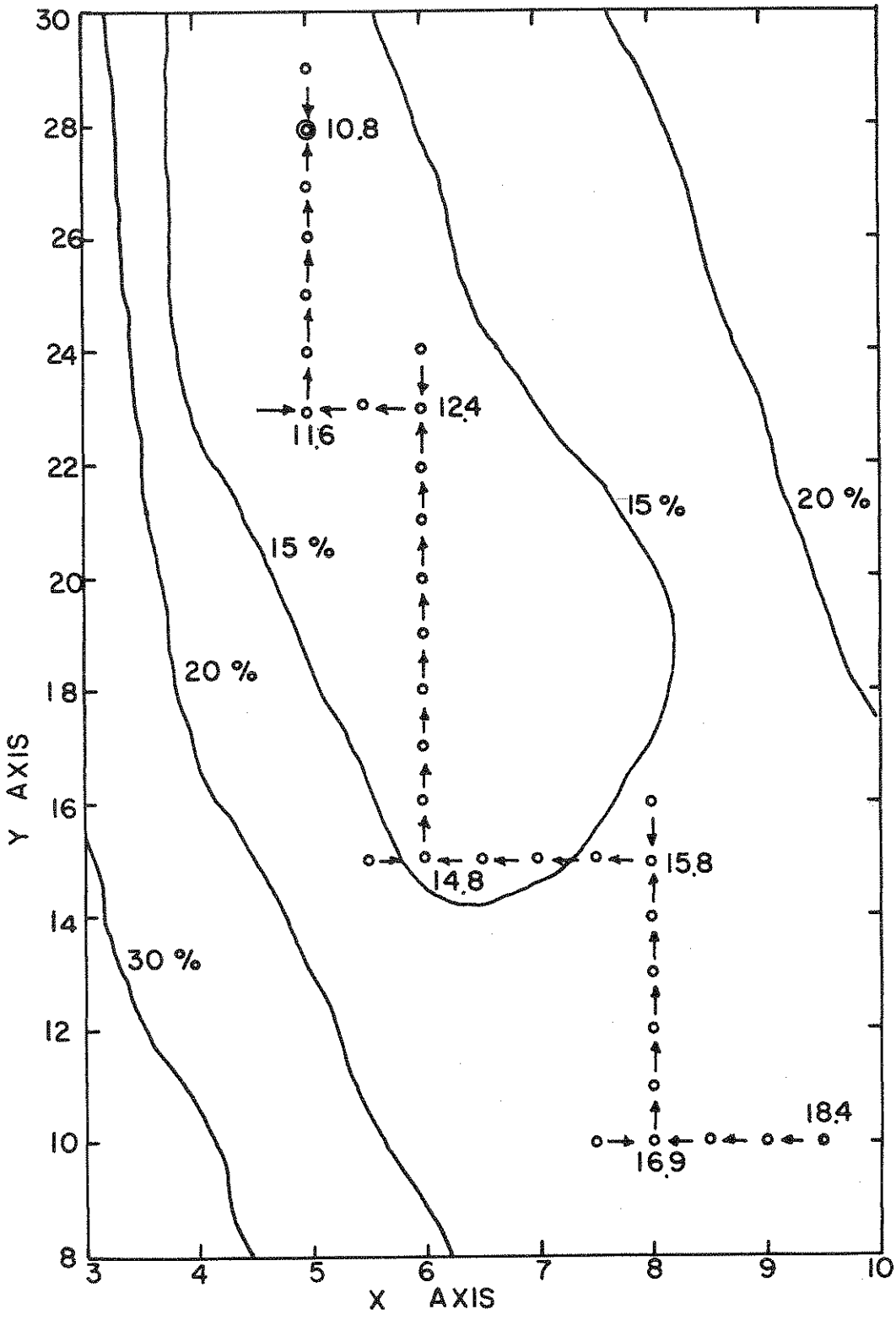

FIGURE 5-9 UNIT DIRECTION SEARCH

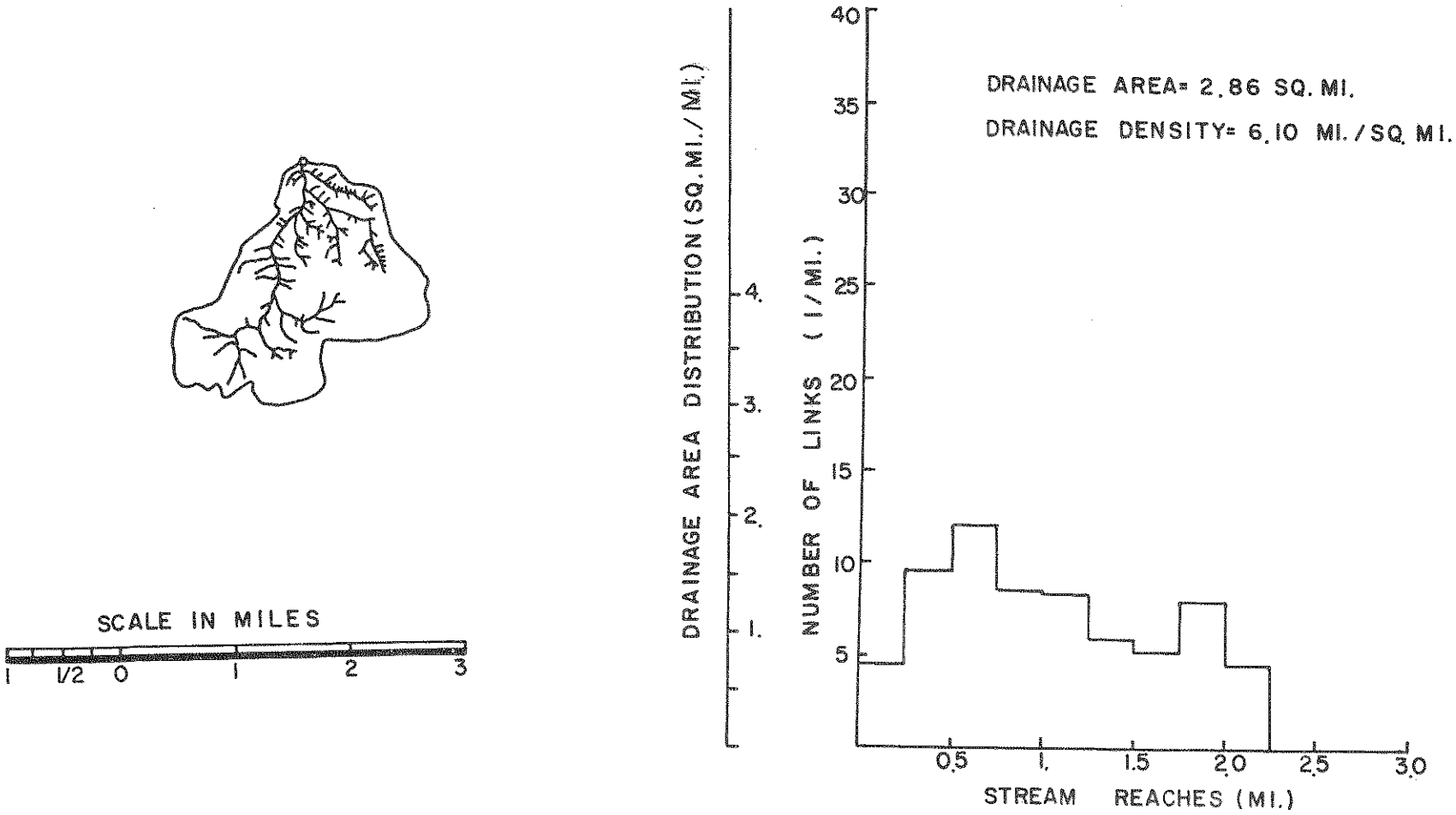

FIGURE 6-1 WATERSHED, LAWRENCE CREEK AT FT BENJAMIN, HARRISON, INDIANA (WATERSHED NO. 1)

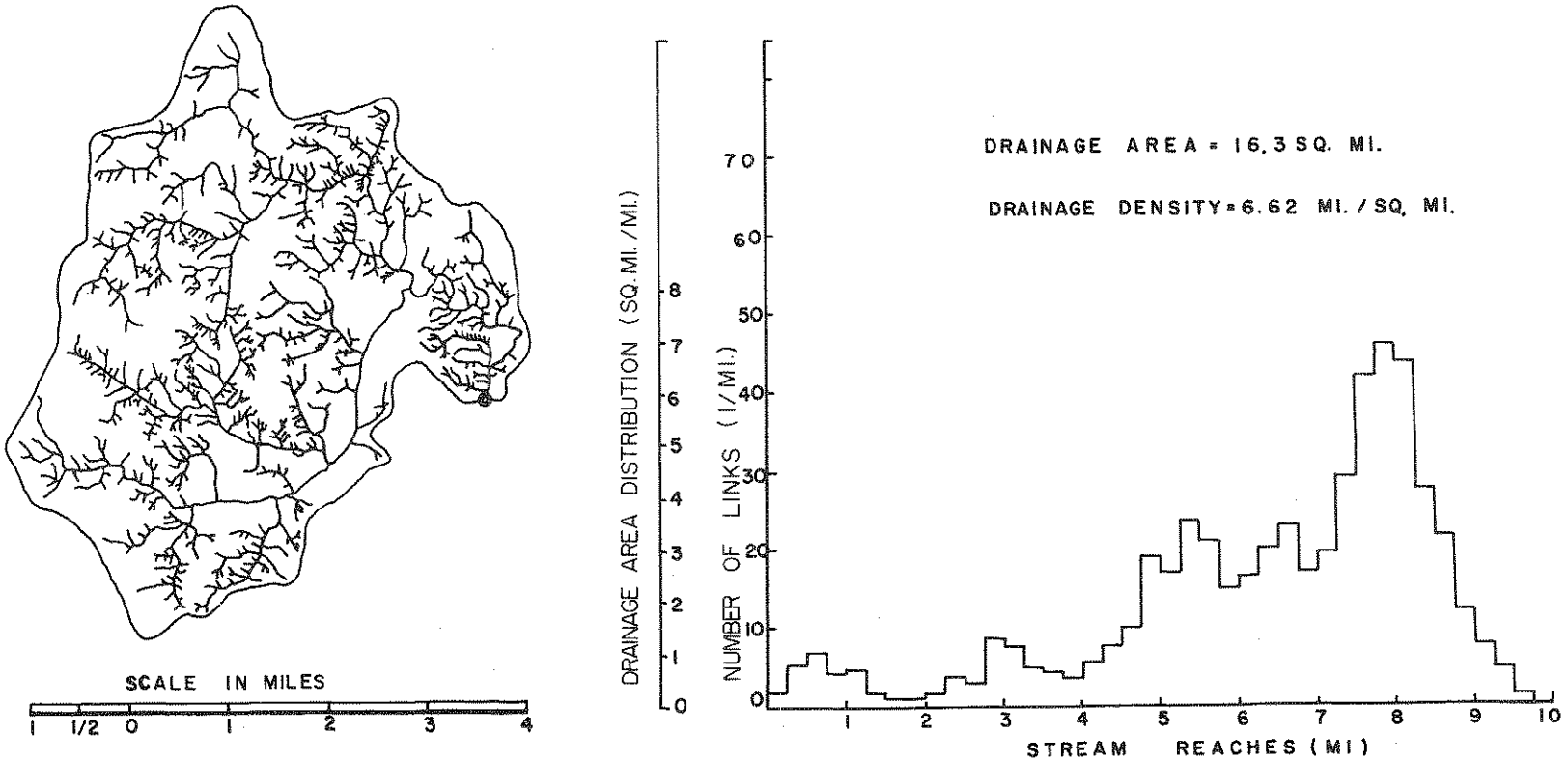

FIGURE 6-2 WATERSHED, HINKLE CREEK NEAR CICERO, INDIANA
(WATERSHED NO. 16)

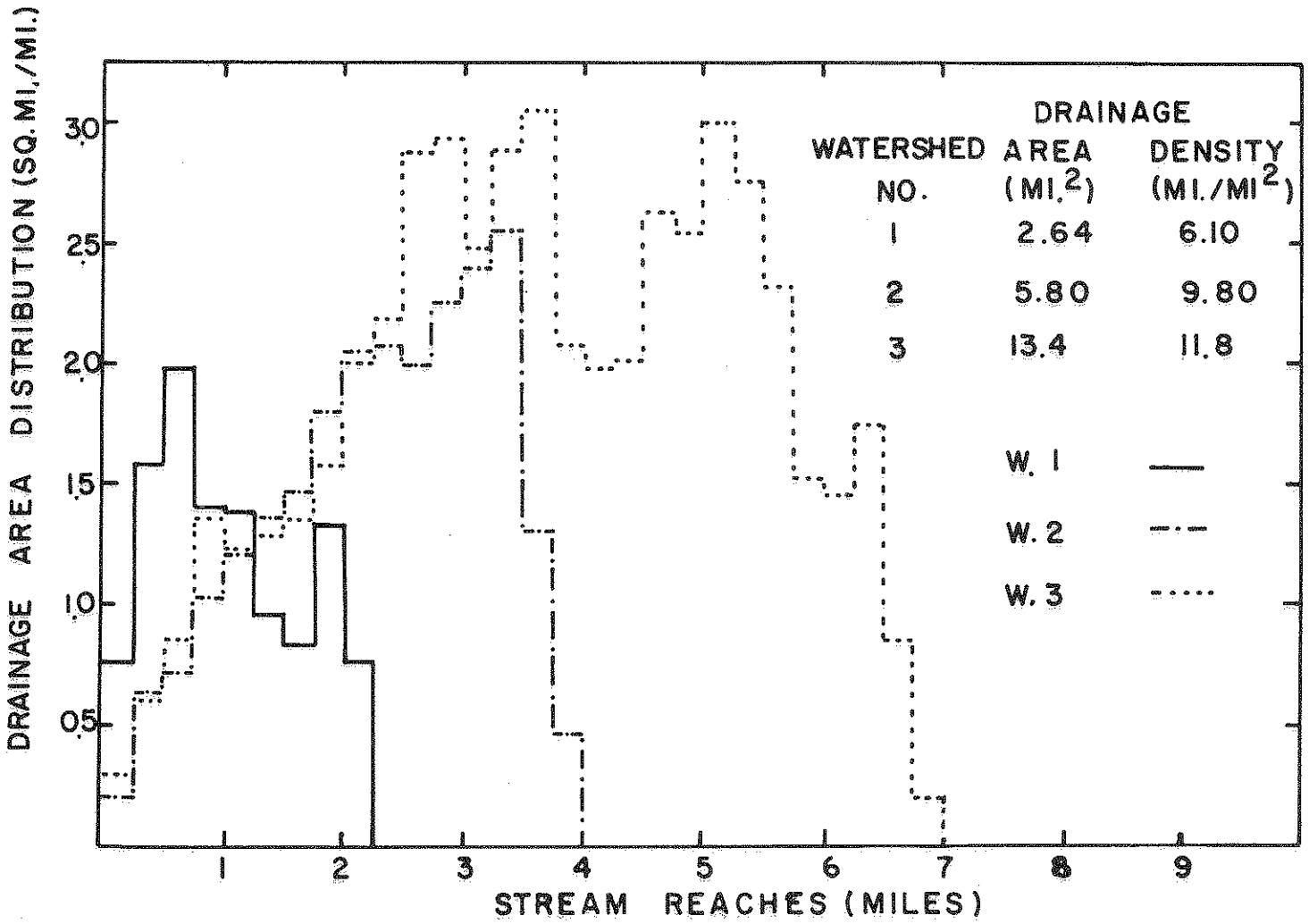

FIGURE 6-3 EXAMPLES OF DRAINAGE AREA DISTRIBUTION ALONG THE STREAM REACHES

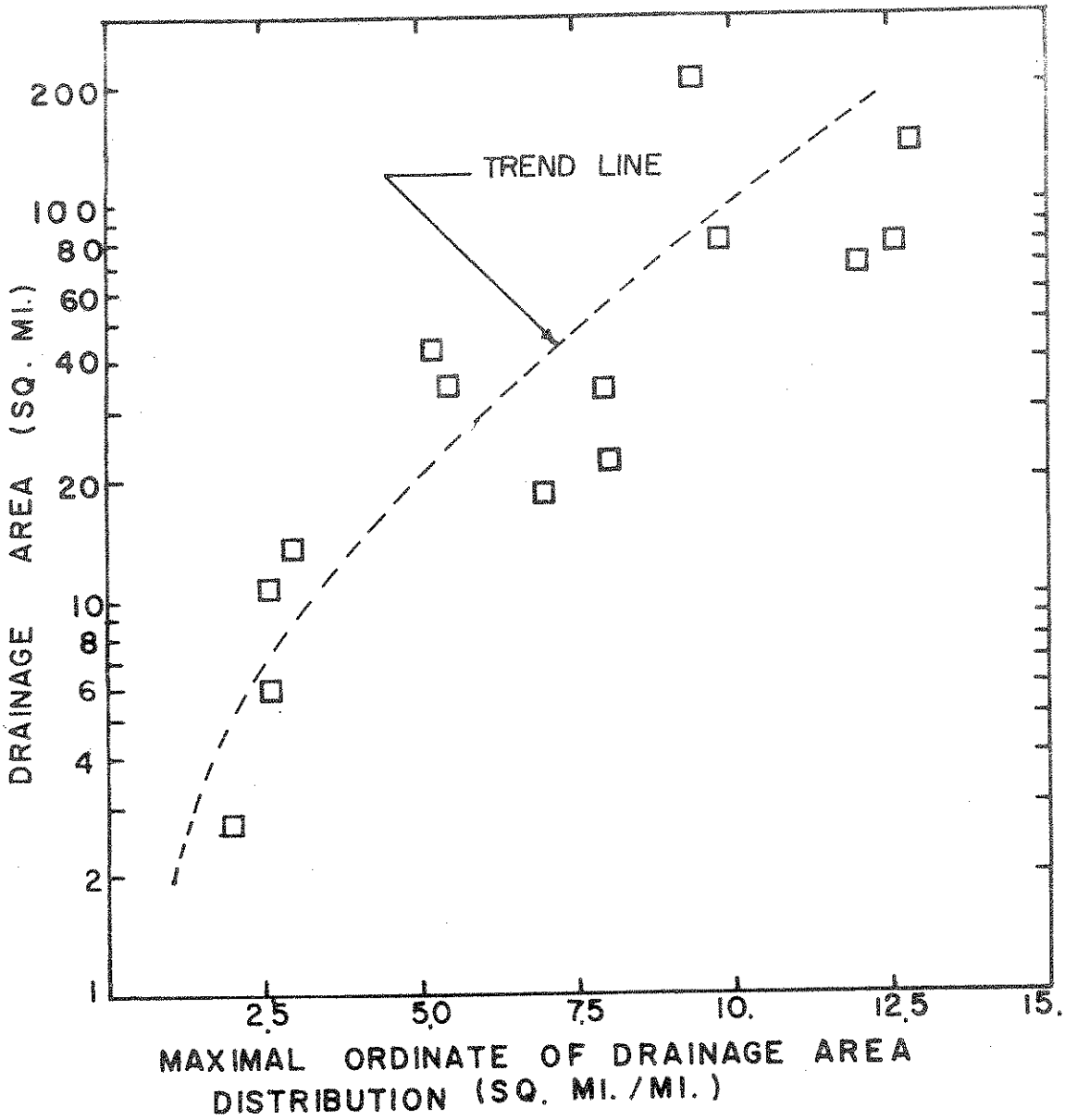

FIGURE 6-4 DRAINAGE AREA AND MAXIMAL ORDINATE OF DRAINAGE AREA DISTRIBUTION

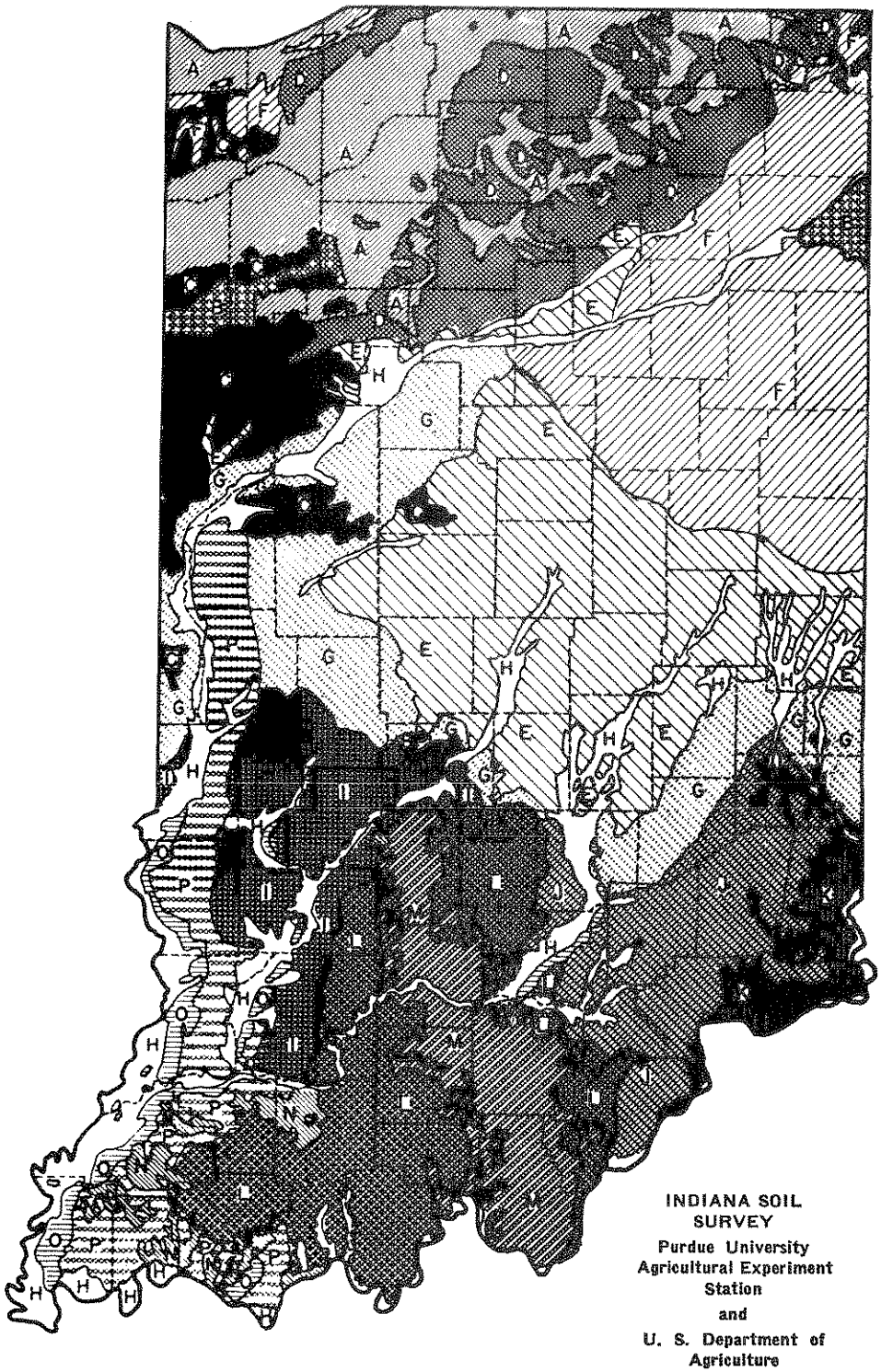

FIGURE 6-5 GENERAL SOIL TYPES OF THE REGIONS OF INDIANA

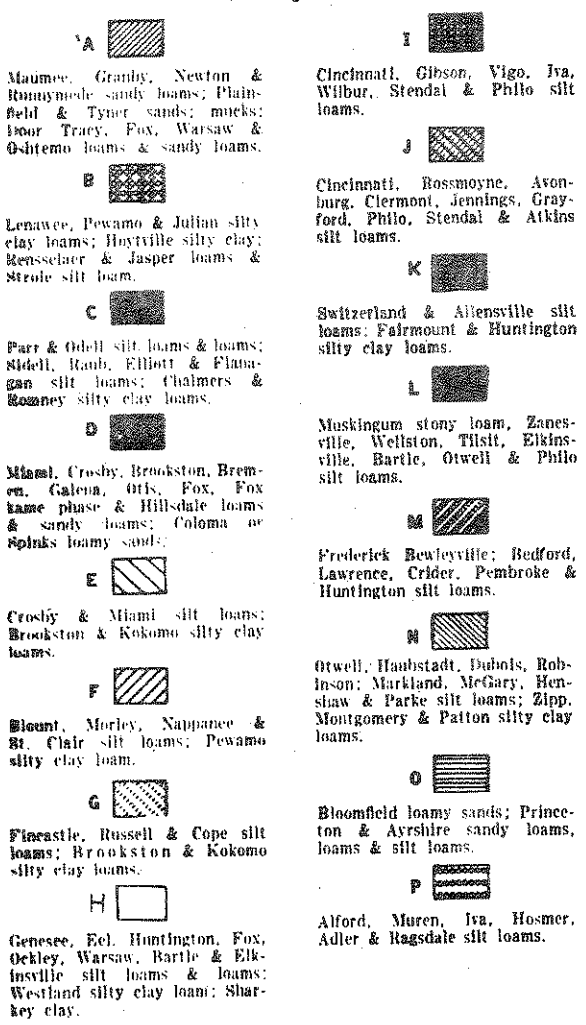

SOIL TYPE	RUN OFF COEFFICIENT
A,	0.30
D, H, O	0.50
C, E, G, M, P	0.70
K, L, N	0.80
B, I, J	1.00
F	0.5 - 0.8

FIGURE 6-5 (CONTINUED)

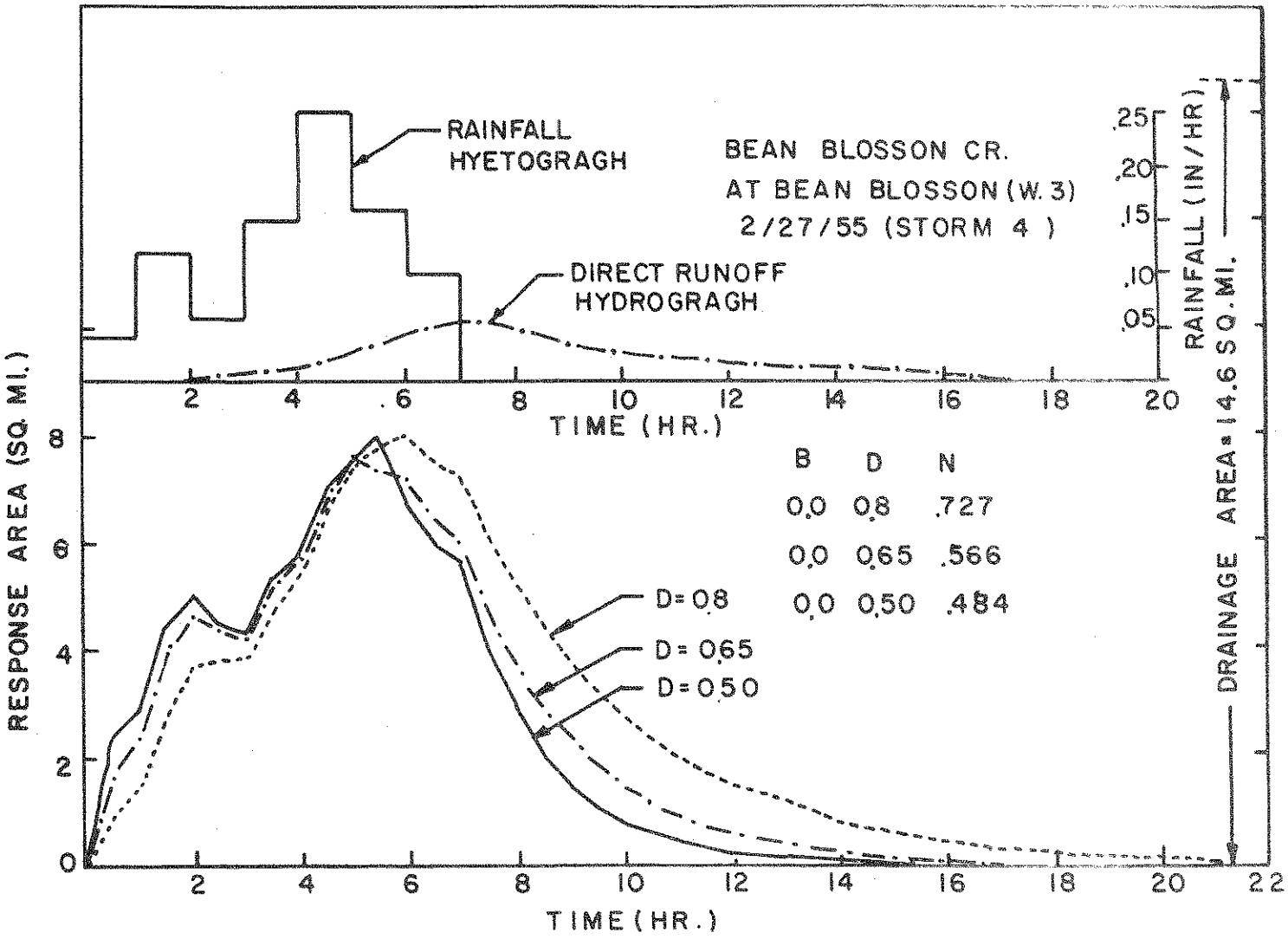

FIGURE 6-6 SENSITIVITY ANALYSIS OF WEIGHT D

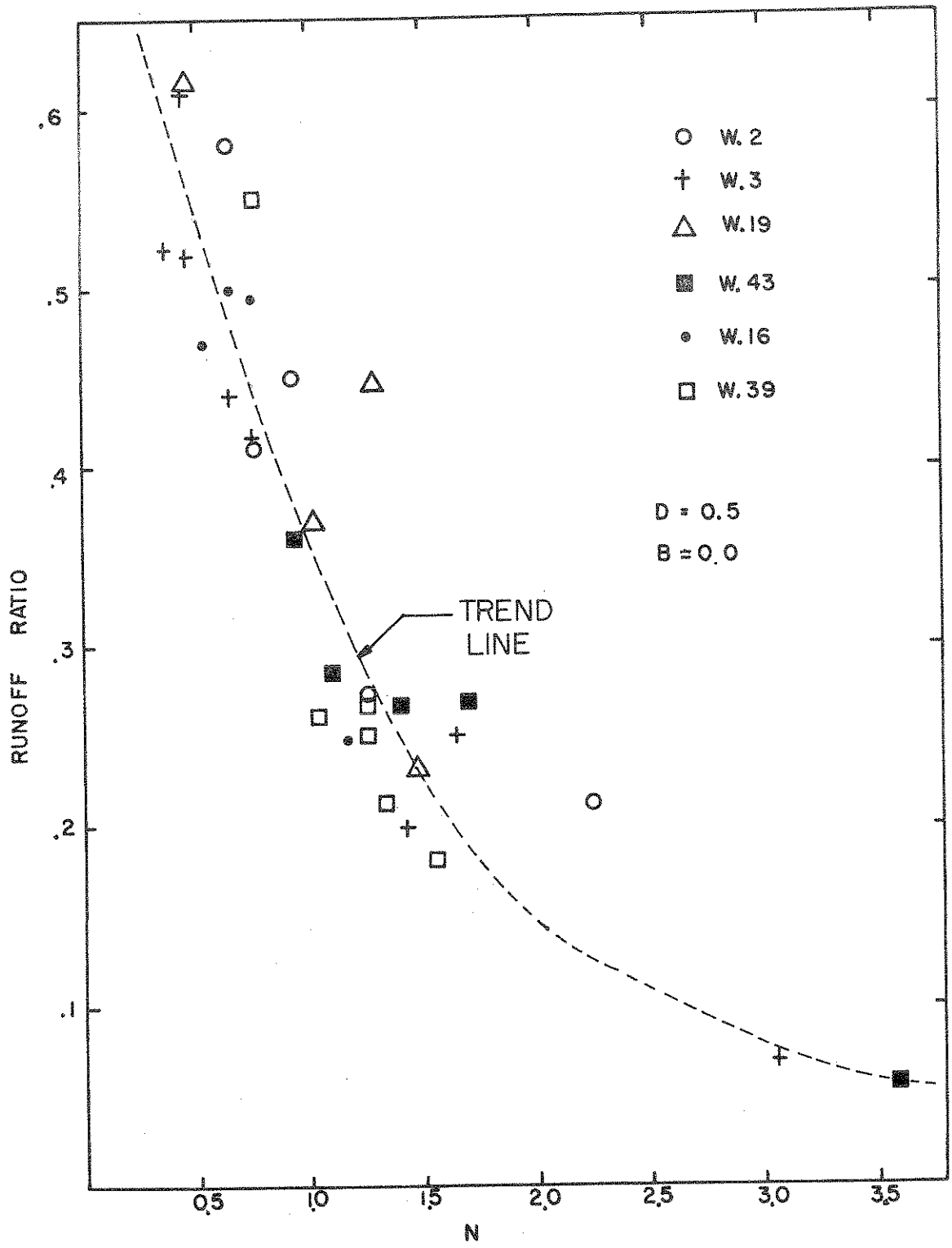

FIGURE 6-7 RUNOFF RATIO VS. N

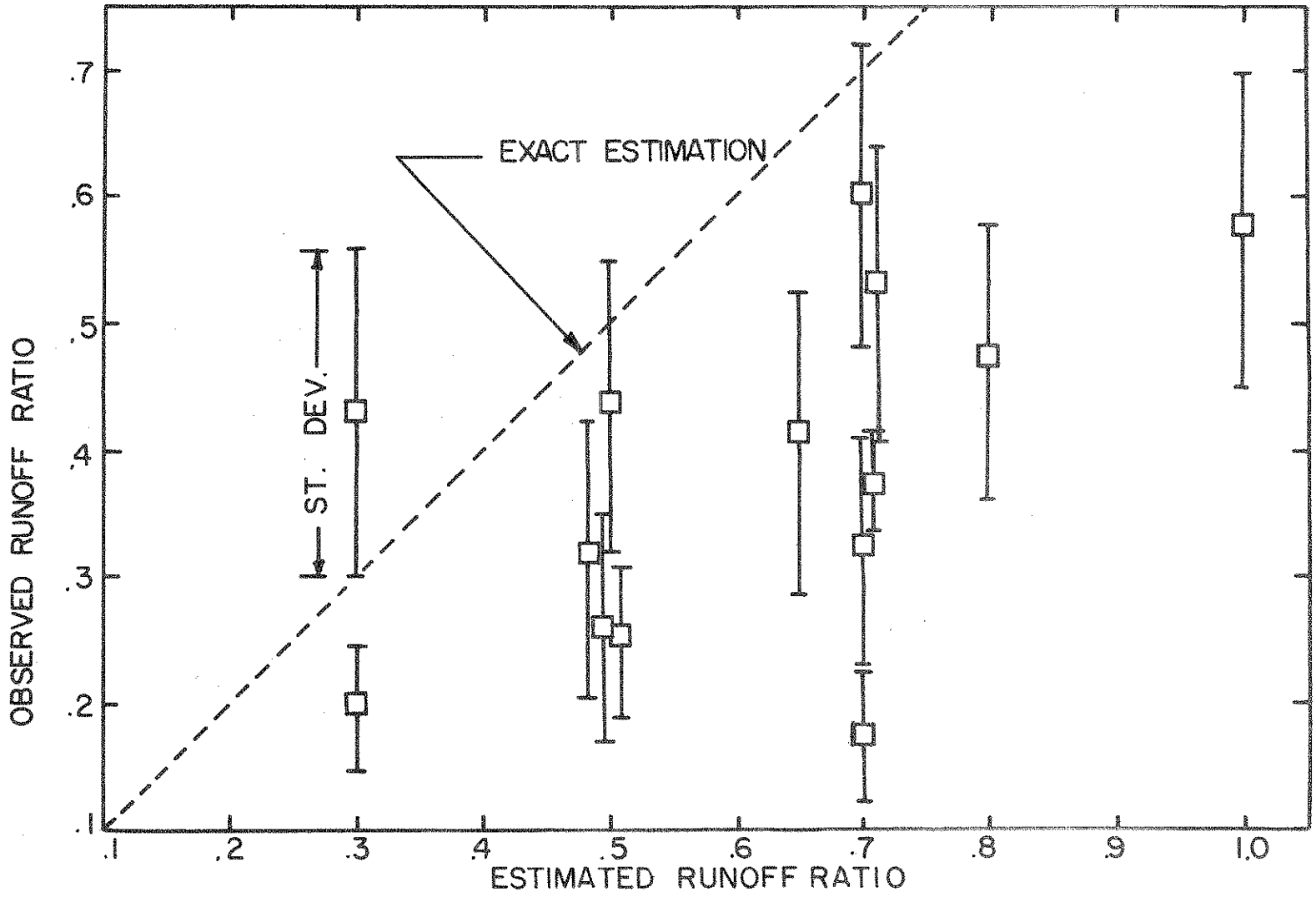

FIGURE 6-8 ESTIMATED RUNOFF RATIO BY WU METHOD

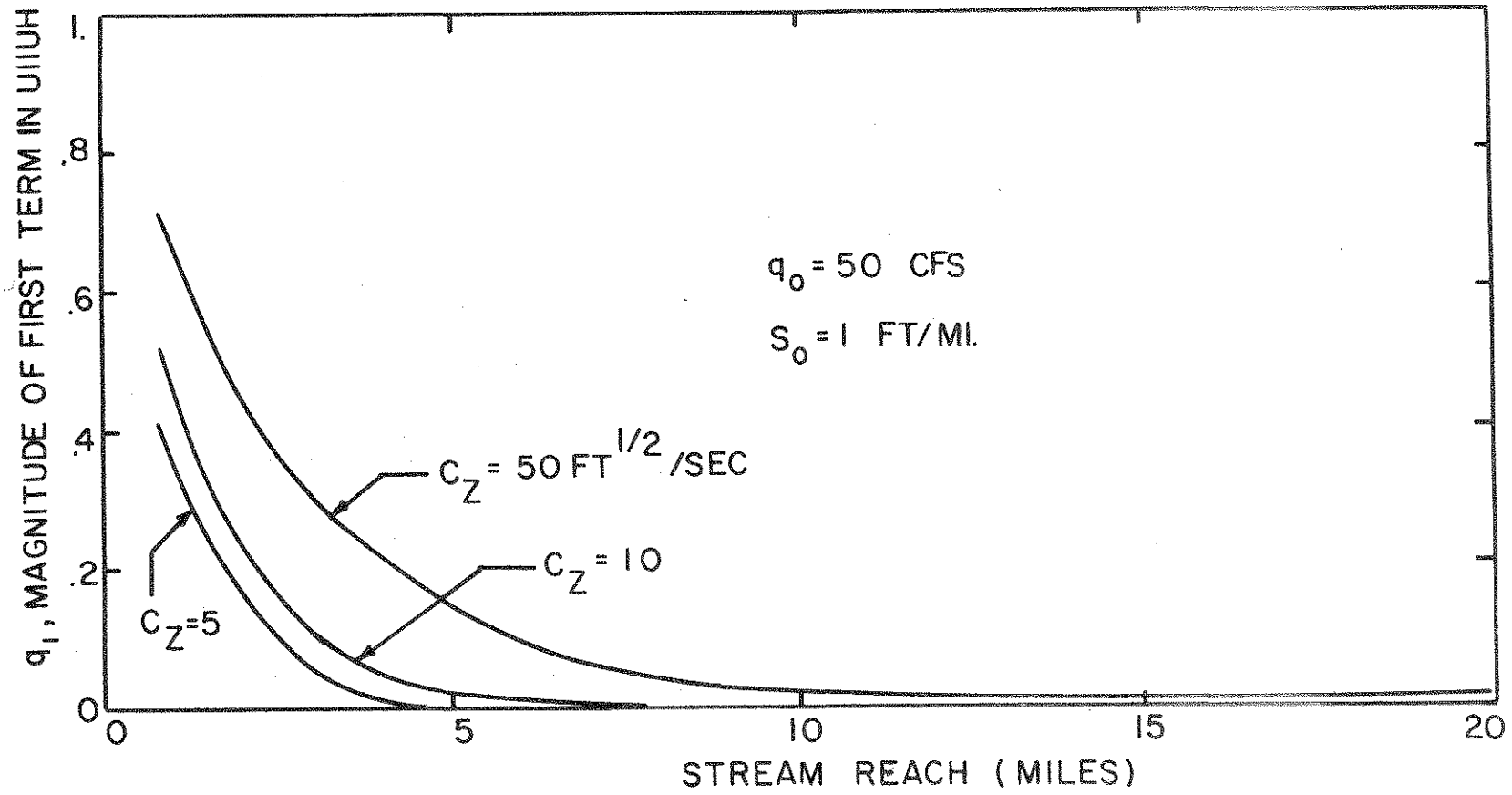

FIGURE 6-9a MAGNITUDE OF FIRST TERM IN UIIUH

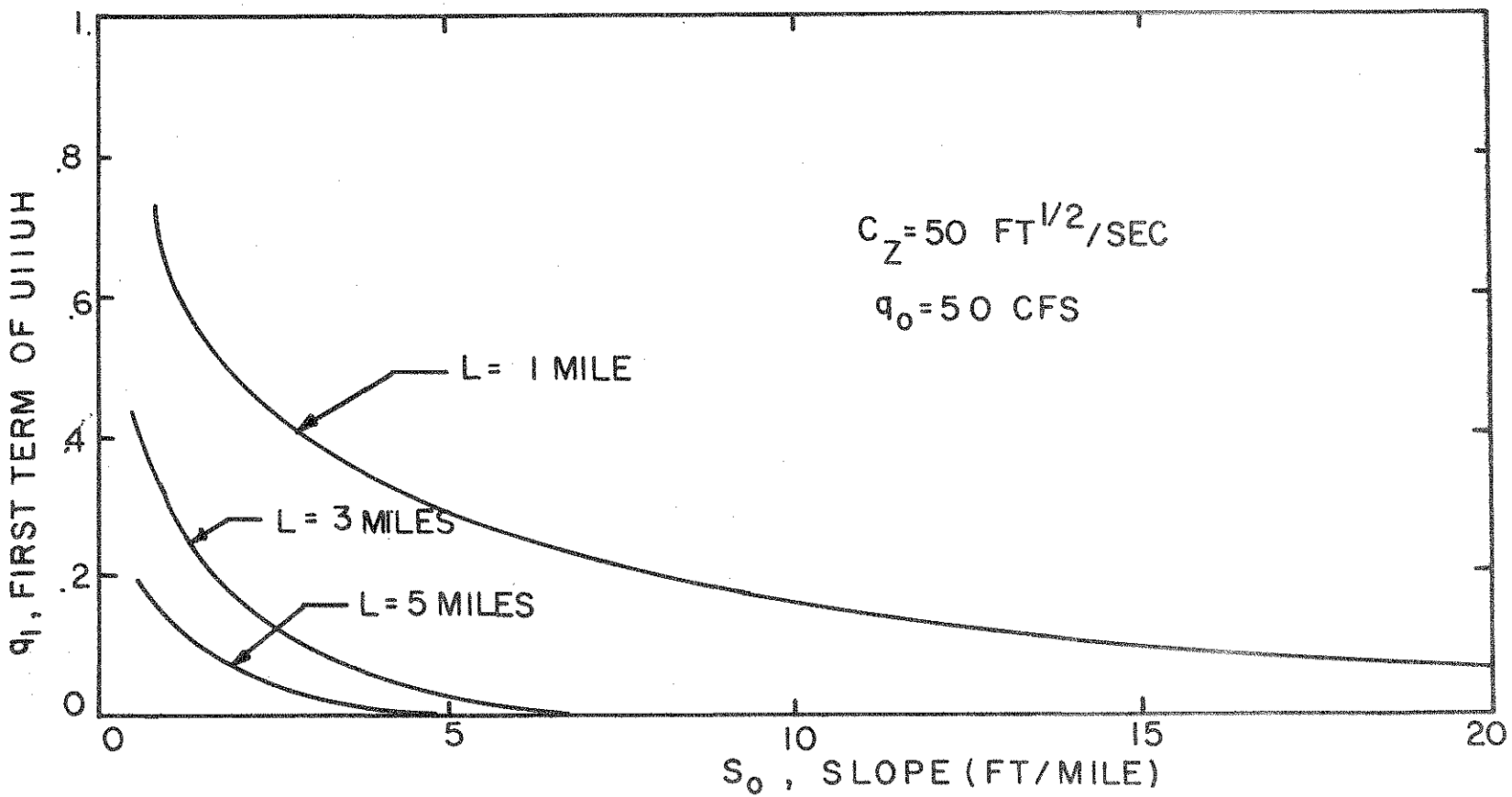

FIGURE 6-9b MAGNITUDE OF FIRST TERM IN UIIUH

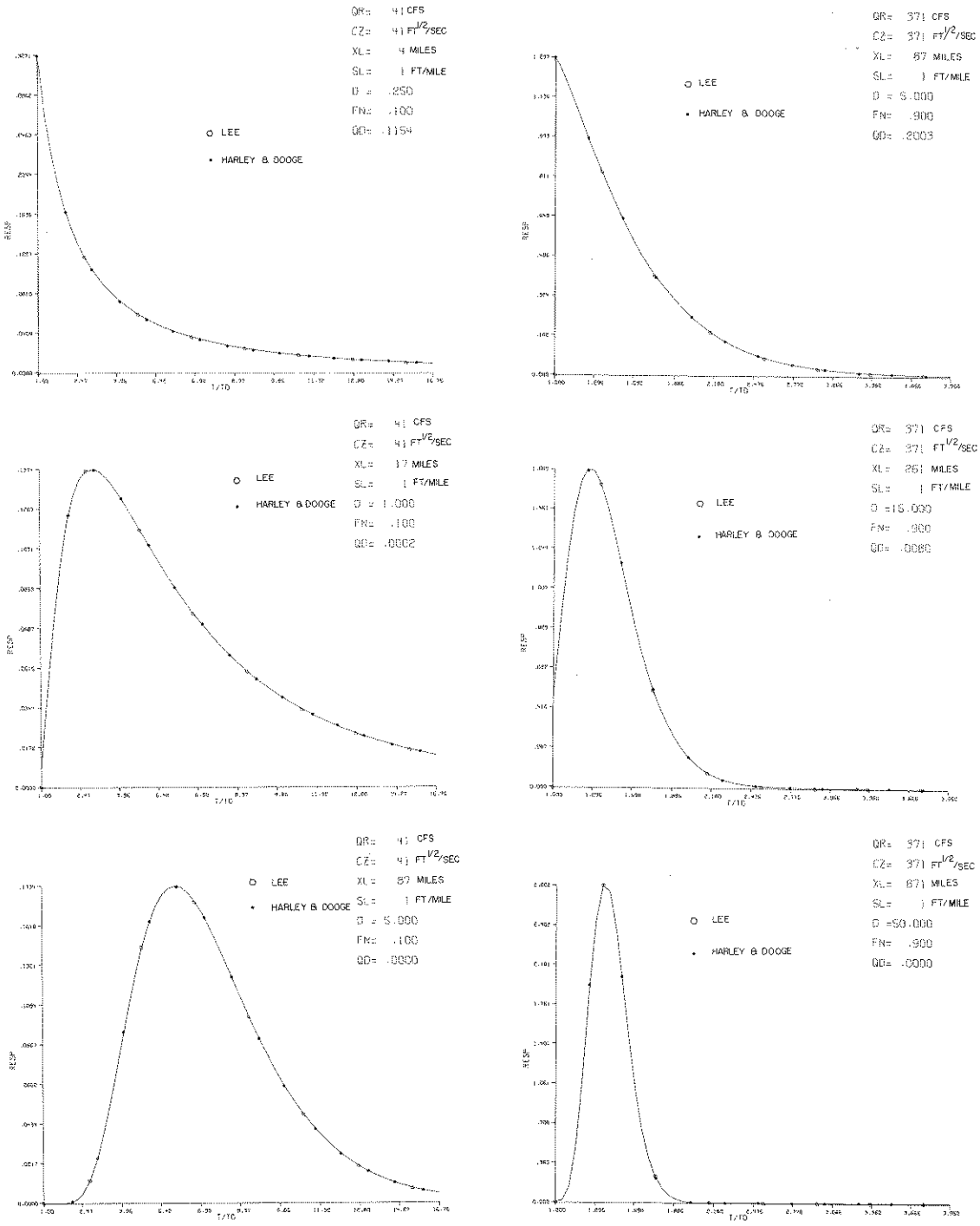

FIGURE 6-10 VERIFICATION OF UIUH

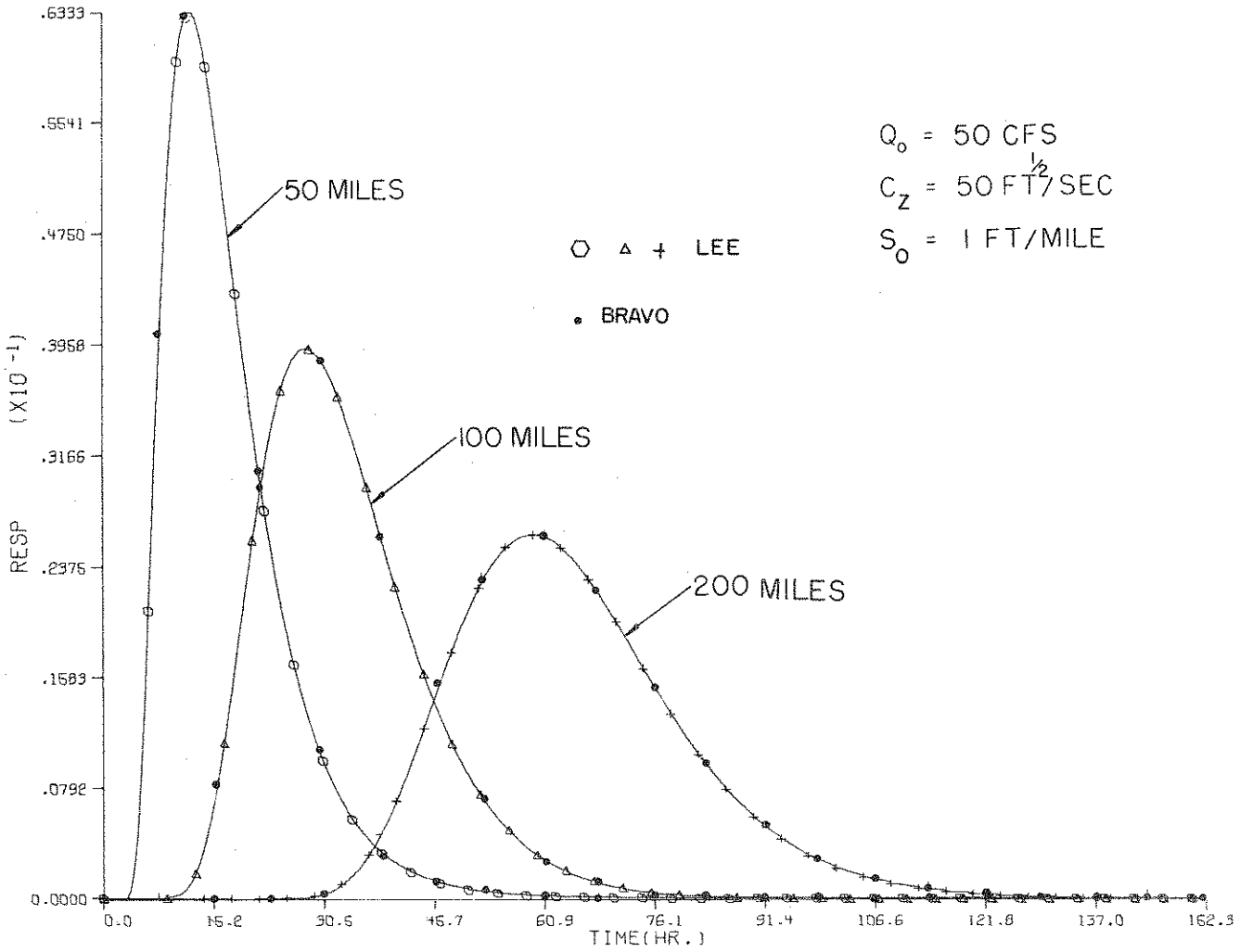

FIGURE 6-11 VERIFICATION OF UIIUH

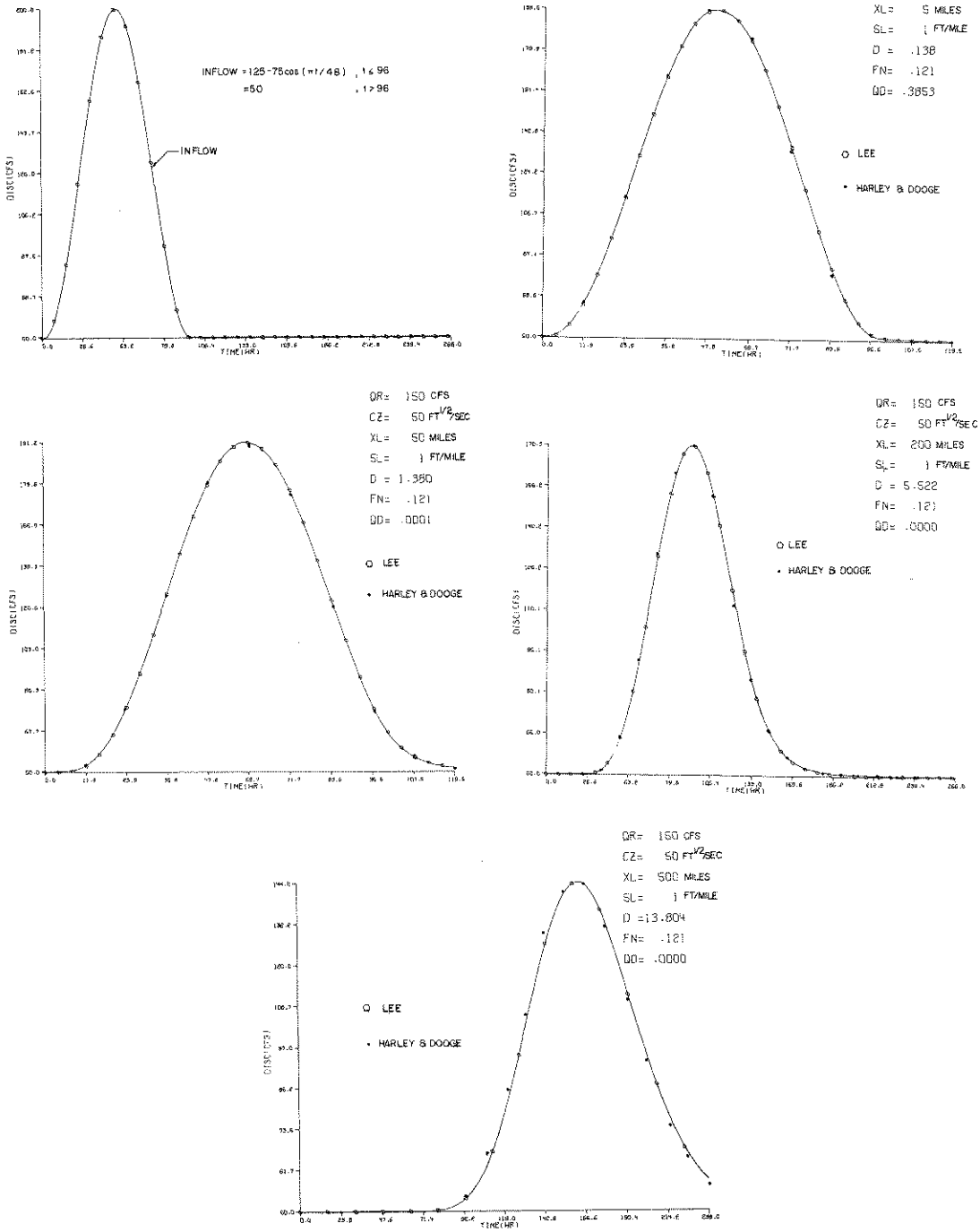

FIGURE 6-12 VERIFICATION OF CONVOLUTION

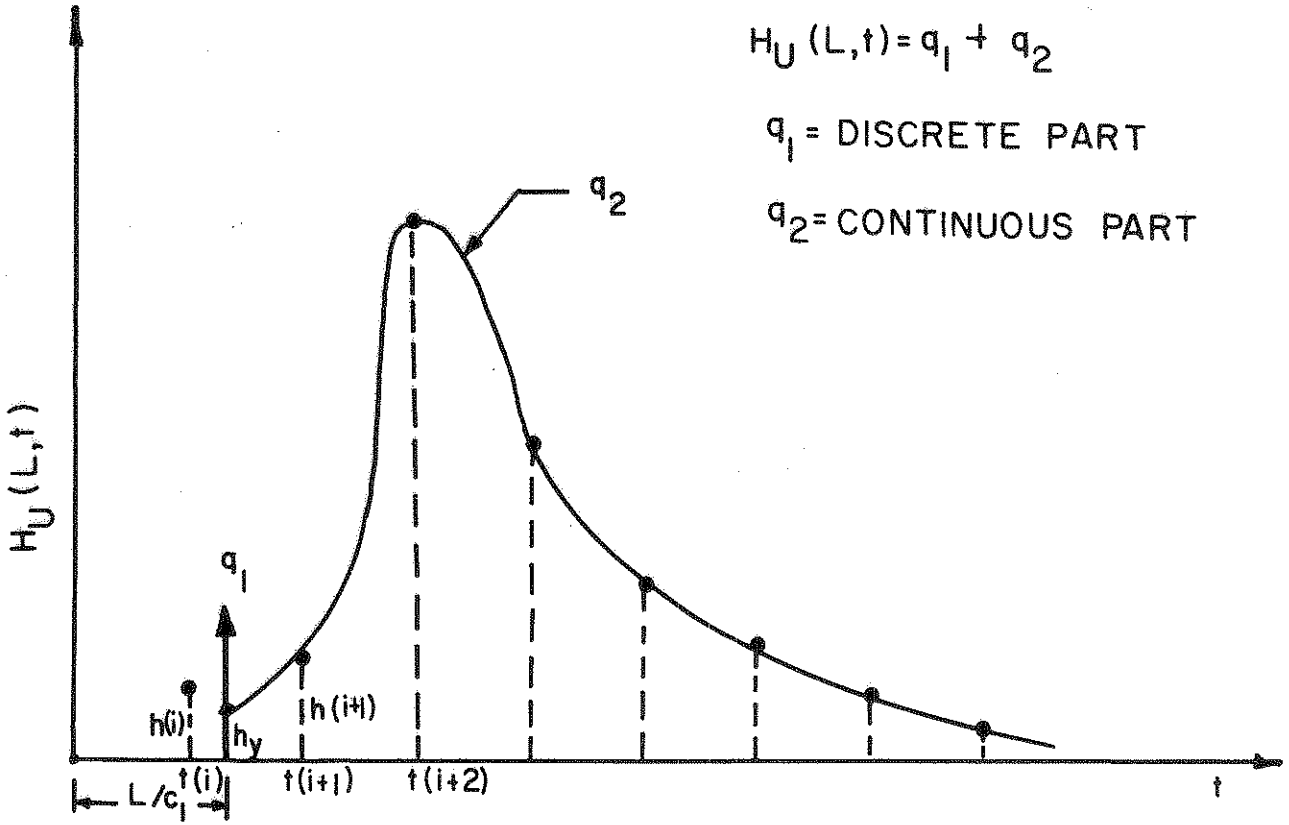

FIGURE 6-13 SAMPLING SCHEME OF UPSTREAM INFLOW INSTANTANEOUS UNIT HYDROGRAGH

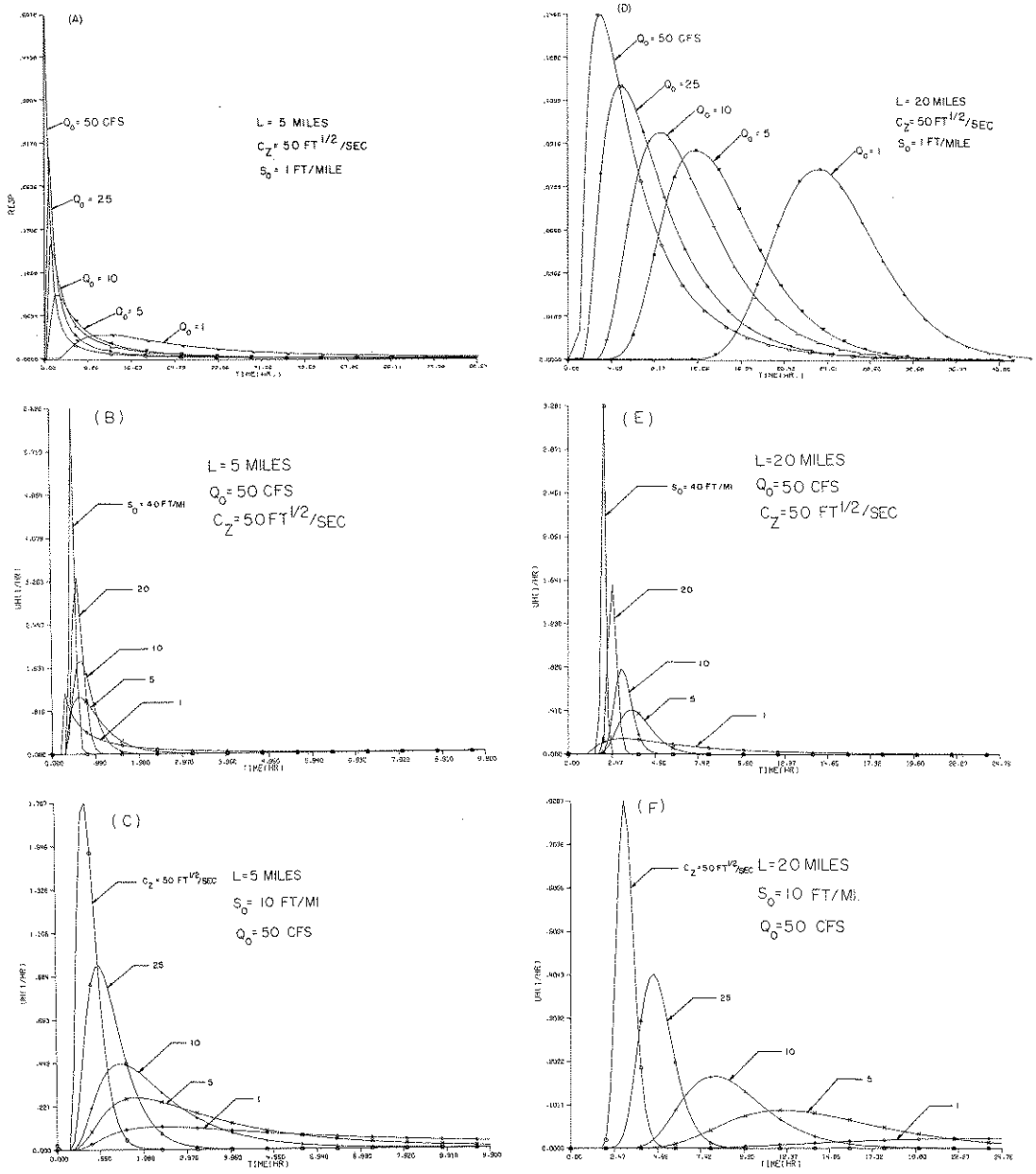

FIGURE 6-14 SENSITIVITY ANALYSIS OF UIUH PARAMETERS

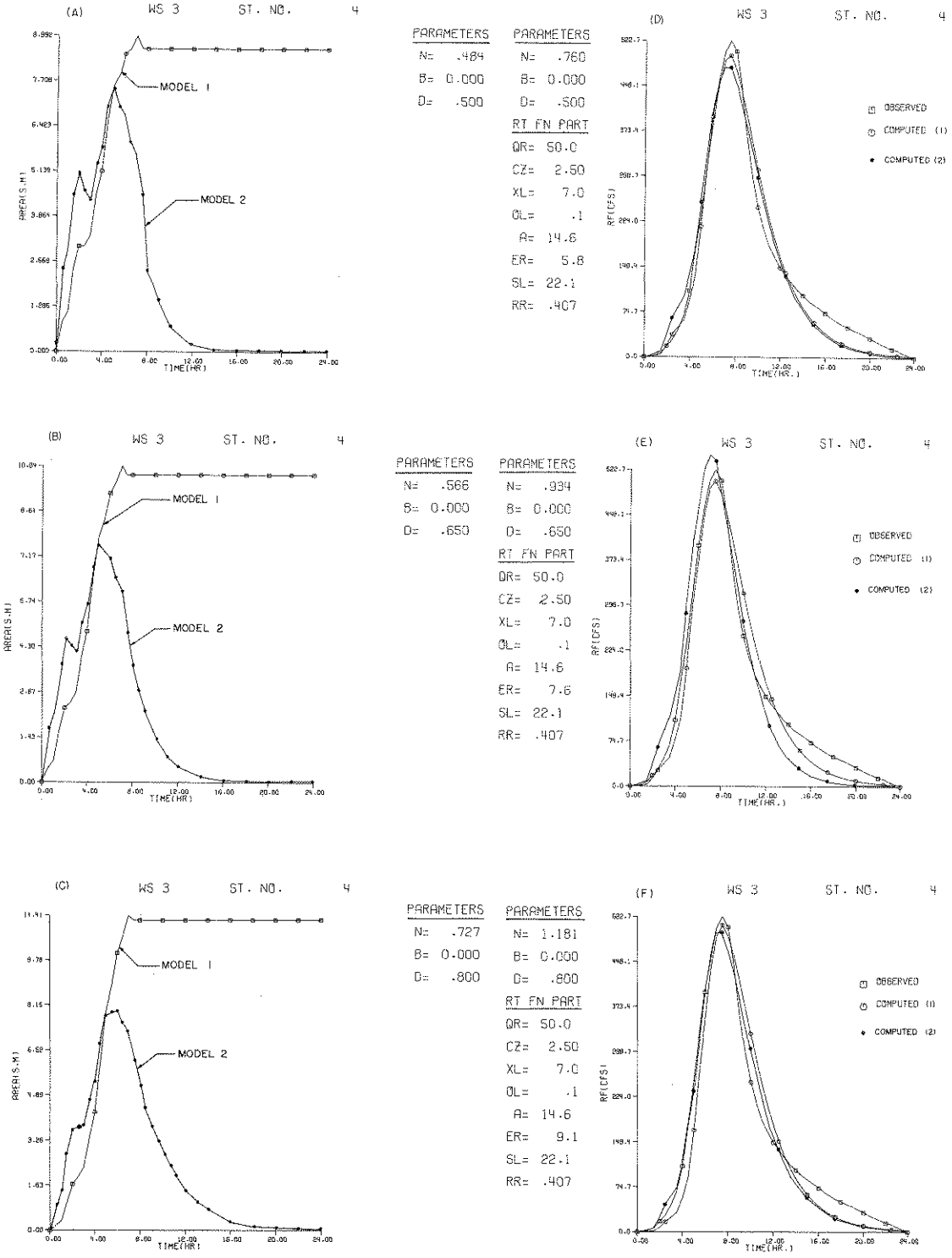

FIGURE 6-15 COMPARISON OF RESPONSE AREA MODELS

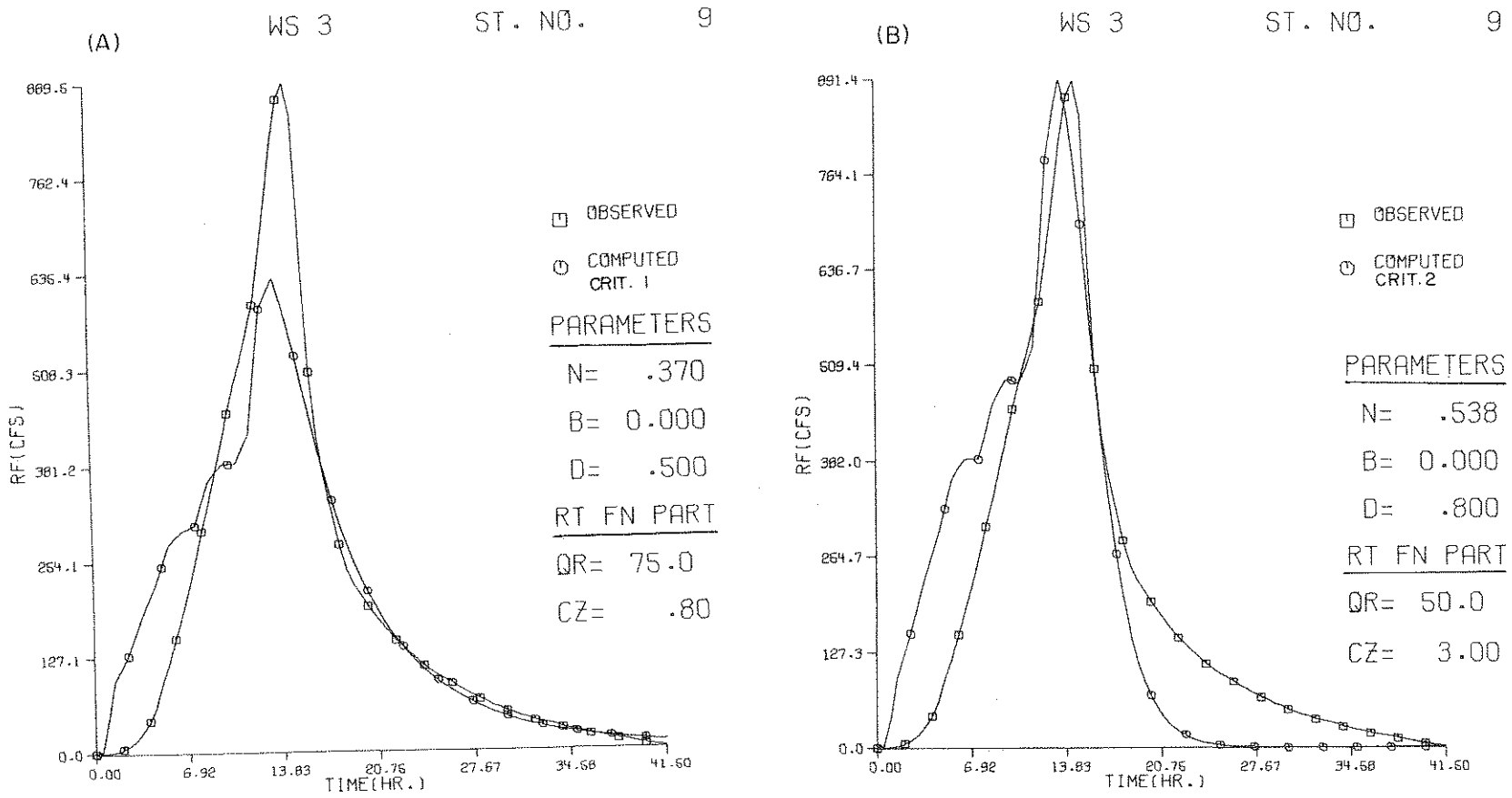

FIGURE 6-16 COMPARISON OF OPTIMIZATION CRITERIA

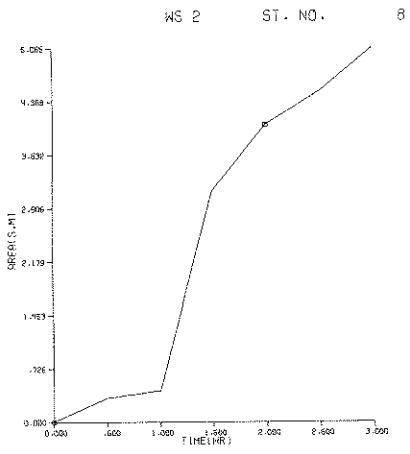

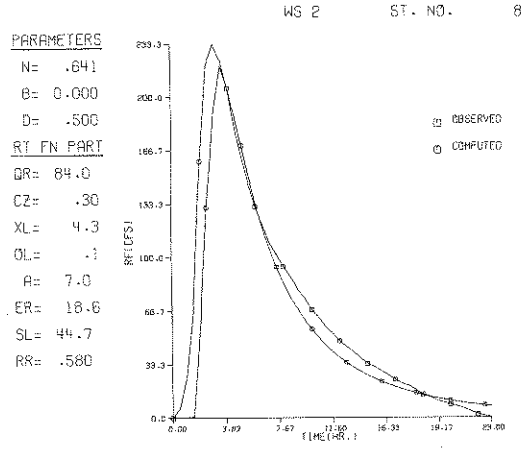

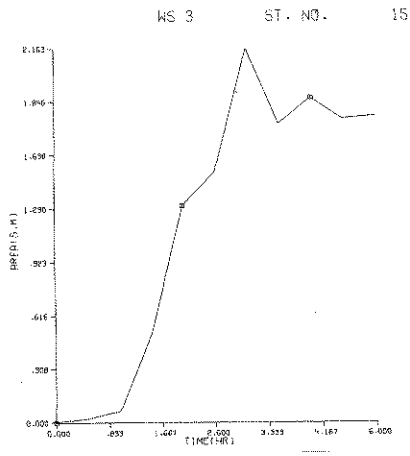

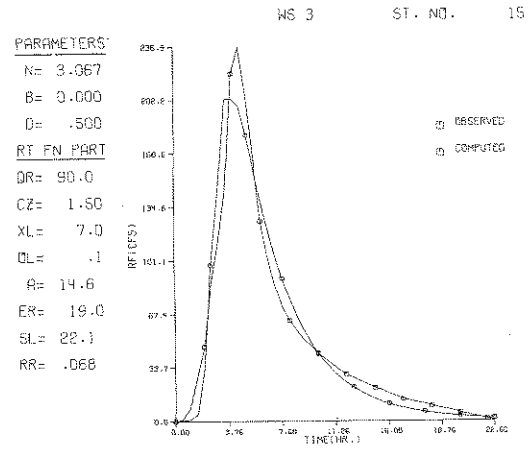

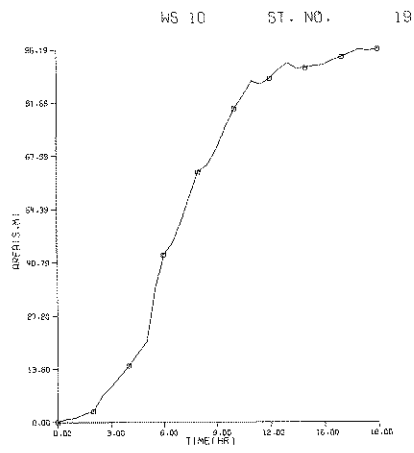

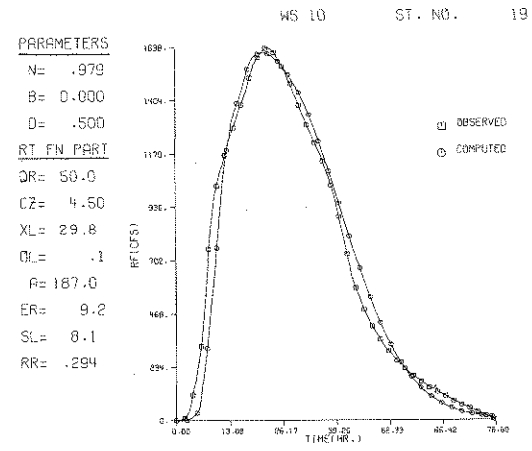

FIGURE 6-17 SAMPLE RESULTS OF WATERSHED NO. 2, 3 AND 10

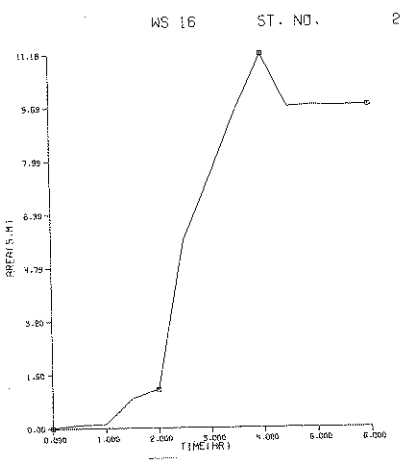

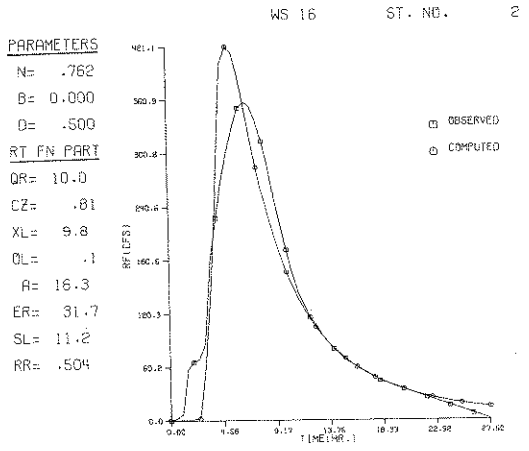

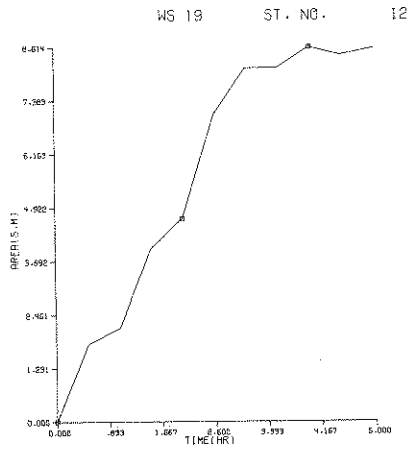

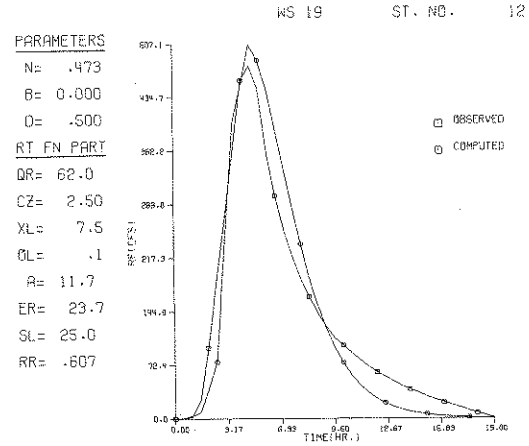

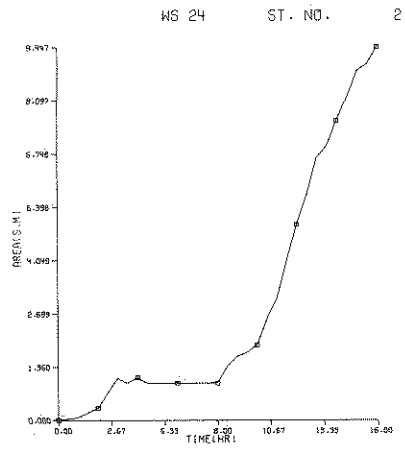

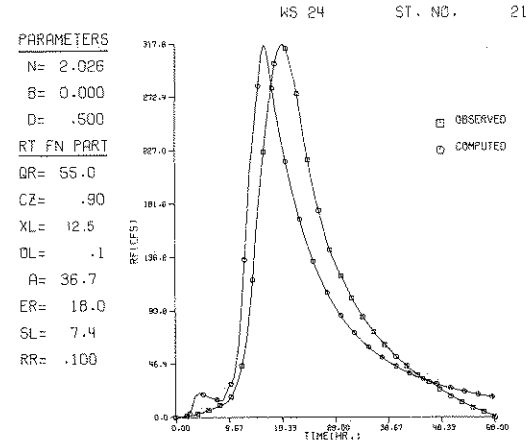

FIGURE 6-18 SAMPLE RESULTS OF WATERSHED NO.16, 19 AND 24

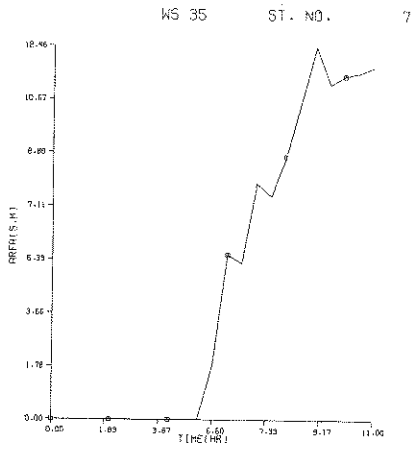

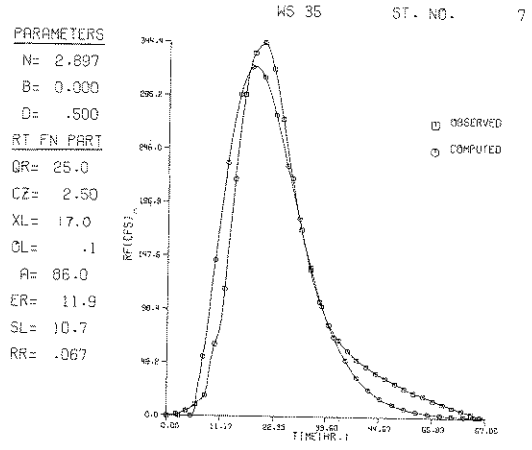

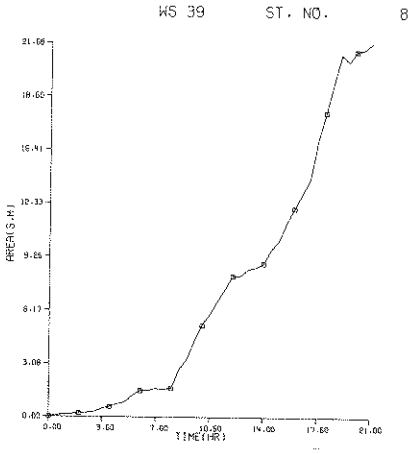

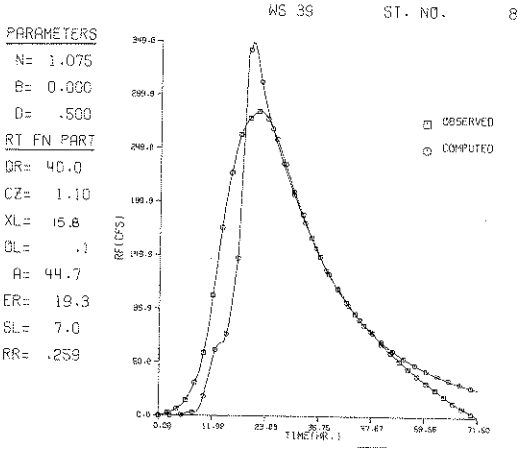

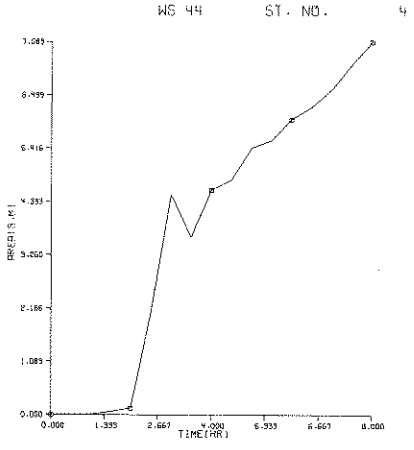

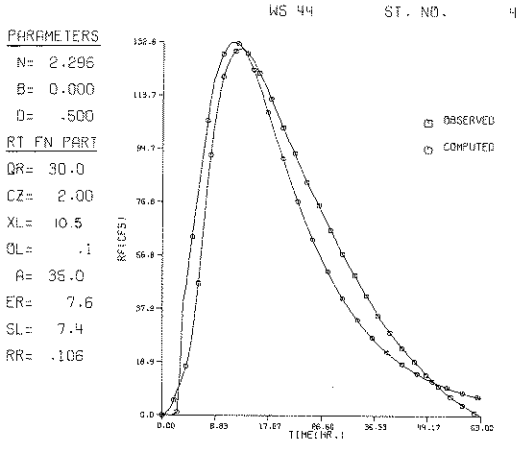

FIGURE 6-19 SAMPLE RESULTS OF WATERSHED NO.35,39 AND 44

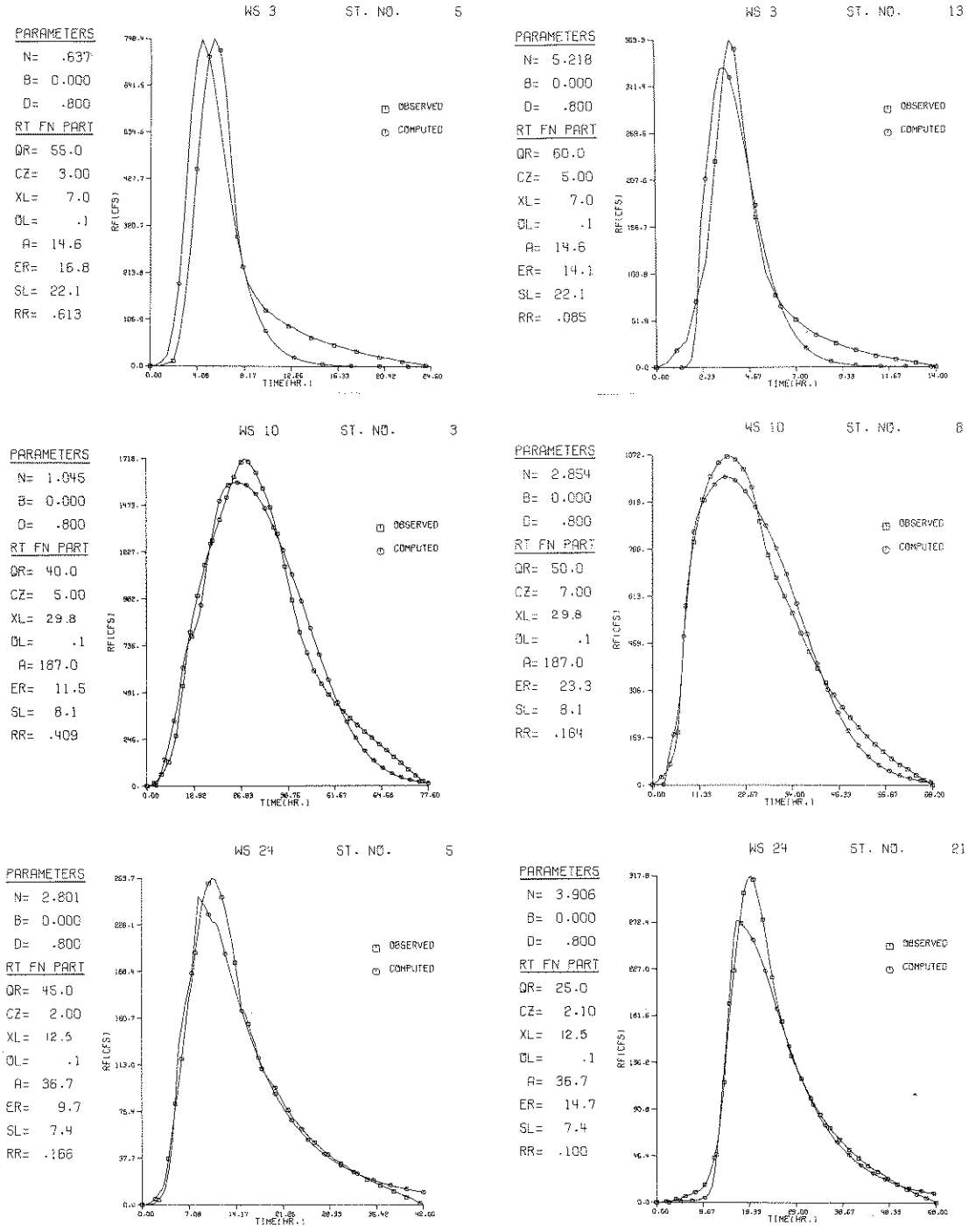

FIGURE 6-20 COMPARISON OF OBSERVED AND COMPUTED DIRECT RUNOFF HYDROGRAPHS

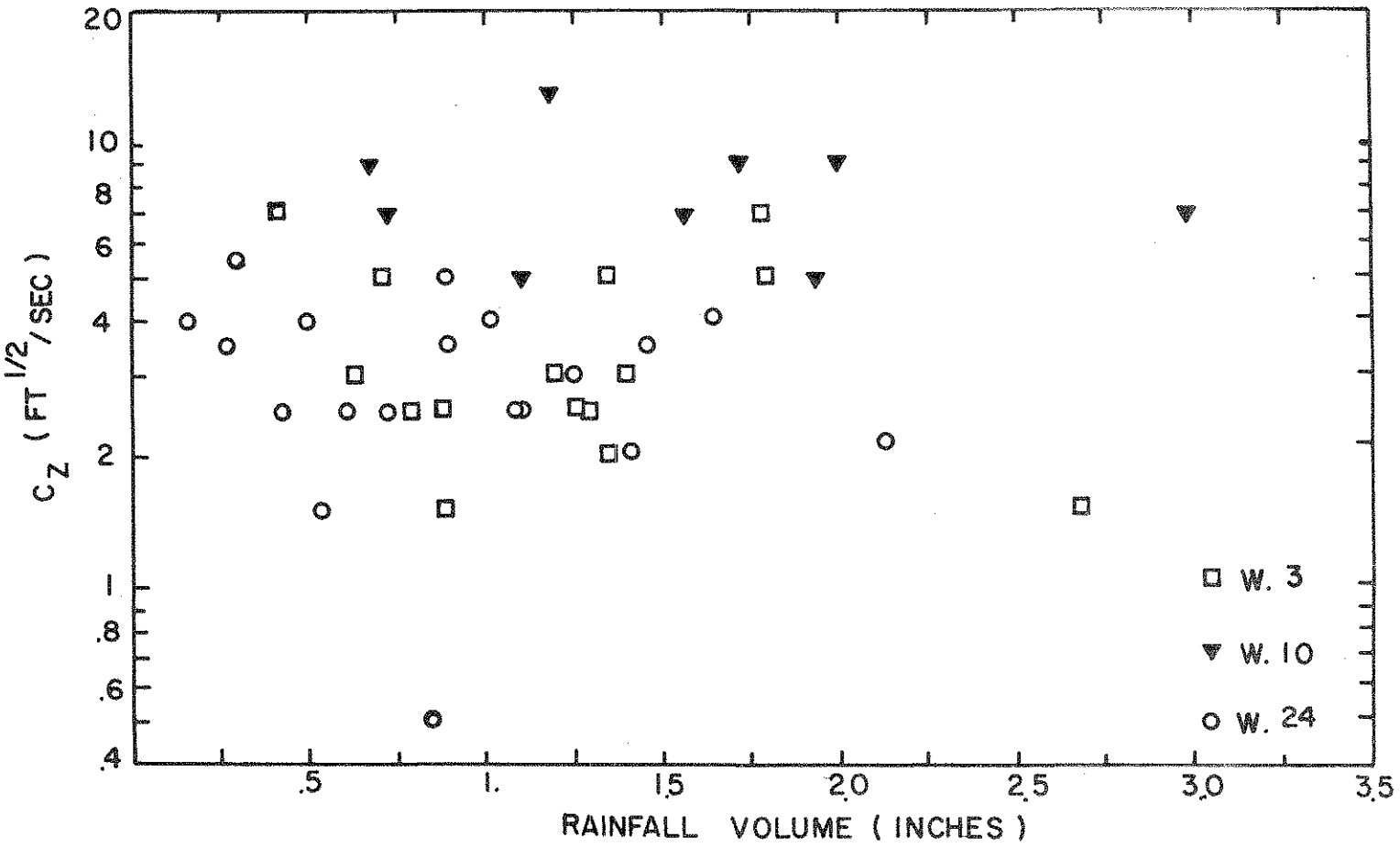

FIGURE 6-21 C_Z VS. RAINFALL VOLUME

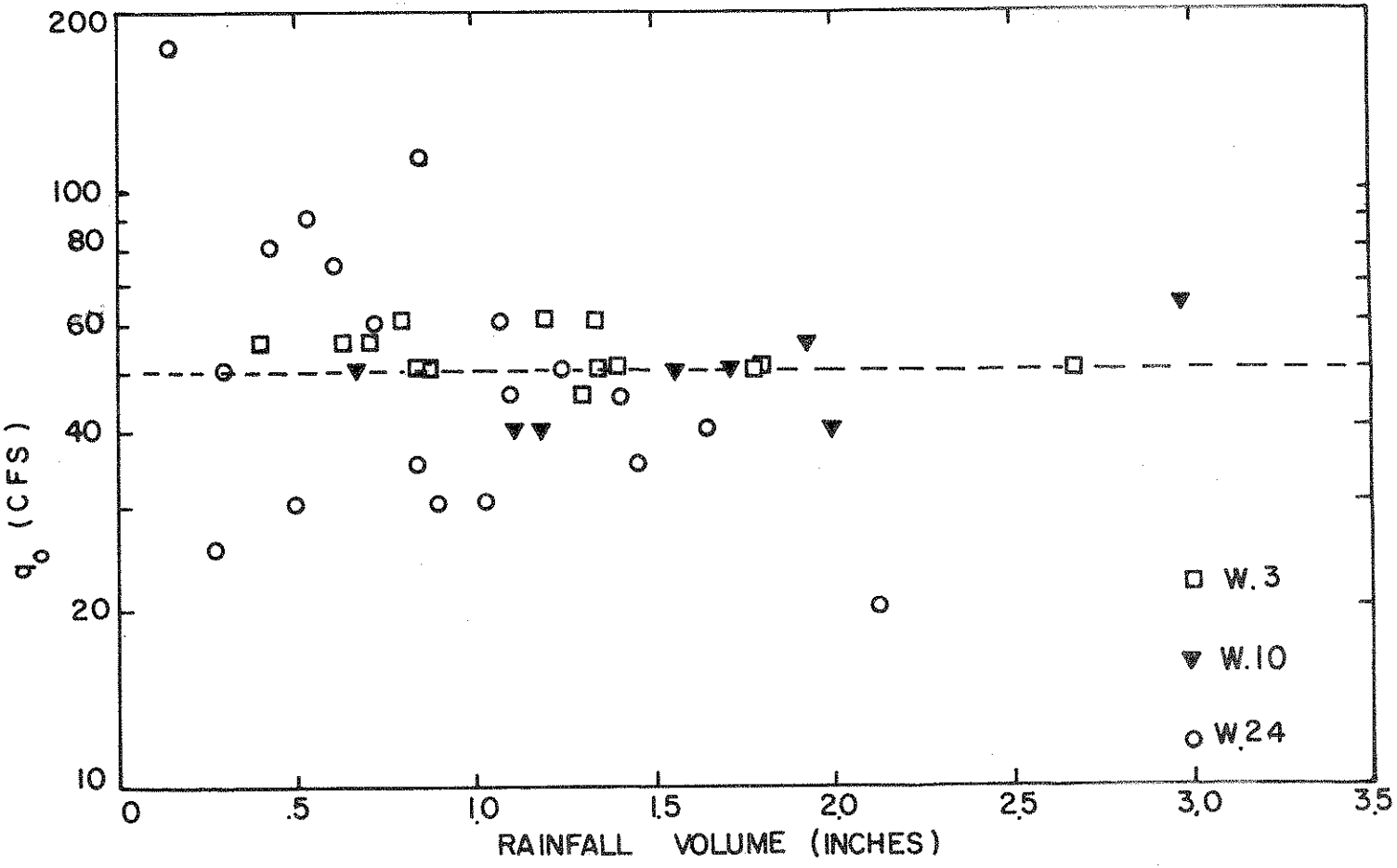

FIGURE 6-22 REFERENCE DISCHARGE VS. RAINFALL VOLUME

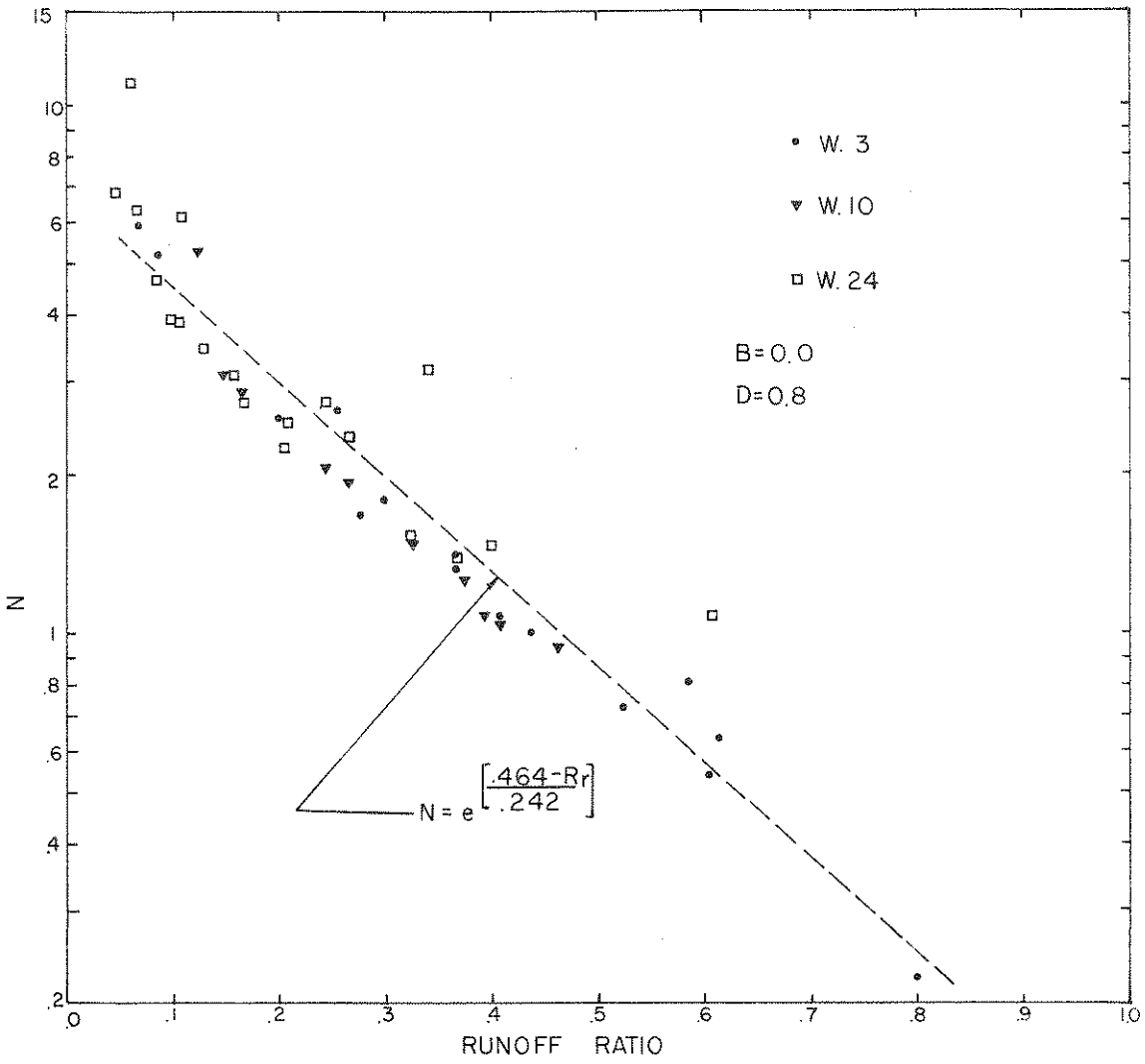

FIGURE 6-23 RUNOFF RATIO VS. N IN WATERSHEDS NO. 3, 10 AND 24

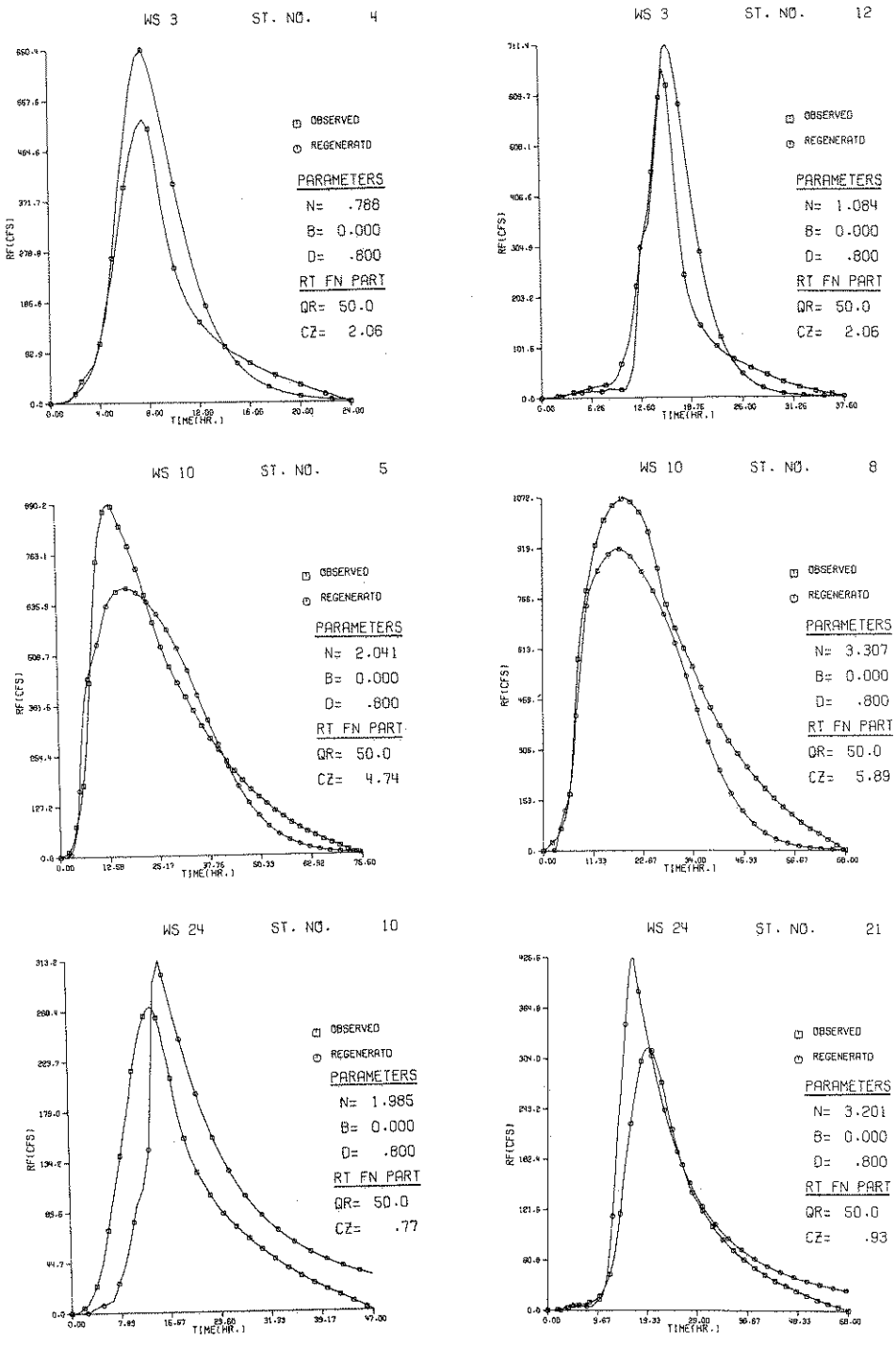

FIGURE 6-24 THE SAMPLE RESULTS OF REGENERATION PERFORMANCE

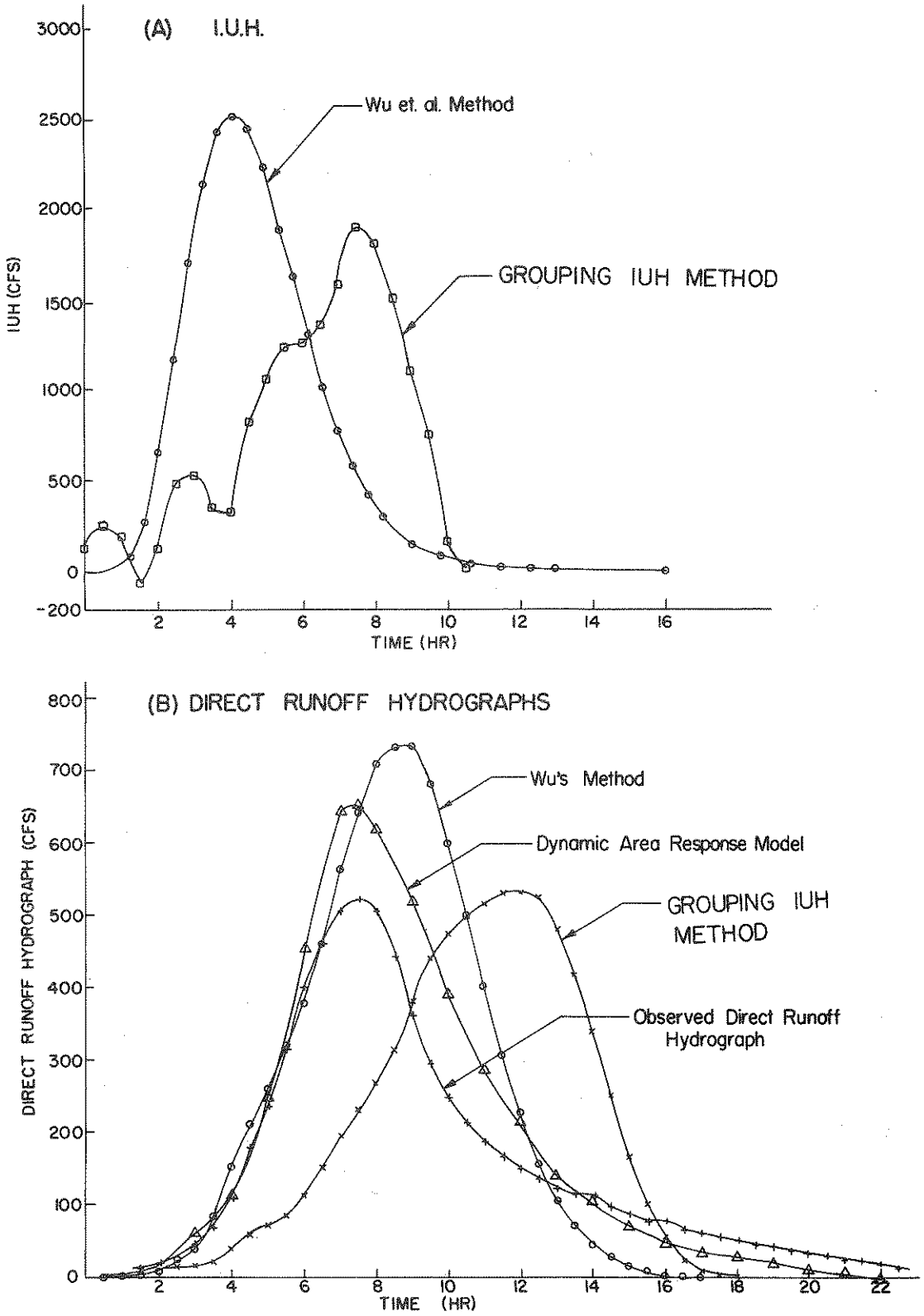

FIGURE 6-25. THE COMPARISON WITH SOME OTHER METHODS